

Aus der  
Medizinischen Universitätsklinik und Poliklinik Tübingen  
Abteilung VIII, Medizinische Onkologie und Pneumologie

**New approaches in the therapy of NUT carcinomas (NCs)  
involving immunovirotherapy and BET-protein inhibitors**

**Inaugural-Dissertation  
zur Erlangung des Doktorgrades  
der Medizin**

**der Medizinischen Fakultät  
der Eberhard Karls Universität  
zu Tübingen**

**vorgelegt von  
Ohnesorge, Paul Vincent**

**2023**

Dekan: Professor Dr. B. Pichler

1. Berichterstatter: Professor Dr. U. Lauer

2. Berichterstatterin: Professorin Dr. B. Schitteck

Tag der Disputation: 09.08.2021

## Table of content

<b>1</b>	<b>Introduction</b>	<b>1</b>
1.1	NUT carcinoma	1
1.1.1	Pathomechanism of the NUT carcinoma	3
1.1.2	NUT carcinoma cell lines	4
1.1.3	Therapy of the NUT carcinoma	6
1.2	Oncolytic Virotherapy	7
1.2.1	History	7
1.2.2	Principles of oncolytic virotherapy	9
1.2.3	Measles virus	11
1.2.3.1	Biology of the oncolytic measles vaccine virus MeV-GFP	12
1.2.3.2	Immunotherapy with oncolytic measles viruses	14
1.2.4	The variola virus and the vaccinia virus	14
1.2.4.1	Biology of the vaccinia virus GLV-0b347	17
1.2.4.2	Immunotherapy with oncolytic vaccinia viruses	18
1.2.5	The herpes simplex virus	18
1.2.5.1	Biology of the modified herpes simplex virus type I T-VEC	20
1.2.5.2	Immunotherapy with T-VEC	21
1.3	The bromodomain and extraterminal domain proteins	22
1.3.1	Inhibitors of the BET protein family	23
1.3.1.1	Approaches combining iBET with other agents to heighten the efficiency	24
1.4	Objective	25
<b>2</b>	<b>Material and methods</b>	<b>27</b>
2.1	Materials	27
2.1.1	NUT carcinoma cell lines	27
2.1.2	Viruses	28
2.1.3	Media, sera and buffer	29
2.1.3.1	Self-made solutions	29
2.1.4	Chemicals	29
2.1.4.1	Self-made solutions	30
2.1.5	Laboratory equipment	30
2.2	Methods	32
2.2.1	Cell culture	32

2.2.1.1	General cell culture _____	32
2.2.1.2	Cryoconservation of cells _____	32
2.2.1.3	Thawing of cells _____	33
2.2.1.4	Determining the concentration of cells via cell counting ____	33
2.2.1.5	Seeding cells for infection _____	34
2.2.2	Virological methods _____	35
2.2.2.1	Infection of adherent cells with MeV-GFP _____	35
2.2.2.2	Infection of adherent cells with GLV-0b347 or T-VEC ____	36
2.2.2.3	Infection of non-adherent cell lines with MeV-GFP, GLV-0b347 or T-VEC _____	36
2.2.3	Methods of molecular treatment approaches _____	37
2.2.3.1	Treatment of cells with BET-inhibitors _____	37
2.2.4	Combinatory treatment of seeded cells with BET-inhibitors and oncolytic viruses _____	38
2.2.5	Analysis of cell viability _____	38
2.2.5.1	Transmitted light and fluorescence photography _____	38
2.2.5.2	Determining cell mass via Sulforhodamine B cytotoxicity assay _____	38
2.2.5.3	Determining cell mass via RealTime-Glo™ MT Cell Viability Assay _____	39
2.2.5.4	Determining cell proliferation under iBET treatment via xCELLigence® assay _____	39
2.2.6	Molecular biology methods _____	40
2.2.6.1	IFN-β ELISA _____	40
2.2.7	Statistical analysis _____	41
<b>3</b>	<b>Results _____</b>	<b>42</b>
3.1	Cell proliferation of NC cell lines HCC2429, 143100 and 690100____	42
3.2	Cytotoxic effect of oncolytic viruses on NC cell lines _____	43
3.2.1	Cytotoxic effect of MeV-GFP, GLV-0b347 and T-VEC on NC cell line HCC2429 _____	44
3.2.2	Cytotoxic effect of MeV-GFP, GLV-0b347 and T-VEC on NC cell line 143100 _____	46
3.2.3	Cytotoxic effect of MeV-GFP, GLV-0b347 and T-VEC on NC cell line 690100 _____	48
3.2.4	Comparison of the cytotoxic effect of different immunovirotherapeutics on adherent NC cell lines _____	50
3.2.5	First studies on semi-adherent BRD4-NUT cell line Ty-82 ____	52

3.2.6	First studies on floating BRD3-NUT cell line 10326	54
3.2.7	Comparison of SRB assay and RealTime-Glo™ assay	56
3.3	Effects of BET-inhibitors on proliferation and cell death of NC cell lines	57
3.3.1	Reaction of NC cell line HCC2429 to iBET treatment	58
3.3.1.1	IC <sub>50</sub> values for the iBET in NC cell line HCC2429	60
3.3.2	Reaction of NC cell line 143100 to iBET treatment	61
3.3.2.1	IC <sub>50</sub> values for the iBET in NC cell line 143100	63
3.3.3	Reaction of NC cell line 690100 to iBET treatment	64
3.3.3.1	IC <sub>50</sub> values for the iBET in NC cell line 143100	66
3.3.4	Comparison of the effects of iBET on the different tested NC cell lines	67
3.4	Combinatorial therapy of NC cell lines with immunovirotherapeutics and BET-inhibitors	70
3.4.1	Combinatorial iBET and OV treatment of the NC cell line HCC2429	71
3.4.2	Combinatorial iBET and OV treatment of the NC cell line 143100	73
3.4.3	Combinatorial iBET and OV treatment of the NC cell line 690100	75
3.4.4	Fluorescence imaging of MeV-GFP and GLV-0b347 infection under iBET treatment	77
3.5	Inhibition of T-VEC with Ganciclovir	79
3.6	IFN-β response of NC cell lines to OV treatment	80
<b>4</b>	<b>Discussion</b>	<b>83</b>
4.1	Oncolytic virotherapy - new hope for NC patients?	83
4.1.1	OV Treatment in BRD4-NUT cell lines leads to promising results	83
4.1.2	Does the translocation type influence the resistance against OVs?	86
4.1.3	Ganciclovir can impede a possible tumor lysis syndrome	88
4.2	iBET therapy in NC cell lines	89
4.3	Oncolytic viruses and iBET - combined therapy as an answer?	90
4.4	Perspectives	92
<b>5</b>	<b>Summary</b>	<b>94</b>
<b>6</b>	<b>Zusammenfassung</b>	<b>96</b>
<b>7</b>	<b>Appendix</b>	<b>98</b>

7.1	List of figures	98
7.2	List of tables	100
<b>8</b>	<b>Citations</b>	<b>101</b>
<b>9</b>	<b>Erklärung zum Eigenanteil</b>	<b>116</b>
<b>10</b>	<b>Veröffentlichungen</b>	<b>117</b>
<b>11</b>	<b>Danksagung</b>	<b>118</b>

## Abbreviations

ANOVA	<i>analysis of variance</i>
BET	<i>bromodomain and extraterminal domain</i>
CAR	<i>chimeric antigen receptor</i>
CD	<i>cluster of differentiation</i>
CDK	<i>cyclin-dependent kinase</i>
cDNA	<i>complementary DNA</i>
CPXV	<i>cowpox virus</i>
DMEM	<i>Dulbecco's Modified Eagle's Medium - high glucose</i>
DMSO	<i>Dimethylsulfoxide</i>
DNA	<i>deoxyribonucleic acid</i>
ds	<i>double stranded</i>
EV	<i>enveloped virus</i>
FCS	<i>Fetal calf serum</i>
GFP	<i>green fluorescent protein</i>
GM-CSF	<i>granulocyte-macrophage colony-stimulating factor</i>
HDACi	<i>histone deacetylase inhibitors</i>
HPV	<i>human papillomavirus</i>
HSV	<i>Herpes simplex virus</i>
HSV-1	<i>herpes simplex virus type 1</i>
iBET	<i>BET-inhibitors</i>
IC <sub>50</sub>	<i>half maximal inhibitory concentration</i>
ICP	<i>infected cell protein</i>
IFN	<i>interferon</i>
kb	<i>kilobase</i>
MeV	<i>measles virus</i>
MeV-Edm	<i>Edmonston vaccine strain measles virus</i>
MeV-GFP	<i>Measles vaccine virus expressing green fluorescent protein</i>
MeV-SCD	<i>suicide gene armed measles virus</i>
MHC	<i>major histocompatibility complex</i>
MOI	<i>multiplicity of infection</i>
MV	<i>mature virus</i>
NC	<i>NUT Carcinoma</i>
NET	<i>neuroendocrine tumor</i>
NMC	<i>NUT Midline Carcinoma</i>
NUT	<i>nuclear protein in testis</i>
OS	<i>overall survival</i>
OV	<i>oncolytic virus</i>
PBS	<i>phosphate buffered saline</i>
PFA	<i>formaldehyde</i>
PFS	<i>progression free survival</i>
PI3K	<i>phosphoinositide 3-kinases</i>
PILR	<i>paired immunoglobulin like-type 2 receptor</i>
PR	<i>partial response</i>
RLU	<i>relative luminescence unit</i>
RNA	<i>ribonucleic acid</i>
rpm	<i>revolutions per minute</i>
RPMI	<i>Roswell Park Memorial Institute</i>
SCD	<i>super-cytosine deaminase</i>
SD	<i>stable disease</i>

siRNA	<i>small interfering RNA</i>
SLAM	<i>signaling lymphocytic activation molecule</i>
SRB	<i>Sulforhodamine B</i>
SSPE	<i>subacute sclerosing panencephalitis</i>
TCA	<i>trichloroacetic acid</i>
TLR	<i>toll-like receptor</i>
TLS	<i>tumor lysis syndrome</i>
T-VEC	<i>Talimogene laherparepvec</i>
VACV	<i>vaccinia vaccine virus</i>
VARV	<i>variola virus</i>
WHO	<i>World Health Organization</i>
WV	<i>wrapped virus</i>



## 1 Introduction

### 1.1 NUT carcinoma

NUT carcinoma (NC), often still referred to as NUT midline carcinoma (NMC), is a rare but very aggressive tumor being genetically defined by a reciprocal translocation involving the *NUTM1* gene (NUT [“nuclear protein in testis”] midline carcinoma family member 1) on chromosome 15q14 (genenames.org). The first case of a t(15;19) (q15;p13) translocation was described in 1992 in Japan (Kuzume et al., 1992). After this, it took another eleven years until the driving pathomechanism of this tumor including the newly discovered cancer-associated genes *NUTM1* and *BRD4*, a gene located on chromosome 19p13.1, was clarified (French et al., 2003).

The incidence is not known yet, as too many cases are not being diagnosed correctly. A large screening of > 14,000 solid tumor samples found 26 cases with NUT rearrangement (Stevens et al., 2019). Comparing this number to the actual small number of published cases as well as the unequal geographic distribution of the cases (the vast majority is located in the U.S. (Bauer et al., 2012)), suggest, that NC is often undiagnosed due to lack of awareness.

Histologically, NC appears as a squamous cell carcinoma. But the degree of the differentiation varies between the different tumors: NC cases without squamous differentiation are described in the literature as well as cases with squamous differentiation (Bauer et al., 2012). Most commonly focal squamous differentiation and abrupt keratinization can be observed (Huang et al., 2019). In contrast to other poorly differentiated tumors NC shows monomorphic cells; the high number of mitotic figures seen in histological cuts correlates with the fast growth of NC (French, 2018).

Clinically, NC is known to be a rapidly growing tumor. People at any age can develop NC, but it mostly affects young patients; the median age of onset varies from 16 years (Bauer et al., 2012) to 23 years (Giridhar et al., 2018). The incidence in men and women is equal. Giridhar et al. as well as Bauer et al. also

found in their systematic patient reviews, that the tumor is most often located in the lung / thorax (35.3 % and 35.56 %, respectively) followed by the head and neck region (35 % and 24.21 %, respectively). As NC of the first described cases were all located in the body midline, the name “NUT midline carcinoma” was established. With higher number of cases the focus of the tumor location in the body midline was no longer maintainable, as case studies with NCs in varying organs and tissues were published. Therefore, the World Health Organization (WHO) officially renamed the NUT midline carcinoma to NUT carcinoma in 2015.

The large cohort studies also showed that the tumor is highly metastatic (31 % (no data for 22 %) and 59.3 %, respectively) and the 2-year overall survival (OS) is very low (9 % and 19 %, respectively) (Giridhar et al., 2018, Bauer et al., 2012). The OS of metastatic NCs arising from the thorax is found to be distinctly lower than in other NCs (Chau et al., 2020).

Now it is known that the driving protein of NCs is the protein encoded by the *NUTM1* gene, as *NUTM1* can be linked to different fusion partners, most often to *BRD4* (70%). Different fusion partners that were found are partly other genes coding for proteins of the bromodomain and extraterminal domain (BET) protein family, like *BRD3* on chromosome 9q34.2 (French et al., 2008). Further research led to the identification of a lot of more possible fusion partners, not belonging to the BET-protein family like *NSD3* (French et al., 2014) and *ZNF532* (Alekseyenko et al., 2017). Recently, more genetic translocations, which lead to the onset of NC were found: *BCORLI* and *MXD1* (Dickson et al., 2018), *CIC* (Schaefer et al., 2018) as well as *MGA* and *MXD4* (Stevens et al., 2019). The NUT fusions do not always lead to the formation of solid tumors, as *BRD9* and *ACIN1* were found to be fused to the NUT gene in acute lymphoblastic leukemia (ALL), in these cases not referred to as NUT carcinomas but “*NUTM1*-rearranged neoplasms” (Andersson et al., 2015). Even more possible gene fusions are listed in the Mitelman Database of Chromosome Aberrations and Gene Fusions in Cancer (Mitelman et al., 2020). The rearrangements not involving BET-proteins are referred to as “NUT variants” in the literature (Stevens et al., 2019).

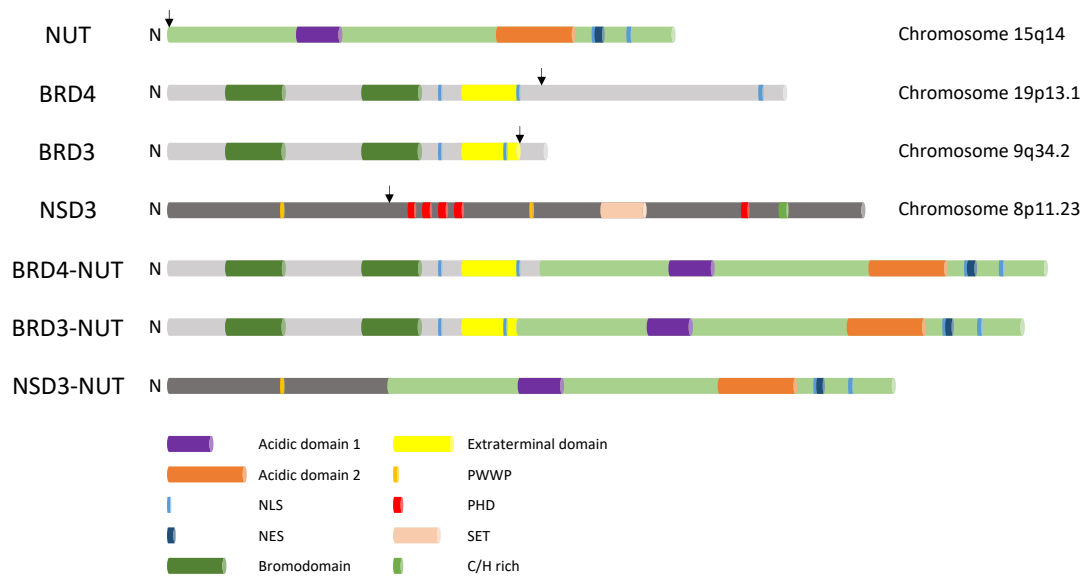


**Figure 1: Schematic display of the genomic structure of the most relevant NUT carcinoma fusion proteins.** In the first four rows, the structures of the normal proteins with the important regions highlighted are shown. The arrows indicate the breakpoints. In the last three rows the fusion proteins leading to the occurrence of the NC are displayed. NLS: Nuclear localization signal; NES: Nuclear export signal; PWWP: proline-tryptophan-tryptophan-proline domain; PHD: PHD zinc finger; SET: gene encoding for SET protein. Modified from (French, 2018).

### 1.1.1 Pathomechanism of the NUT carcinoma

The pathomechanism of NC is closely related to a higher transcription rate of the *MYC* Oncogene Locus, which is also known to play a leading part in the pathomechanism of other tumors like the diffuse large B-cell carcinoma (DLBCC) (Sun et al., 2017), and the *TP63* locus (Alekseyenko et al., 2017). Alekseyenko et al. and Reynoird et al. specified the underlying mechanism: The binding of the EP300 histone acetyltransferase to the NUT protein intensely enhances its activity (Reynoird et al., 2010) leading to the acetylation of whole topologically associated domains (TADs), which were named “*Megadomains*”. The bromodomains of the *BRD4-NUT* fusion protein bind to these “*Megadomains*”, which results in a higher transcription of the named loci (Alekseyenko et al., 2017). These findings fit with the results of Grayson et al., who demonstrated that by knocking down the *MYC* gene, cell growth is blocked and squamous differentiation increases (Grayson et al., 2014). When the *BRD4-NUT* fusion protein is knocked down by NUT specific siRNAs, this also induces a squamous differentiation (Schwartz et al., 2011) as well as autophagy (Sakamaki et al., 2017).

Most other proteins involved in less frequent cases of the NC interact with the BRD4 protein and therefore follow the same pathomechanism: For example, ZNF532 and the N-terminal side of NDS3 seem to act as a linker protein between NUT and BRD4 (Alekseyenko et al., 2017, French et al., 2014). The pathomechanism of other recently identified fusion proteins has not yet been elucidated.

As the *MYC* locus itself was found to be “undruggable” (Sun et al., 2017), different molecular approaches, trying to downregulate the transcription of *MYC*, play an important role in newly developed therapies.

### 1.1.2 *NUT* carcinoma cell lines

Table 1: Currently published *NUT* carcinoma cell lines

NC cell line	Translocation	Origin	Source / Literature
<b>HCC2429</b>	BRD4-NUT t(15;19) (q14;p13.1) (ex11:ex2)	Lung 34-year old female	(Haruki et al., 2005, Dang et al., 2000)
<b>143100</b>	BRD4-NUT t(15;19) (q14;p13.1) (ex14:ex2)		(Brägelmann et al., 2017)
<b>690100</b>	BRD4-NUT t(15;19) (q14;p13.1) (ex13:ex2)		(Brägelmann et al., 2017)
<b>Ty-82</b>	BRD4-NUT	Thymus 22-year old female	JCRB Cell Bank (Kuzume et al., 1992)
<b>10326</b>	BRD3-NUT		(French et al., 2008)
10-15	BRD4-NUT t(15;19) (q15;p13) (ex15:ex2)		(Grayson et al., 2014, Wang et al., 2014)
14169	BRD4-NUT t(15;19) (q15;p13) (ex15:ex2)		(Wang et al., 2014)

TC-797	t(11;15;19) (p15;q12;p13.3)	Thymus 15-year old male	(Toretsky et al., 2003)
1221	NSD3-NUT		(French et al., 2014)
00134	BRD4-NUT		(Schwartz et al., 2011, French et al., 2001)
P896-CL	BRD4-NUT (ex15;ex2)	Sinonasal 14-year old female	(Stirnweiss et al., 2017, Stirnweiss et al., 2015)
PER-403	BRD4-NUT t(15;19) (p12;q13)	Intrathoracic 11-year old female	(Kees et al., 1991)
PER-624	BRD4-NUT t(6;19) (q13;p13.1) (ex15;ex2)	Lung 16-year old female	(Beesley et al., 2014, Thompson-Wicking et al., 2013)
PER-704	BRD4-NUT t(15;19) (q14;p13.1) (ex15;ex2)	Larynx 8-year old male	(Beesley et al., 2014)
RPMI2650	BRD4-NUT	Nasal septum 52-year old male	DSMZ - German Collection of Micro- organisms and Cell Cultures GmbH  (Stirnweiss et al., 2017, Klijn et al., 2015, Moorhead, 1965)
11060	BRD4-NUT	Mediastinum 29-year old	(Filippakopoulos et al., 2010)
8645		10-year old male	(Schwartz et al., 2011)
24335	ZNF532-NUT 47, XX, +7 t(15;18) (q14;q23)	Established from pleural fluid female	(Alekseyenko et al., 2017)

	t(15;19) (q15;p13)	Thymus 22-year old female	(French et al., 2001, Kubonishi et al., 1991)
	t(15;19) (q13;p13.1)	Epiglottis 13-year old female	(Vargas et al., 2001, French et al., 2001, Lee et al., 1993)

*Cell lines that have been worked with in this thesis are marked with grey background.*

### **1.1.3 Therapy of the NUT carcinoma**

As a result of a missing specialized therapy for NC the standard approach still is a multimodal approach with a surgical resection before or after an (neo-)adjuvant radiochemotherapy. Studies comparing the effect of those approaches come to different results about the benefits: One study found initial surgery being the only therapy that increases the overall survival significantly (Chau et al., 2016). On the contrary Giridhar et al. found a significant increase of the OS after radiotherapy but not after surgery, whereas Bauer et al. found both, surgery and initial radiotherapy, leading to a significant benefit of the OS (Giridhar et al., 2018, Bauer et al., 2012). But as none of these therapies was able to cure patients and not even led to a long-lasting progression free survival (PFS) in most cases, many other approaches are being tested. These therapies mostly try to intervene in the epigenetic mechanism of the tumor.

One approach to attack the epigenetic changes is the use of BET inhibitors (iBET). Different iBET are already tested in phase-I-clinical studies and showed promising results for the treatment of NC (see also 1.3.1). In addition, other substances target the molecular pathomechanism of the tumor as well, like histone deacetylase inhibitors (HDACi) (Schwartz et al., 2011, Maher et al., 2015) or aurora kinase inhibitors (iAURK) (Stirnweiss et al., 2017). Also combining different therapies, like HDACi and phosphoinositide 3-kinases (PI3K) seems favorable (Sun et al., 2017). Inhibition of the cyclin-dependent kinase (CDK) 9, which is needed by BRD4 to perform the transcriptional elongation, with Flavopiridol was successfully tested as another treatment option for NC *in vitro* as well as *in vivo* (Beesley et al., 2014).

About the possible response of NC to immunotherapy the present research is insufficient: Unfortunately, no surface protein being ubiquitously and specifically expressed on NC cells has been detected yet, making chimeric antigen receptor (CAR) T-cell therapy, a very potent therapy option for other tumors, impossible. Another innovative and not yet investigated approach to target NC without knowledge and need of expressed surface proteins is the oncolytic virotherapy.

## **1.2 Oncolytic Virotherapy**

Oncolytic virotherapy is a relatively new approach in the area of immunotherapy. Oncolytic viruses, which are used as the therapeutic, are modified to meet the demand only to replicate in tumor cells and lead to their lysis, while normal cells are able to cope with the virus infection. The following chapter will give an overview about the history of oncolytic virotherapy and its principles along with examples of oncolytic viruses and their usage in malignant neoplasms, focusing on the viruses being investigated in this thesis.

### **1.2.1 History**

The idea to use viruses as therapeutics occurred when a remission of malignant diseases was observed during a virus infection. This was first documented in the beginning of the 20<sup>th</sup> century (Dock, 1904), even before viruses were first photographed under the microscope (Kausche et al., 1939). In the following years different studies were published, which showed that the physical well-being of people suffering from malignancies can be improved by viral infections transmitted through body fluids. For example, the effect of APC (adenoidal-pharyngeal-conjunctival) viruses on cervix carcinoma was tested (Smith et al., 1956) and viral hepatitis was found to cause remission of Hodgkin's disease (Hoster et al., 1949). Early on, also measles virus was included in these studies and good results in Hodgkin's disease (Zygiert, 1971, Taqi et al., 1981) and leukemia (Pasquinucci, 1971) were observed.

At this time, scientists still had to deal with a lot of problems as it was not yet possible to genetically engineer the viruses to attenuate their virulence. Therefore, it was not possible to control the virus infection and keep the viral replication in the tumor cells. As a result, a lot of patients were suffering heavily from side

effects of the virus infection (Kelly and Russell, 2007). Furthermore, at the beginning neither *ex vivo* human cell culture was available, nor animal models were used. So, the excitement around the topic decreased again.

The improvement of technical possibilities made it easier to understand the impact of viral infection on tumor cells: Levaditi and Nicolau were one of the first using mouse and rat tumor models to show a decrease in tumor masses of various tumor entities after treatment with a vaccinia virus (Levaditi and Nicolau, 1922). Further on, cultivation of isolated tissue cells was established *in vitro* successfully, which also led to a lot of new knowledge in oncolytic virotherapy due to a better understanding of the oncolytic mechanisms of each virus (Sanford et al., 1948).

Another critical step was accomplished in 1991: It has been shown in mouse models, that through genetic modification, a HSV virus selectively replicated in fast proliferating cells, while not being able to do so in non-dividing cells or the human nervous system (Martuza et al., 1991).

These findings gave oncolytic virotherapy a much larger potential. In the following, more viruses were genetically modified to either lower their pathogenicity, to enhance their oncolytic potential or their tumor cell specificity (Kelly and Russell, 2007). A good overview about viruses used for oncolytic therapy is given in the review from 2017 (Lawler et al., 2017).

The first oncolytic virus approved by a governmental agency was the adenovirus rAd-p53, which was approved by the State Food and Drug Administration of China (SFDA) for the treatment of head and neck squamous cell carcinoma in 2003 (Peng, 2005). Shortly afterwards, a second adenovirus, H101, got approval in China for squamous cell carcinoma of head and neck after a phase-III study showed a response rate of 79 % with viral treatment and only 40 % with cisplatin and 5-FU therapy (Xia et al., 2004, Garber, 2006). In the EU and USA, it took another 10 years until the first oncolytic virus, the herpes simplex virus *Talimogene laherparepvec* (T-VEC) was approved in 2015 by the European Medical Agency (EMA) and the U.S. Food and Drug Administration (FDA) for the treatment of melanoma (Greig, 2016) (see 1.2.5.2).



### **1.2.2 Principles of oncolytic virotherapy**

As stated in the introduction of this chapter, the aim of oncolytic virotherapy is the use of naturally occurring or genetically optimized viruses to specifically attack and kill tumor cells. This is possible due to the genetic and epigenetic transformations in the malignant cells: As tumor cells develop mechanisms to hide tumor-specific antigens from the immune system, they are able to escape the immune effector T-cells, which depend on these antigens to distinguish between endogenous cells and malignant cells. These T-cells normally also attack virus infected cells to prevent spreading of the infection. Furthermore, in tumor cells often other pathways for immune response activation are mutated, like the interferon (IFN)  $\beta$  (belonging to the group of type I IFN) pathway (Berchtold et al., 2013). In healthy cells the viral genome gets recognized by pattern recognition receptors (PRRs), like cytosolic RIG-I-like receptors (RLRs) or endosomal toll-like receptors (TLR3,7,8) for viral RNA and  $\gamma$ -activation sequence (cGAS) and TLR9 for viral DNA. This recognition leads to an activation of downstream signaling cascades ending in the production of proinflammatory cytokines and IFN type I (Matz et al., 2019). The IFN then activates neighboring cells, which react with inhibition of RNA translation or activation of T-cell response to contain the viral infection (Samuel, 2001).

Hence, tumor cells offer an optimal room for viruses to replicate. This excessive replication finally leads to bursting of the tumor cell, when it can no longer cope with the high viral load or is killed by toxic viral proteins (Kirn, 1996). The bursting of the tumor cell triggers three mechanisms that are characteristic for oncolytic virotherapy: Firstly, a mass of viral particles is released, which now can infect new tumor cells. Secondly, some viruses are able to change the tumor micro-environment by disruption of the tumoral blood vessels (Breitbach et al., 2013). And thirdly, also tumor-specific antigens are released, that are hidden by intact tumor cells. These antigens can now be recognized by the immune system, making a specific immune response possible and leading to *in situ* tumor vaccination (Toda et al., 1999, Savage et al., 1986). Many different mechanisms, either occurring naturally or being enhanced by genomic engineering, secure that oncolytic viruses can replicate predominantly in tumor cells. As normal cells react

with IFN production or induction of apoptosis, viral spreading even is obtained in the case of normal cell infection (Russell and Peng, 2007). Thus, viral infection is contained as soon as the tumor burden is successfully destroyed.

To archive this optimal course of virotherapy, oncolytic viruses have to meet some criteria: They need to replicate specifically in tumor cells and have a high oncolytic potential to lead to cell lysis, while still not effecting normal tissue cells. This is important to keep side effects of the therapy to a minimum. Possible infections should still be characterized well so they can be treated in case of severe sickness. Furthermore, oncolytic viruses need to be genetically stable to minimize possible virus mutation. Even though non-human viruses seem to be ideal, as they often are not able to replicate in human tissue, they must be used with great care, to prevent their evolvement to a human pathogen (Kelly and Russell, 2007). As wild-type viruses not necessarily meet all of these criteria, most viruses used for oncolytic therapy, are genetically engineered, including deletion or insertion of certain genes. With this engineering, it is possible to specifically adapt the characteristics of the viruses: Some genes allow the detection *in vitro* / *in vivo* (e.g. GFP) or the systemic immune response (e.g. GM-CSF) or heighten their oncolytic capacity (e.g. SCD).

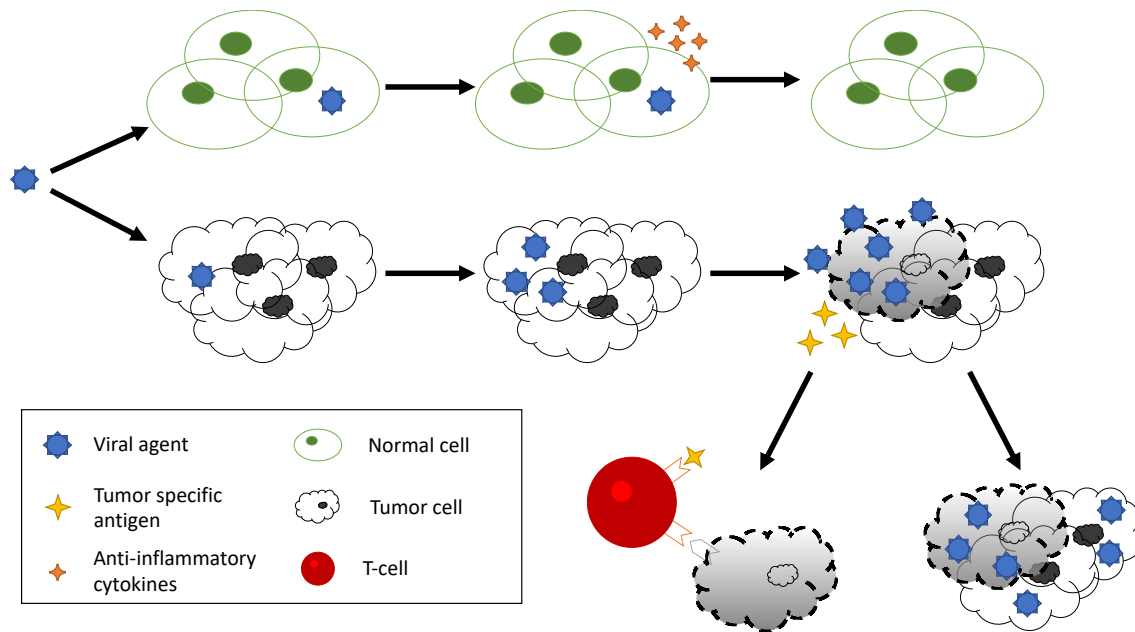


Figure 2: Principle of oncolytic virotherapy.

The viral agent infects tumor cells but also normal cells. Due to the intact immune response of normal cells, they are able to inhibit the spreading of the virus, e.g. through secreting anti-inflammatory cytokines as IFN- $\beta$ . Tumor cells however can't cope with the viral infection, so the virus starts replicating. As the viral load increases it kills the tumor cell and viral particles are released together with tumor specific antigens. These viral particles now can infect other tumor cells, while tumor specific antigens get recognized by T-cells, which now can also attack the tumor cells.

### 1.2.3 Measles virus

Measles virus (MeV) is classified in the genus of the *Morbillivirus* of the family of the *Paramyxoviruses*. Genetically, it is a negative sense, single stranded [ss (-)] RNA-virus. All measles viruses belong to the same serotype but can be differentiated into 24 genotypes, which is important for the differentiation of wild type measles and vaccine measles strains (rki.de, 2014).

Measles disease is highly infectious: the contagiousity index is close to 100 % (rki.de, 2014) and also the manifestation rate of 95-98 % is one of the highest of all viruses (Hof and Schlüter, 2019). Clinical symptoms of the acute disease include high fever, conjunctivitis, maculopapular exanthema and respiratory symptoms (Hof and Schlüter, 2019). While the lethality of the acute symptoms is rather low, the possible complications can be very dangerous. These complications often are bacterial superinfections causing an otitis media or pneumonia but can also lead to a postinfectious encephalitis (lethal in 10-20 % of the cases) or subacute sclerosing panencephalitis (SSPE). SSPE is very rare

but always leads to the death of the patient. For this complication the risk of getting sick is five times higher for young children (20-60 cases /100,000 measles disease cases) than for grown up people (4-11 cases / 100,000 measles disease cases) (rki.de, 2014).

### 1.2.3.1 Biology of the oncolytic measles vaccine virus MeV-GFP

MeV consists of six genes coding for eight proteins of which six are found in the virion (**Figure 3**): hemagglutinin (H) and fusion protein (F), two surface proteins whose function is described in detail below; matrix protein (M), which is located directly under the envelope and interacts with the ribonucleocapsid; nucleocapsid protein (N), which is wrapped around the RNA strands; large protein (L), a RNA-polymerase; and phosphoprotein (P), which is necessary for the polymerase function (Griffin, 2018).

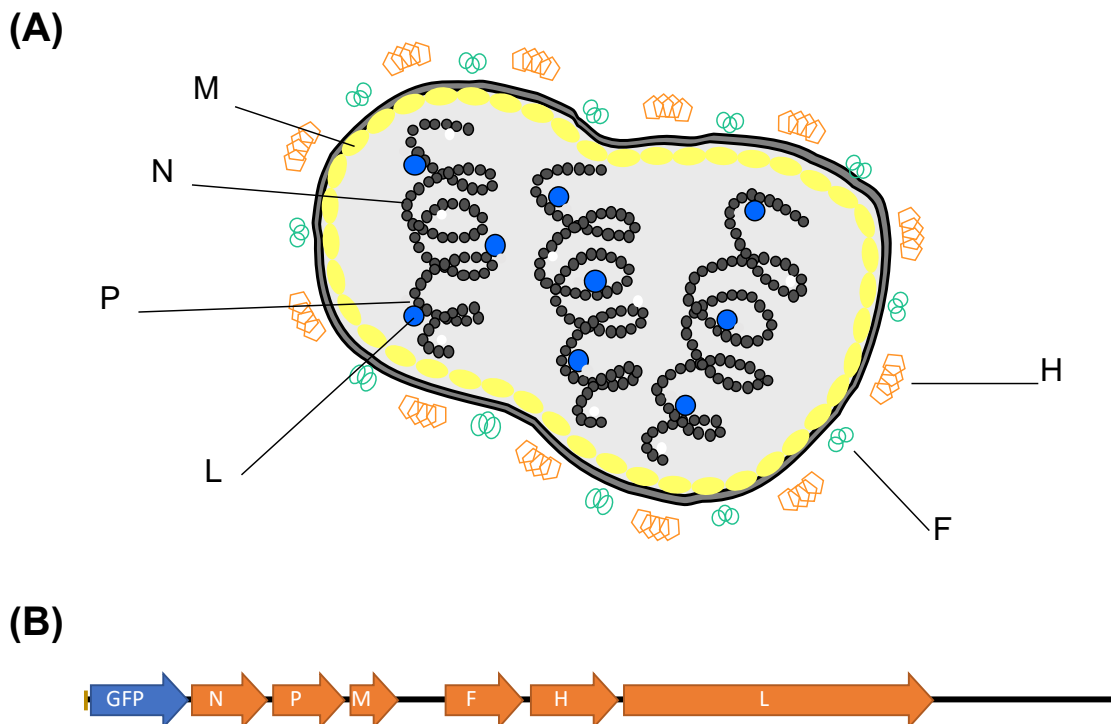


Figure 3: Structure of the measles virus and its genome.

(A) Schematic display of the measles virion with its six proteins: hemagglutinin (H), fusion protein (F), matrix protein (M), nucleocapsid protein (N), large protein (L) and phosphoprotein (P). (B) Schematic display of the genome of MeV-GFP: The sequence coding for the GFP is inserted in the normal measles virus genome at genome position one. © Guy Ungerechts, NCT Heidelberg

The two surface proteins H and F are responsible for entering of the virus into the host cell. H can bind to three different cell receptors. In 1993 the cluster of

differentiation (CD) 46 (membrane cofactor protein [MCP]) molecule was determined as a receptor for measles vaccine strains (Dörig et al., 1993, Naniche et al., 1993), but later it was found that this is not valid for the wild-type strains (Buckland and Wild, 1997). CD46, a regulatory protein of the complement system, is expressed on nearly all cell types excluding erythrocytes (Johnstone et al., 1993, Liszewski et al., 1991). In 2000 the signaling lymphocytic activation molecule (SLAM, also named CD150) was found to be another possible binding site for measles vaccine strains as well as wild type measles strains (Tatsuo et al., 2000). But it is used more efficient by the wild-type strains (Schneider et al., 2002). The binding to SLAM results in the lymphotropism of measles virus, as it is mostly expressed on lymphocytes, monocytes and dendritic cells (Aref et al., 2016). In 2011 a third receptor, Nectin-4 / poliovirus-receptor-like-4 (PRVL4), was identified allowing vaccine strains as well as wild-type strains to enter the host cell. This receptor is located on epithelial cells, e.g. of the respiratory tract, explaining the respiratory symptoms that can be caused by a measles infection. This binding allows the F protein to fuse the viral lipid shell with the cell membrane, after which the viral genome and internal proteins can enter the host cell (Mühlebach et al., 2011, Noyce et al., 2011).

The distinction between the entry mechanisms of wild-type and vaccine measles strains is important because the MeV-GFP virus used in this thesis is a derivate from the Schwarz vaccine strain (Berchtold et al., 2013), which itself originates from the Edmonston vaccine strain (MeV-Edm) (Rota et al., 1994). Therefore, it is able to enter host cells through all three named receptors. Most interesting for the usage of the virus in immunotherapy, however, is the entry via CD46, since this molecule is overexpressed on many tumor cells. This is reasonable because it blocks the activation of C3 in the cascade of the complement system (Fishelson et al., 2003) and thus helps the tumor to evade the immune system. But also, the entry via Nectin-4 could be used for oncolytic therapy as it is often overexpressed in adenocarcinomas (Noyce et al., 2011). The cytotoxic effect of MeV-Edm viruses is highly induced by the ability of forming syncytia with 50-100 neighboring cells, which are then all led into apoptosis (Galanis, 2010).

For the development of MeV-GFP only one adaptation to the MeV-Edm strain had been made: GFP (green fluorescent protein) was inserted into the viral cDNA by insertion of an additional transcription unit (ATU) at genome position one (Berchtold et al., 2013).

### **1.2.3.2 Immunotherapy with oncolytic measles viruses**

Even though none of the currently investigated oncolytic measles viruses achieved official approval by any governmental agency so far, many *in vitro* and *in vivo* trials showed promising results.

In a comprehensive *in vitro* analysis of the efficiency of suicide gene armed measles virus (MeV-SCD) using the NCI-60 tumor panel, 27 out of 54 tested cell lines proved to be susceptible (< 50 % remnant tumor cell mass in comparison to control at MOI 1) while only six cell lines were rated resistant (remnant tumor cell mass > 75 %). When the prodrug 5-FU, which gets converted to the chemotherapeutic 5-FU by the virus-encoded protein super-cytosine deaminase (SCD), was added to all MeV-SCD infected cell lines the remnant cell mass dropped to < 50% (Noll et al., 2013).

Other measles viruses also being derivatives of the MeV-Edm strain were already tested in clinical studies. MeV-NIS, expressing the human sodium iodide symporter allowing non-invasive monitoring of the virus distribution and leading to a higher viral proliferation rate and thus to higher viral titers, was tested for the treatment of ovarian cancer (Galanis et al., 2015) as well as multiple myeloma (Dispenzieri et al., 2017). The MeV-CEA virus with an inserted gene coding for the soluble extracellular domain of human carcinoembryonic antigen (CEA) allowing quantitative monitoring of viral gene expression has also shown good tolerability and biological activity in ovarian cancer in a phase-I study (Galanis et al., 2010). In another phase-I study the Edm-Zagreb vaccine strain was tested for cutaneous T-cell lymphoma (CTCL) and 5 out of 6 lesions injected showed regression (Heinzerling et al., 2005).

### **1.2.4 The variola virus and the vaccinia virus**

The history of the variola virus (VARV), which caused the smallpox disease, is thought to be dated back till 10,000 BC with the first cases in north-eastern Africa

(Barquet and Domingo, 1997). The disease spread globally and caused 100,000s of deaths in the 18<sup>th</sup> century. As it was observed that survivors of the smallpox disease afterwards became immune to the disease, variolation came into the focus of interest. In the beginning this was performed with infective material of affected humans. Edward Jenner, who was convinced that vaccination with cowpox also protected against the human smallpox disease, conducted the first successful vaccination with the cowpox virus CPXV in 1796 (Riedel, 2005). This success started an era of vaccination, leading to the eradication of smallpox in Europe and North America in the 1950s. In 1976 the World Health Organization started a campaign with the aim of the worldwide eradication of the disease, which was finally announced by a report of the WHO in 1980 (WHO, 1980). For this campaign the vaccinia vaccine virus VACV, whose origin is still unknown but is thought to be either a derivate of VARV, of CPXV or a hybrid of both, was used (Sánchez-Sampedro et al., 2015).

Clinically, the variola virus showed a typical exanthem affecting the whole body, where all efflorescences developed simultaneously from maculae, over papulae and vesiculae to crustae (Hof and Schlüter, 2019). The vaccinia virus rarely showed adverse reactions after vaccination. Noticed symptoms include harmless local skin reactions, serious events like general vaccinia as well as life-threatening postvaccinal encephalitis (Cono et al., 2003).

With diameters of 100-300 nm the smallpox virus is one of the largest viruses known. It has a double stranded [ds (±)] DNA genome. Depending on the section of the replication cycle the *Poxviridae* occur in three different forms: the extracellular enveloped virus (EV) with two lipid layers, the mature viruses (MV) with one lipid layer and the wrapped viruses (WV) with three lipid layers. Within the most inner lipid layer all forms look the same: Two lateral bodies press the core into a dumbbell shape. The core coats the genome as well as virus specific enzymes and regulatory proteins (Hof and Schlüter, 2019).

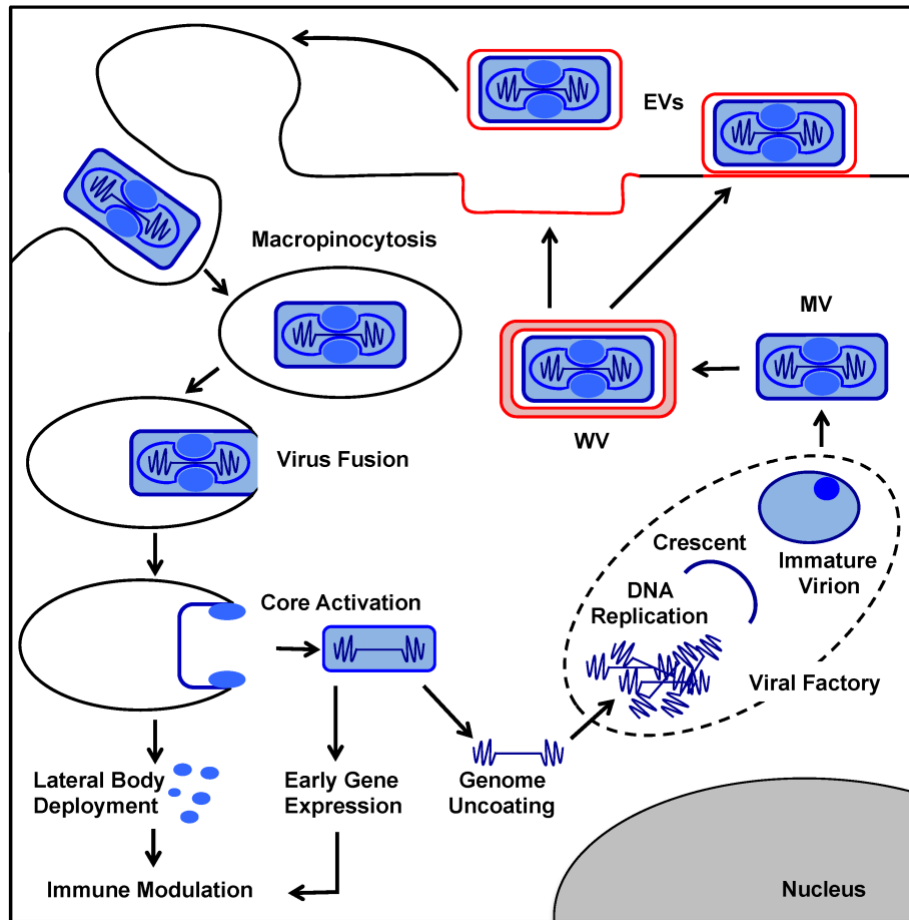


Figure 4: Replication cycle of Poxviridae.

WV: wrapped virus; EV: enveloped virus; MV: mature virus. Image taken from (Bidgood and Mercer, 2015)

The replication cycle of the *Poxviridae* is a complex process and only takes place in the cytoplasm of the host cell, in contrast to most other viruses, which replicate in the nucleus of the host cell. This replication cycle is described in detail by Bidgood and Mercer: The poxvirus invades the host cell via macropinocytosis. Binding of the *Poxviridae* to the host cell membrane is mostly mediated by glycosaminoglycans (GAGs), but also binding to heparan sulphate and to chondroitin sulphate has been described to initiate virus uptake (Schmidt et al., 2012). The virus particle then fuses with the membrane of the macropinosome and releases its core. As the lateral bodies detach from the core, it gets activated and the transcription and translation of viral proteins, replication of the viral genome and production of crescent-shaped membrane parts starts in so-called “viral factories”. These products get assembled to a new MV. The MVs exit the host cell via lysis after approximately 72 h. To achieve a faster spreading of the viral



particles, WVs can be formed by wrapping two additional trans-Golgi or endosomal membranes around the MV. This WV with a triple membrane now can leave the host cell after 6 hours via exocytosis, forming EVs (Bidgood and Mercer, 2015).

Chen et al. state eight reasons, why VACV is suitable for oncolytic virotherapy: “(a) It has a short, well-characterized life cycle and spreads very rapidly from cell to cell; (b) it is highly cytolytic for a broad range of tumor cell types; (c) it has a large insertion capacity (> 25 kb) for the expression of exogenous genes; (d) it is genetically very stable; (e) it enables large-scale production of high levels of infectious viruses; (f) it does not cause any known diseases in humans; (g) it does not integrate into the host genome; and (h) it was used as smallpox vaccine in millions of people and thus has well-documented side effects” (Chen et al., 2009), that in case can be treated (Cono et al., 2003).

#### 1.2.4.1 Biology of the vaccinia virus GLV-0b347

VACV as well as VARV itself are part of the virus family of *Chordopoxviridae* and the genus of *Orthopoxviridae*. The viral construct GLV-0b347 used in this thesis is a derivative of VACV, more precisely of the Western Reserve strain. This strain is known to be the most virulent strain of VACV (Zeh et al., 2015) and naturally selective for tumor cells (Mejías-Pérez et al., 2018).

The only genomic change made to derive GLV-0b347 from the Western Reserve strain was the insertion of the fluorophore turboFP635 into the non-essential thymidine kinase J2R gene locus (**Figure 3**). This leads to deletional mutation of J2R, making the virus less pathogenic (Buller et al., 1985) and more specific for tumor cells (Puhlmann et al., 2000).

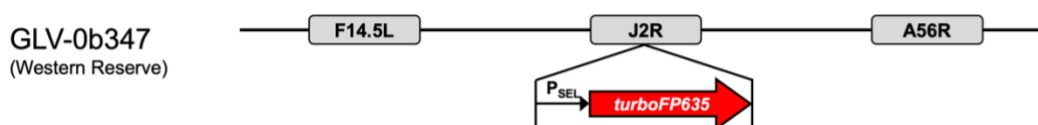


Figure 5: Genome of the GLV-0b347 virus.

The fluorophore turboFP635 is a far-red mutant of the red fluorescent protein from sea anemone *Entacmaea quadricolor* and was inserted into the thymidine kinase J2R gene (non-essential gene encoding thymidine kinase (TK)) of GLV-0b347. This leads to a red fluorescent signal of virus-infected cells with excitation/emission maxima of 588/635 nm. Image taken from: Oral abstract at SITC 27<sup>th</sup> Annual Meeting 2012: Chen et al.

### **1.2.4.2 Immunotherapy with oncolytic vaccinia viruses**

As for measles viruses, none of the engineered vaccinia viruses has attained approval so far, but again different clinical studies show the potential the virus might play in future for the treatment of several cancer types.

A promising candidate for a soon approval is *Pexastimogene Devacirepvec* (Pexa-Vec; JX-594). This oncolytic vaccinia virus is derived from the Wyeth vaccine strain (Heo et al., 2013), in which the viral thymidine kinase gene has been disrupted and genes coding for human GM-CSF and  $\beta$ -galactosidase have been inserted. It showed great clinical potential in phase-II studies in hepatocellular, colorectal and renal cell carcinoma (Breitbach et al., 2015). By now, the PHOCUS phase-III study is comparing the efficiency of JX-594 given in addition to the sorafenib to sorafenib alone, which is the standard treatment (NCT02562755).

First phase-I studies with the vaccinia virus GL-ONC1 (GLV-1h68) as a treatment for peritoneal carcinoma or head and neck carcinoma also showed good toleration and in-patient replication and oncolysis could be proven, making further phase-II studies feasible (Lauer et al., 2018, Mell et al., 2017). GL-ONC1 is derived from the Lister strain of vaccinia virus. Three genes were inserted (coding for Ruc-GFP,  $\beta$ -glucuronidase and  $\beta$ -galactosidase) for attenuation, higher tumor-specificity and easier monitoring. JX-929 (vvDD-CDSR), a virus derived from the Western Reserve strain, like the virus used in this thesis, showed good tumor specificity and replication in a first clinical study (Zeh et al., 2015).

### **1.2.5 The herpes simplex virus**

The herpes simplex virus type 1 (HSV-1) belongs to the family of the *Alphaherpesviridae*. It has a double stranded [ds ( $\pm$ )] DNA genome (Hof and Schlüter, 2019). HSV-1 is spread globally and has a worldwide prevalence of 67 % in under 50-year old persons (Who.int, 2017). As the virus is highly contagious and is transmitted through close physical contact, the initial infection often occurs in the childhood. The virus enters the body through small lesions in the epithelium, most often orally. In contrast to measles virus the manifestation rate of HSV-1 is very low: Only 10 % of the primary infections develop clinical

symptoms. These typically include blisters and ulcers around the mouth (*herpes labialis*). Infected children more often suffer from *stomatitis aphthosa* including a pharyngitis. Seldom, the HSV-1 virus also leads to *herpes genitalis* making the infection of neonates possible. This so-called *herpes neonatorum* occurs mostly when a woman has her primary infection with *herpes genitalis* during the birth. It is a rare disease, affecting 10 out of 100,000 neonates, but can have severe consequences as it can lead to neurologic disabilities and even death (Hof and Schlüter, 2019, Who.int, 2017).

After primary infection, the virus penetrates neurons and stays in the *ganglion trigeminale* in a latency stadium. Therefore, an HSV-1 infection usually lasts lifelong and it can come to a recurrence at any time.

The genome of the herpes simplex virus is located around the protein-core and enclosed by the capsid. The capsid itself is surrounded by the tegument, whose proteins have mostly regulatory functions, as controlling the capsid channels, and also are important during virus infection (Shen and Nemunaitis, 2006). A bilipid layer forms the outer envelope including several glycoproteins (Kukhanova et al., 2014), five of which playing an important role during virus invasion into the host cell (Akhtar and Shukla, 2009). HSV-1 is able to bind to multiple different receptors: Nectin-1 and Nectin-2, 3-O sulphated heparan sulphate, and the herpes entry mediator (HVEM). All receptors are recognized by the viral glycoprotein gD and the paired immunoglobulin like-type 2 receptor (PILR), which is bound to glycoprotein gB. Nectin-1 (Galen et al., 2006) and Nectin-2 (Lopez et al., 2000) are expressed on epithelial cells, fibroblasts and neurons, HVEM belongs to the tumor necrosis factor (TNF) receptor family and can also be found on epithelial cells and fibroblasts but also on leucocytes, making it the main entry receptor of HSV-1 into T-cells (Spear, 2004). PILR is also mainly expressed on immune cells including monocytes, dendritic cells and granulocytes (Fournier et al., 2000). 3-O sulphated heparan sulphate results from additional sulphate groups being added to heparan sulphate by D-glucosaminyl 3-O-sulfotransferases, which are expressed on multiple cell types (Shukla et al., 1999).

### **1.2.5.1 Biology of the modified herpes simplex virus type I T-VEC**

*Talimogene laherparepvec* (T-VEC, trademark name: Imlygic® of Amgen®, Inc) was developed from the JS-1 strain of HSV-1, originally originating from a cold sore (Kohlhapp and Kaufman, 2016).

The oncolytic virus takes benefit of the suppression of protein kinase K (PRK) and type I interferon, which is commonly seen in cancer cells. The suppression of both pathways, which are usually upregulated in healthy cells during a virus infection, leads to a selective infection of tumor cells (Conry et al., 2018). Additionally, Conry et al. stated the four different genome adaptations, which were made to make the virus more tumor specific and heighten the oncolytic potential. The deletion of both copies of the infected cell protein (ICP) 34.5 reduces the neurovirulence of HSV-1, since only cells that suppress PRK by other routes become infected and can suppress latency. The deletion of ICP 47 leads to a higher tumor antigen presentation via MHC class I, making tumor cells more visible for the immune system. Also infected non-tumor cells can be detected easier by the immune system avoiding viral spreading in healthy cells. This deletion translocated the downstream herpes unique short 11 gene (US 11) under an early promoter enhancing the lytic activity of the virus. Finally, two copies of the human granulocyte-macrophage colony-stimulating factor (GM-CSF) gene were inserted into the genomic locus where ICP 34.5 was deleted. By this insertion a systemic anti-tumoral immune response can be achieved, while without GM-CSF only the injected tumor itself showed a response (Liu et al., 2003).

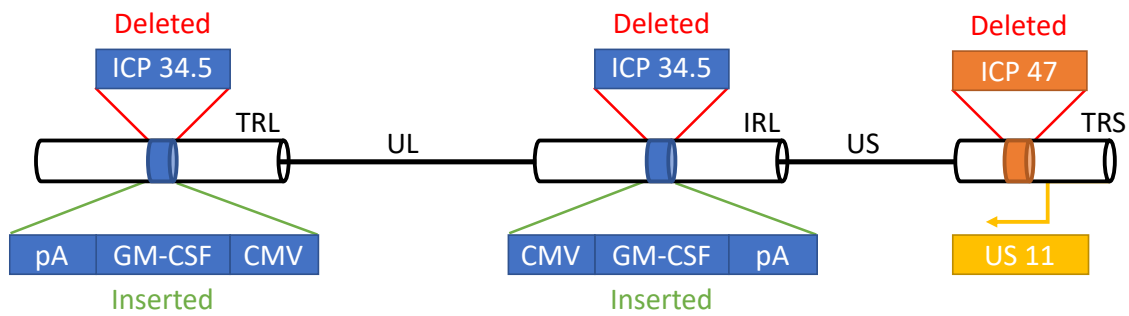


Figure 6: Genomic structure of *Talimogene laherparepvec*.

The two copies of infected cell protein (ICP) 34.5 were replaced by human granulocyte-macrophage colony-stimulating factor (GM-CSF) to achieve a systemic anti-tumoral immune response. Expression of GM-CSF is attained by intermediate early promoters of cytomegalovirus (CMV) and polyadenylation signal (pA). ICP 47 was deleted for higher tumor antigen expression via MHC I, which leads to an earlier expression of US11. UL: Unique long sequence; US: Unique short sequence; TRL: terminally repeated long sequence; IRL: internally repeated long sequence; TRS: terminally repeated short sequence; Modified from (Eissa et al., 2017).

The tumor lysis syndrome (TLS) is a severe adverse effect of oncological treatment. It can be caused by a too aggressive treatment regimen, leading to high number of apoptotic cells in a very short time. These cells release too many intracellular minerals, as potassium, phosphorus and nucleic acids, to be eliminated by the kidneys, so the balance of minerals in the body gets out of order. Clinically, the TLS often leads to kidney failure, arrhythmias and neuromuscular irritability (Howard et al., 2011). As these conditions are very lethal, a preventive therapy for patients with a high risk of developing an TLS is important (Adeyinka and Bashir, 2020). As T-VEC proved to be a very potent oncolytic virus a TLS seems possible and therefore an antidote should be available. Ganciclovir proved to be a possible candidate for inhibiting T-VEC function in neuroendocrine tumor (NET) cell lines (Kloker et al., 2019). Ganciclovir is a nucleoside analog of guanine, which is incorporated into the elongating viral DNA and therefore inhibits the replication of the virus by slowing down the synthesis of viral DNA (Crumpacker, 1996).

### 1.2.5.2 Immunotherapy with T-VEC

T-VEC has been approved in the USA and the EU for the treatment of advanced metastatic melanoma, which cannot be removed by surgery. Its clinical efficiency and safety have been proven in many clinical phase-I, -II and -III trials. A phase-I study showed good toleration and safe administration even when applied

intratumoral every 2-3 weeks and also could achieve a stabilization of the tumor (Hu et al., 2006). These results led to further investigations in a phase-II study, where patients with advanced melanoma were treated successfully with intratumoral injections (Senzer et al., 2009). The phase-III study finally leading to the approval was the randomized *OPTiM* study, where the efficiency of intratumoral T-VEC injection was compared to subcutaneous GM-CSF injection. The study could prove, that T-VEC is well tolerated, had an higher durable response rate and a longer median OS (Andtbacka et al., 2013).

By now clinical studies could also show, that therapy approaches combining intratumorally injected T-VEC with immune checkpoint inhibitors, like anti-CTLA-4 (Ipilimumab) or anti-PD-1 (Pembrolizumab), result in better response rates than either of one given alone (Chesney et al., 2018, Ribas et al., 2017).

### **1.3 The bromodomain and extraterminal domain proteins**

Bromodomain and extraterminal domain (BET) proteins are characterized by the existence of two tandem bromodomains, an extraterminal domain as well as a C-terminal domain (Stathis and Bertoni, 2018). Members of this family include the Bromodomain-containing proteins BRD2, BRD3, BRD4 and the Bromodomain testis-specific protein BRDT.

The first BET protein was found in 1986 in a drosophila encoded by the gen *fs(1)h* (Digan et al., 1986). A few years later a similar gene was found, now known as *BRD2*, encoding for a nuclear kinase in a human cell line which is thought to play an important role in cell growth control (French, 2016, Denis and Green, 1996).

For NUT carcinoma especially the BRD4 protein plays an important role, as in around 70 % of all known NC cases the NUT protein forms a fusion protein with BRD4. Therefore, it is not surprising that this protein was first found in human cell lines in the context of NC research (French et al., 2001).

Three of the four human BET proteins (BRD2, BRD3, BRD4) are found ubiquitously in human tissues; BRDT, the fourth human BET protein, is only present in the testes and rarely in tumors (Stonestrom et al., 2016).

In order to modify the transcription rates of certain genes and thereby influence cell growth, the BRD4 requires its two bromodomains, which have various amino acid sequences. With these bromodomains BRD4 binds to acetylated histones, thereby being capable to distinguish between different acetylation patterns (Dey et al., 2003). This mechanism of binding to the chromosomes is maintained during mitosis, which is why BET proteins are thought to be important for cellular transcriptional memory (Yang et al., 2008).

By inhibiting BET proteins, it has been shown that these proteins also have an inflammatory effect, because their inhibition led to a decrease of pro-inflammatory cytokines (Nicodeme et al., 2010). Furthermore, a higher transcription of pro-inflammatory genes by BRD4 was found (Huang et al., 2009).

### **1.3.1 Inhibitors of the BET protein family**

Nicodeme et al. were the first to synthetically generate an iBET compound, which was found to suppress inflammations and therefore could help against bacteria-induced sepsis (Nicodeme et al., 2010).

The BRD4 protein is essential for many tumors including NC to archive their increased proliferation rates by inducing higher transcription rates of the *MYC* gene. So, it was tested if inhibition of this protein could lead to a decreased proliferation. In a first approach, the newly developed iBET JQ1 was proven to initiate differentiation as well as cause growth arrest in NC cells and mice xenograft models (Filippakopoulos et al., 2010). Later, it was shown in gastric and ovarian cancer cells that a reason of the decreasing proliferation is the induction of cellular senescence (Dong et al., 2018, Liu et al., 2018).

The promising results of the drug's efficacy in NC tumor cells led to a huge increase of interest in BET inhibitors. For this reason, iBET were tested in other *MYC*-dependent tumors like leukemia (Zuber et al., 2011) or multiple myeloma (Chaidos et al., 2014) and the number of clinical trials increased, mostly including patients with solid tumors, especially with NC (Doroshov et al., 2017). These clinical trials could show an extension of progression-free survival (PFS) in NC patients, but permanent tumor remission was rarely achieved.

Still, there are two other major problems with the usage of iBET for cancer therapy: Firstly, as already mentioned, BET proteins are ubiquitously present in human tissues. Secondly, secondary resistance has been observed in cancer cells treated with iBET. The ubiquitous presentation of BET proteins leads to a lot of unwanted side effects, most important a thrombocytopenia, limiting the administrable dose of the drug and therefore the effect on cancer cells (Napolitano et al., 2019). By performing CRISPR and ORF (open reading frame) screening for more than 900 genes known to be tumor drivers, five pathways were identified leading to resistance of NC cells to iBET (Liao et al., 2018). One of these pathways is the preservation of *MYC* function during BRD4 inhibition by finding ways to bypass the need of BRD4 for *MYC* transcription. This is for example achieved by increasing the Wnt/ $\beta$ -catenin signaling (Fong et al., 2015), the NF- $\kappa$ B (Wu et al., 2018) or the BLC2 pathways (Esteve-Arenys et al., 2018). These findings led to further studies combining iBET therapy with other agents to overcome the bypass.

### **1.3.1.1 Approaches combining iBET with other agents to heighten the efficiency**

Since iBET proved to be suitable for reducing the tumor burden, but also proved to be an inadequate therapy for treating NC alone, researchers began to investigate whether synergistic activity with other agents could increase therapeutic efficiency.

As immune checkpoint inhibitors had a great breakthrough in cancer therapy over the past years, showing great efficiency in many different tumors, these substances were also tested in combination with iBET. iBET JQ1 combined with a PD-1 blockade was shown to lead to a further reduction of tumor mass in non-small cell lung cancer (NSCLC) mouse models (Adeegbe et al., 2018). Synergistic effects of combined iBET and HDACi therapy, both substances that have already shown promising effects in NC therapy, were also found in mouse models of lymphoma (Bhadury et al., 2014). As another substance class that has already demonstrated positive effects in NC, CDK inhibitors showed synergistic effects with iBET when tested in NC cell lines and xenograft mouse models (Liao



et al., 2018). In a review of Bechter and Schöffski preclinical studies testing iBET in combination with a variety of other therapy approaches are described (Bechter and Schöffski, 2020). As this review indicates, combination approaches are mostly limited to other agents targeting the molecular pathways, while only immune checkpoint blockade was tested as a representative of immunotherapy. Therefore, more research is needed on this field.

#### **1.4 Objective**

Despite increased efforts to find an efficient therapy leading to a prolonged overall survival in the last years, the prognosis of patients with NUT carcinomas (NC) is still poor and the tumor itself is not curable. Hence, novel treatment regimens are urgently needed. Since oncolytic virotherapy already achieved encouraging results in other malignant neoplasms with the *MYC* oncogene locus as a leading driver of tumor cell proliferation, such as medulloblastoma (Lal et al., 2018), it was hoped that human NC cell lines would also respond well to oncolytic virotherapy.

In a first step, human NC cell lines were infected with different oncolytic DNA- and RNA-viruses to generate so-called “virograms”. Thereby, it was intended to identify a distinct virotherapeutic agent showing the most promising oncolytic effect on each and every human NC cell line. Human NC cell lines with the two most common translocations, exhibiting fusion proteins *BRD4-NUT* or *BRD3-NUT*, were selected to build up a respective test platform.

In a second step, it was planned to test also monotherapies with two different BET inhibitors (iBET) on a panel of human NC cell lines by employing compounds BI894999 (provided by Boehringer-Ingelheim, Vienna, Austria) and GSK525762 (provided by Glaxo-Smith-Kline, London-Brendford, Great Britain). The aim of these experiments was to find out, if inhibition of BET proteins leads to an enhanced differentiation, determined by slowing down the growth rates of tumor cells.

Since iBET compounds so far have not been found to achieve long-lasting tumor remissions, the third part of this thesis was to find out, if the combination of

## 1 Introduction

---

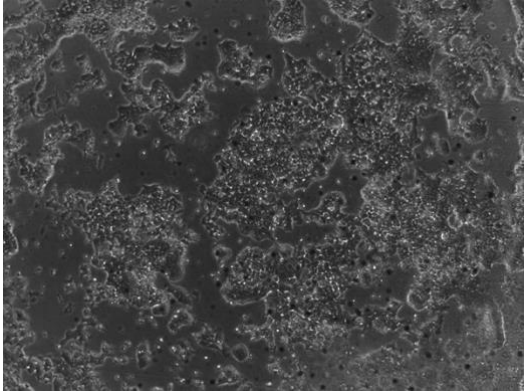
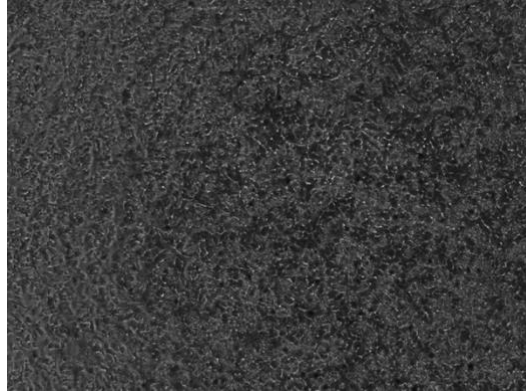
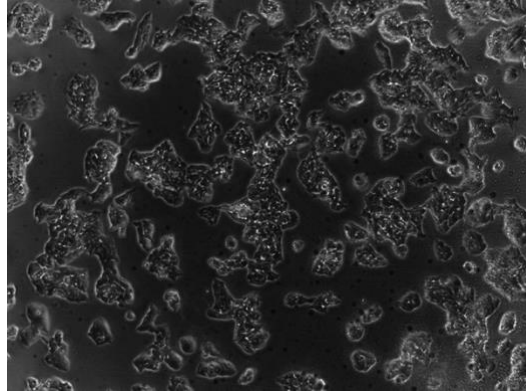
oncolytic viruses with iBET compounds could result in an increased rate of oncolysis on the NC cell lines when compared to the respective monotherapies.

## 2 Material and methods

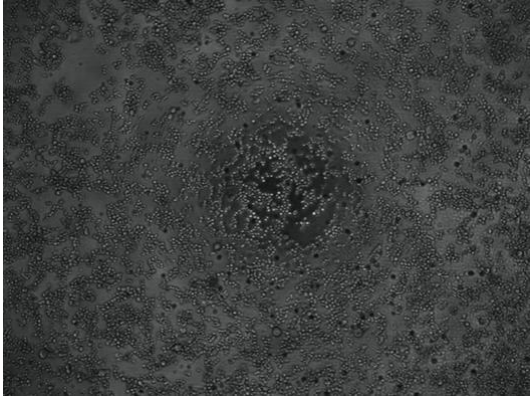
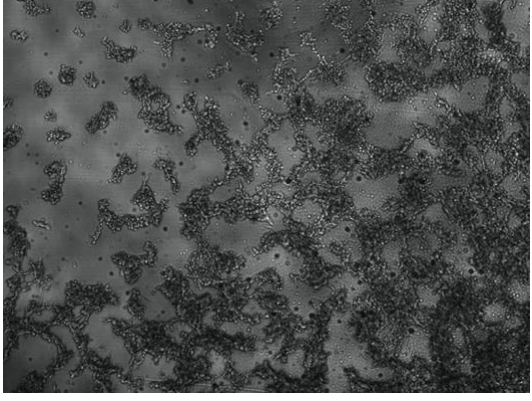
### 2.1 Materials

#### 2.1.1 *NUT* carcinoma cell lines

Table 2: *NUT* carcinoma cell lines used in this thesis

Name	Cell culture medium	Growth	Morphology
HCC2429 †	DMEM + 10 % FCS	Adherent	
143100 †	DMEM + 10 % FCS	Adherent	
690100 †	DMEM + 10 % FCS	Adherent	

## 2 Material and methods

<b>Ty-82</b> *	RPMI 1640 + 10 % FCS	Semi- adherent	
<b>10326</b> †	DMEM + 10 % FCS	Floating	

† Cell lines kindly provided by Prof. Christopher A. French (Brigham and Women's Hospital and Harvard Medical School).

\* Cell line purchased from JRCB Cell Bank (JCRB No.: JCRB1330).

### 2.1.2 Viruses

Table 3: Oncolytic viruses used in this thesis.

Name	Gene disruptions	Gene insertions	Source
<b>MeV-GFP</b>	none	GFP	(Scheubeck et al., 2019)
<b>GLV-0b347</b>	J2R	TurboFP635	Genelux Corporation, San Diego, CA, USA
<b>T-VEC</b>	ICP 34.5, ICP 47	GM-CSF	Amgen®, Thousand Oaks, CA, USA

**2.1.3 Media, sera and buffer**

DMEM	Sigma-Aldrich
RPMI 1640	Gibco
FCS	Sigma-Aldrich
Opti-MEM	Gibco
PBS (cell culture use)	Sigma-Aldrich
Accutase <sup>®</sup> Solution	Sigma-Aldrich
0.05 % Trypsin-EDTA	Sigma-Aldrich

**2.1.3.1 Self-made solutions**

PBS (non-cell culture use)

NaCl	137 mM (8 g)
KCl	2.7 mM (0.2 g)
Na <sub>2</sub> HPO <sub>4</sub>	10 mM (1.44 g)
KH <sub>2</sub> PO <sub>4</sub>	1.8 mM (0.24 g)
H <sub>2</sub> O <sub>dd</sub>	filled up to 1 l

**2.1.4 Chemicals**

Acetic Acid (glacial) 100%	Merck
Antifect <sup>®</sup> N liquid	Schülke & Mayr
Dimethyl sulfoxide (DMSO)	AppliChem
Isopropanol (70 %)	SAV Liquid Production
Hydrochloric acid fuming 37%	Merck
KCl	Carl ROTH
NaCl	Merck
Na <sub>2</sub> HPO <sub>4</sub>	Merck
PFA (4%)	Otto Fischar GmbH

## 2 Material and methods

---

Secusept	ECOLAB
Sulforhodamine B (SRB)	Sigma-Aldrich
Trichloroacetic acid (TCA)	Carl ROTH
Trizma® Base (TRIS)	Sigma-Aldrich
Trypan Blue	Sigma-Aldrich

### 2.1.4.1 Self-made solutions

#### TCA solution (10 %)

TCA	100 g
H <sub>2</sub> O <sub>dd</sub>	filled up to 1 l

#### SRB staining solution (0.4 % in 1 % acetic acid)

SRB	4 g
Acetic acid	10 ml
H <sub>2</sub> O <sub>dd</sub>	filled up to 1 l

#### TRIS base (10 mM)

TRIS	1.21 g
H <sub>2</sub> O <sub>dd</sub>	filled up to 1 l
pH	10.5

### 2.1.5 Laboratory equipment

Autoclave 3850 EL	Systec
Centrifuge	Eppendorf / Heraeus
Fluorescence Microscope	Olympus
Freezing container Mr. Frosty	Nalgene
Hemocytometer	Hecht Assistant
Incubator (37 °C, 5 % CO <sub>2</sub> , > 95 % Humidity)	Memmert / Sanyo / Heraeus
Laminar Flow Work Bench	Heraeus

Light Microscope CK40	Olympus
Multichannel Pipette (100 µl, 1200 µl)	Eppendorf
Multistepper Pipette	Eppendorf / BrandTech
pH-Meter	HANNA instruments
Multi-Detection Microplate Reader Synergy HT with GEN 5 1.11 Software	BioTek
Pipette Boy	Integra
Pipettes (10 µl, 100 µl, 200 µl, 1000 µl)	Eppendorf
Refrigerator (-18 °C, -80 °C, -120 °C)	Liebherr
Shaker	Heidolph
Sonifier	Branson Ultrasonics
Varioklav	H.P. Medizintechnik
Vortex mixer	NeoLab
Water Bath 3042 (37 °C)	Köttermann

### 2.2 Methods

#### 2.2.1 Cell culture

##### 2.2.1.1 General cell culture

The cells were cultivated in tissue culture flasks (75 mm<sup>2</sup> / 150 mm<sup>2</sup>) in Dulbecco's Modified Eagle's Medium - high glucose (DMEM) or Roswell Park Memorial Institute (RPMI) containing 10 % Fetal Calf Serum (FCS) (in the following referred to as "cell culture medium") (see 2.1.1). They were stored in an incubator at 37 °C in a humidified atmosphere with 5 % CO<sub>2</sub>. The cell growth was estimated once a day by light microscopy with 4x magnification. When the cell layer was confluent the cells were passaged, which was necessary approximately twice a week.

For passaging the adherent cells were washed with warmed (37 °C) sterile phosphate buffered saline (PBS). Afterwards warmed 0.05 % trypsin-EDTA was added onto the cell layer to detach the cells from the flask. After 4 min of incubation, trypsin was diluted with cell culture medium for inactivation. The suspension was transferred into a conical tube and centrifuged at 1000 revolutions per minute (rpm) for 4 min. The supernatant was removed. The cell pellet was suspended with cell culture medium and depending on the desired dilution factor a certain amount of the cell suspension was transferred into the tissue culture flask, which was filled up with cell culture medium.

For the semi-adherent cell line, the supernatant containing floating cells was centrifuged as well, so floating cells were not discarded.

The suspension cell line was split by taking out a part of the cell solution of the tissue culture flask and replacing it with fresh cell culture medium.

##### 2.2.1.2 Cryoconservation of cells

As the doubling time of the used cell lines increased with the number of passages, it was necessary to freeze cells with a low passage count for later use. Therefore, a cell pellet was prepared as described above (see 2.2.1.1). The pellet was suspended with freezing solution (10 % Dimethyl sulfoxide (DMSO), 20 % FCS, 70 % DMEM / RPMI). 1 ml of the solution was filled into cryoconservation tubes,



which were stored in a freezing container at -80 °C. After 24 h the frozen cells were transferred to -145 °C.

### **2.2.1.3 Thawing of cells**

To reculture cells with a lower passage number, the frozen cells were thawed in a water bath. The cell suspension was mixed with 8 ml warmed cell culture medium and centrifuged for 4 min at 1000 rpm. The supernatant was removed, and the cell pellet was resuspended in cell culture medium. The cell suspension was transferred into a new tissue culture flask. Before the thawed cells could be used for further experiments, they had to be passaged at least once.

### **2.2.1.4 Determining the concentration of cells via cell counting**

For quantification of the cell number 10 µl of cell solution and 90 µl of trypan blue were mixed (dilution factor 1/10). When less than 10 cells / ml were counted, the dilution factor had to be lowered to achieve a more accurate cell count. The cells were counted using an improved Neubauer hemocytometer. The Neubauer hemocytometer was arranged by attaching a moistened cover glass on the hemocytometer. 10 µl of the prepared solution were pipetted under the cover glass. The vital cells, being not colored by trypan blue in contrast to the dead cells, were counted in four large squares of the hemocytometer (**Figure 7**). As one large square contains the volume of 0.1 µl, the cell concentration per ml could be calculated with the following formula:

$$\text{Concentration} = \frac{\text{Counted cell number} \times 10,000 \times \text{Dilution factor}}{\text{Number of counted large squares}}$$

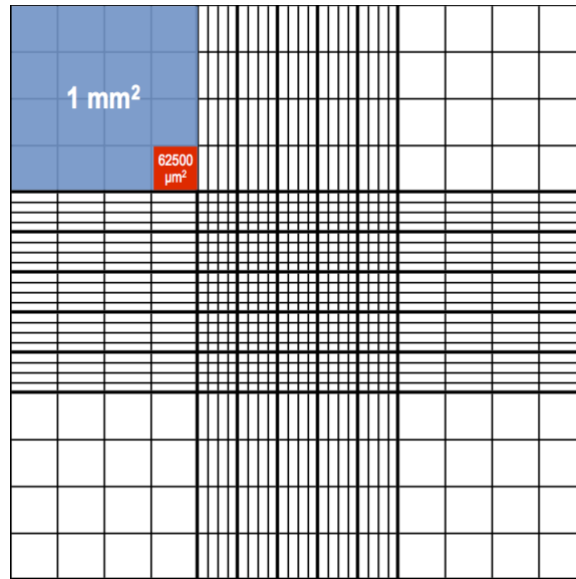


Figure 7: Grid of the improved Neubauer hemocytometer.

All cells in the four large squares (marked with 1 mm<sup>2</sup>) in the corners of the chamber are counted. Image taken from <https://www.hemocytometer.org/hemocytometer-square-size/> (22.10.2019)

### 2.2.1.5 Seeding cells for infection

24 h before infection or treatment a defined number of cells had to be seeded into cell culture plates, the number of wells depending on the later performed assay. For seeding, cells were counted as described in 2.2.1.1. Subsequently, a dilution with cell culture medium was prepared containing a defined number of cells per ml adjusted to fit the well size and the doubling time of the cell line. So, for different assay types, different plates and cell numbers were required (**Table 4**).

Table 4: Conditions used for the different assay types

Assay Type	Used plate	Amount of medium / well	Cell line	Number of seeded cells / well
<b>SRB-Assay, IFN-<math>\beta</math> ELISA</b>	24-Well-Plate clear, flat bottom	500 $\mu$ l	HCC2429	4 x 10 <sup>4</sup> cells / well
			143100	4 x 10 <sup>4</sup> cells / well
			690100	4 x 10 <sup>4</sup> cells / well
<b>RealTime-Glo™ MT Cell Viability Assay</b>	96-Well-Plate White walled, clear flat bottom	50 $\mu$ l	Ty-82	4 x 10 <sup>4</sup> cells / well
			143100	5 x 10 <sup>3</sup> cells / well
		100 $\mu$ l	10326	2 x 10 <sup>4</sup> cells / well
<b>xCELLigence® Assay</b>	E-96-well-plate	200 $\mu$ l	HCC2429	5 x 10 <sup>3</sup> cells / well
			143100	5 x 10 <sup>3</sup> cells / well
			690100	5 x 10 <sup>3</sup> cells / well

## 2.2.2 Virological methods

### 2.2.2.1 Infection of adherent cells with MeV-GFP

The cells seeded in cell culture plates (see 2.2.1.5) were infected with five different MOIs (multiplicity of infection) (MOI 10, 1, 0.1, 0.01, 0.001), MOI 1 meaning 1 virus particle per cell, plus a negative control (MOCK). To prepare the MOIs the virus (stored at -80 °C) was thawed in the water bath and viral particles were added to Opti-MEM in a concentration corresponding to the highest MOI. The other MOIs were prepared in a 1 to 10 dilution series.

Before the virus containing solution was given onto the cell layer, cells were washed with warmed PBS. In each case four wells were infected with 250  $\mu$ l of a virus- or MOCK-solution. After 3 h of incubation in an incubator the inoculum was removed and replaced with 500  $\mu$ l of cell culture medium. The cells were then further incubated for 72 or 96 hours in an incubator.

## 2 Material and methods

---

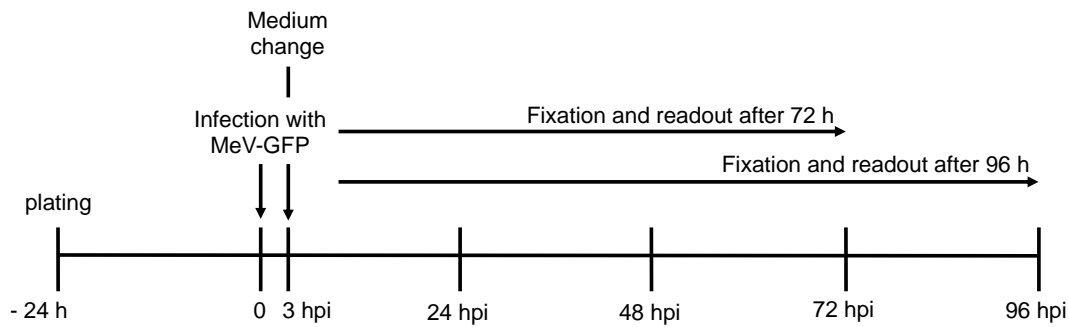


Figure 8: Setting of MeV-GFP single agent treatment for adherent cell lines.  
hpi: hours post infection

### 2.2.2.2 Infection of adherent cells with GLV-0b347 or T-VEC

Before GLV-0b347 or T-VEC (both stored at -80 °C) could be used for infection of seeded cells (see 2.2.1.5), they had to be sonicated for 30 seconds. The sonication was necessary to dissolve viral aggregates. After sonication the MOIs could be prepared as above (see 2.2.2.1) using DMEM + 2 % FCS (for GLV-0b347) / DMEM (for T-VEC) as medium instead of Opti-MEM. The MOIs used were MOI 1, 0.1, 0.01, 0.001 and 0.0001.

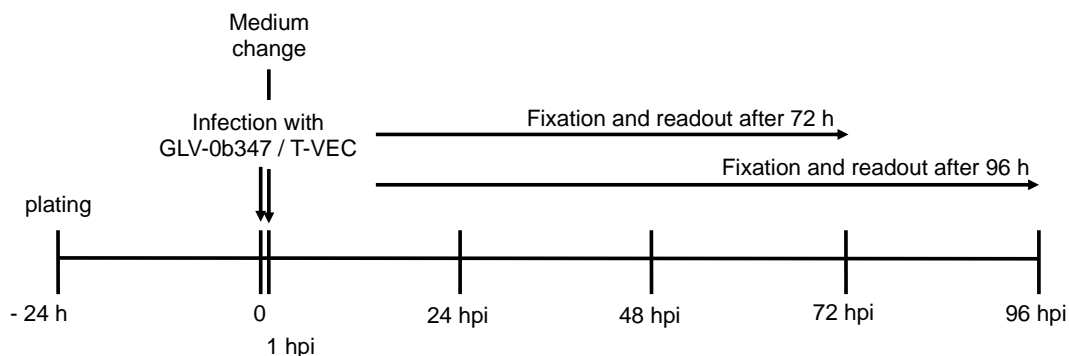


Figure 9: Setting of GLV-0b347 and T-VEC single agent treatment for adherent cell lines.  
hpi: hours post infection

### 2.2.2.3 Infection of non-adherent cell lines with MeV-GFP, GLV-0b347 or T-VEC

As the non-adherent cell lines Ty-82 and 10326 could not be washed with PBS, the inoculum was prepared in cell culture medium and then added to the cells. Because medium could not be changed afterwards either, the virus containing medium was left with the cells until the end of the incubation time.



Figure 10: Setting of MeV-GFP, GLV-0b347 and T-VEC single agent treatment for non-adherent cell lines. hpi: hours post infection

### 2.2.3 Methods of molecular treatment approaches

#### 2.2.3.1 Treatment of cells with BET-inhibitors

In this thesis two different BET-inhibitors were used: The compound BI894999 (generated by Boehringer-Ingelheim, Vienna, Austria) and GSK525762 (generated by Glaxo-Smith-Kline, London-Brendford, Great Britain). The dissolved iBET were stored at  $-20\text{ }^{\circ}\text{C}$  at a concentration of 10 mM. For treatment, the inhibitor was diluted with cell culture medium to attain the desired concentrations. Cells were seeded in 24 well plates (see 2.2.1.5) and incubated for 24 h. Then medium was removed and the iBET solution was directly pipetted onto the cell layer. After the treatment, the cells were incubated for 24 h, 48 h, 72 h or 96 h in an incubator.

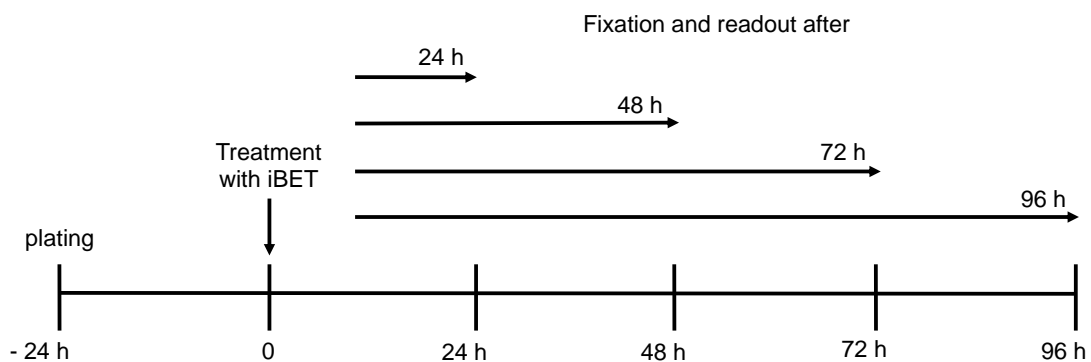


Figure 11: Setting of iBET single agent treatment for adherent cell lines.

### **2.2.4 Combinatory treatment of seeded cells with BET-inhibitors and oncolytic viruses**

After the suitable concentrations of iBET and virus were found in preliminary experiments, leaving around 75 % of the cells viable in comparison to the MOCK value, experiments combining both approaches could be started.

Two different concentrations of iBET were tested with one MOI of the oncolytic viruses. As controls MOCK, monoinfection with OV and monotreatment with both concentrations of iBET were needed. As for the monotherapeutic approaches the cells were seeded in 24 well plates (see 2.2.1.5) and infected at 24 h after seeding. The virus and MOCK solutions were prepared as described in 2.2.2. First, the medium was taken off and either 250 µl virus or MOCK solution were given onto the cell layer. After 3 h (for MeV-GFP) or 1 h (for GLV-0b347 and T-VEC) the inoculum was taken off again and replaced by medium containing the BET-inhibitor (preparation see 2.2.3.1). The plates were incubated for either 72 or 96 hours post infection (hpi) in an incubator.

The settings are visualized in **Figure 8** and **Figure 9**. But instead of “medium change” after 1 h respectively 3 h medium containing iBET was added.

### **2.2.5 Analysis of cell viability**

#### **2.2.5.1 Transmitted light and fluorescence photography**

To visualize virus proliferation and the cell death, phase contrast and fluorescence photos of the same regions of the wells were taken. MeV-GFP expresses green fluorescent protein (GFP), GLV-0b347 encodes a far-red mutant of the red fluorescent protein from sea anemone *Entacmaea quadricolor* (turboFP635). As the T-VEC virus as well as the iBETs did not have a fluorescent marker only phase contrast photos were taken.

#### **2.2.5.2 Determining cell mass via Sulforhodamine B cytotoxicity assay**

Using the SRB assay, first described by Skehan et al., the cytotoxicity of solutions can be portrayed (Skehan et al., 1990): After infection or treatment and the following incubation the remaining viable cell mass was quantified by staining the cells with Sulforhodamine B (SRB). First, cells were washed with cold (4 °C) PBS

and covered with 250 µl of cold 10 % trichloroacetic acid (TCA) for at least 30 min at 4 °C to make the cell membrane porous. Next, the TCA was removed, and the wells were washed thrice with tap water. After washing, the plates were dried for at least 3 h in a drying chamber at 40 °C.

The dried wells were filled with 250 µl SRB staining solution per well, which was removed after a minimum of 15 min. Now, the wells were washed three times with 1 % acidic acid to remove unbound staining solution. The plates were dried again in the drying chamber for at least 3 h.

Subsequently, the stained cells were covered with 1-2 ml 10 mM Tris pH 10.5 solution, as in this basic condition the stain fixated in the cells dissolved again. The plates were incubated for at least 10 min on a shaker until the color was evenly distributed in the fluid. The amount of Tris was estimated due to the amount of stain fixated by the cells, which was necessary as the resulting optical density is only linear until a measured optical density of 2. 80 µl of solution were transferred into a transparent flat-bottom 96-well-plate in technical duplicates.

The optical density was measured at a wavelength of 550 nm with the microplate reader.

### **2.2.5.3 Determining cell mass via RealTime-Glo™ MT Cell Viability Assay**

The assay was used as an end-point assay. The 2x RealTime-Glo™ reagent was prepared according to the manufacturer's instructions. To get 1x concentration of the solution, the same volume of 2x RealTime-Glo™ reagent, that was already in the well in medium, was given in each well. The luminescence then was measured in the microplate reader after 10 min, 30 min, 60 min and every following 60 min until the luminescence signal weakened again. The measurement resulting in the highest luminescence signal was used, as this way the background was blanked as good as possible and the differences between the different treatment approaches were presented best.

### **2.2.5.4 Determining cell proliferation under iBET treatment via xCELLigence® assay**

To determine the rate of cell proliferation the xCELLigence® assay was used.

To get reasonable results, first, the appropriate cell number, where cells remained in an exponential growth phase during the whole measurement period, had to be found out. Cells were counted as described in 2.2.1.4. The E-96-Well-Plate was prepared by pipetting 150 µl of PBS in the interspaces between the wells and 50 µl of cell culture medium into each well as a background. The background was determined by a single measurement in the xCELLigence®-reader. Then, 150 µl of cell solution (preparation see 2.2.1.5) were pipetted into the wells with cell numbers ranging from  $1 \times 10^3$  to  $2 \times 10^4$  per well (3 wells per concentration), leaving the side wells with only background medium. The cell impedance was measured in the xCELLigence®-reader over 96 h in 30 min intervals.

In the second approach, the suitable cell number identified before was treated with different concentrations of the iBET compound. For this experiment the E-96-well-plate was prepared for the background measurement as described above. Afterwards again 150 µl of cell solution, this time containing the same number of cells for each well, were pipetted into each well. The cell impedance was now measured for 24 h in 30 min intervals in the xCELLigence®-reader. After 24 h, 20 µl cell culture medium containing different iBET concentrations, which led to a reduction of cell mass between 10 % and 60 % in the monotherapy experiments analyzed via SRB assay, were added to the medium (4 wells per concentration). As the old medium could not be taken off, the iBET concentrations were prepared 10x higher than needed and an amount equaling 1/10 of the amount of medium already present in the well, was pipetted on top of the old medium. This treatment had to be performed within 30 min between two sweeps, so a gapless result could be obtained at the end of the experiment. The proliferation of the treated cells was measured for another 96 h in 30 min intervals, resulting in a total of 241 single measurements.

### **2.2.6 Molecular biology methods**

#### **2.2.6.1 IFN-β ELISA**

Cells were seeded in 24 well plates (see 2.2.1.5) and infected with OV (see 2.2.2) and / or treated with iBET (see 2.2.3.1). After 24, 48, 72 and 96 h supernatants were harvested and centrifuged at 4500 rpm for 5 min. Afterwards the



supernatant was pipetted into a new Eppendorf tube, which were stored at -80 °C until the assay was performed.

For the determination of the interferon  $\beta$  concentration in each sample the *VeriKine<sup>TM</sup> Human IFN Beta* ELISA Kit (pbl assay science) was used according to the manufacturer's protocol.

### **2.2.7 Statistical analysis**

The results were analyzed using an ordinary one-way ANOVA with multiple comparisons in GraphPad Prism version 8.00 for Windows (GraphPad Software, San Diego, California, USA, [www.graphpad.com](http://www.graphpad.com)). The Bonferroni Test was used for correction of the p-value. For the monotherapy experiments all different MOIs respectively concentrations were compared with the MOCK value. For the combinatory treatment of T-VEC + Ganciclovir, the MOCK value was compared to every single Ganciclovir treatment and the T-VEC value was compared to all T-VEC + Ganciclovir combinatory treatments. For the combinatory treatment four comparisons were performed: virus vs. virus + iBET low concentration, virus vs. virus + iBET high concentration, iBET low concentration vs. virus + iBET low concentration, iBET high concentration vs. virus + iBET high concentration.

To calculate the half maximal inhibitory concentration ( $IC_{50}$ ), the data was analyzed in *GraphPad Prism 8* with a non-linear regression using the predetermined formula "log[Inhibitor] vs. response - Variable slope (four parameters)". For more accurate results the used concentrations of the inhibitor were transformed to  $\log(x)$ ; due to the calculation of  $\log(x)$  for "0" is impossible, these values were set as " $1 \times 10^{-10}$ ".

### 3 Results

#### 3.1 Cell proliferation of NC cell lines HCC2429, 143100 and 690100

To achieve good results in the xCELLigence® experiments of the same cell lines when treated with the iBET, first, the proliferation activity of the cell lines in the E-96-well-plate with different cell densities had to be monitored. Thereby it was important, to seed as many cells as possible without having to face a proliferation stop due to a too high cell density or shortage of medium. That these problems occurred became apparent when the impedance curve changed from a linear growth to a sigmoidal curve.

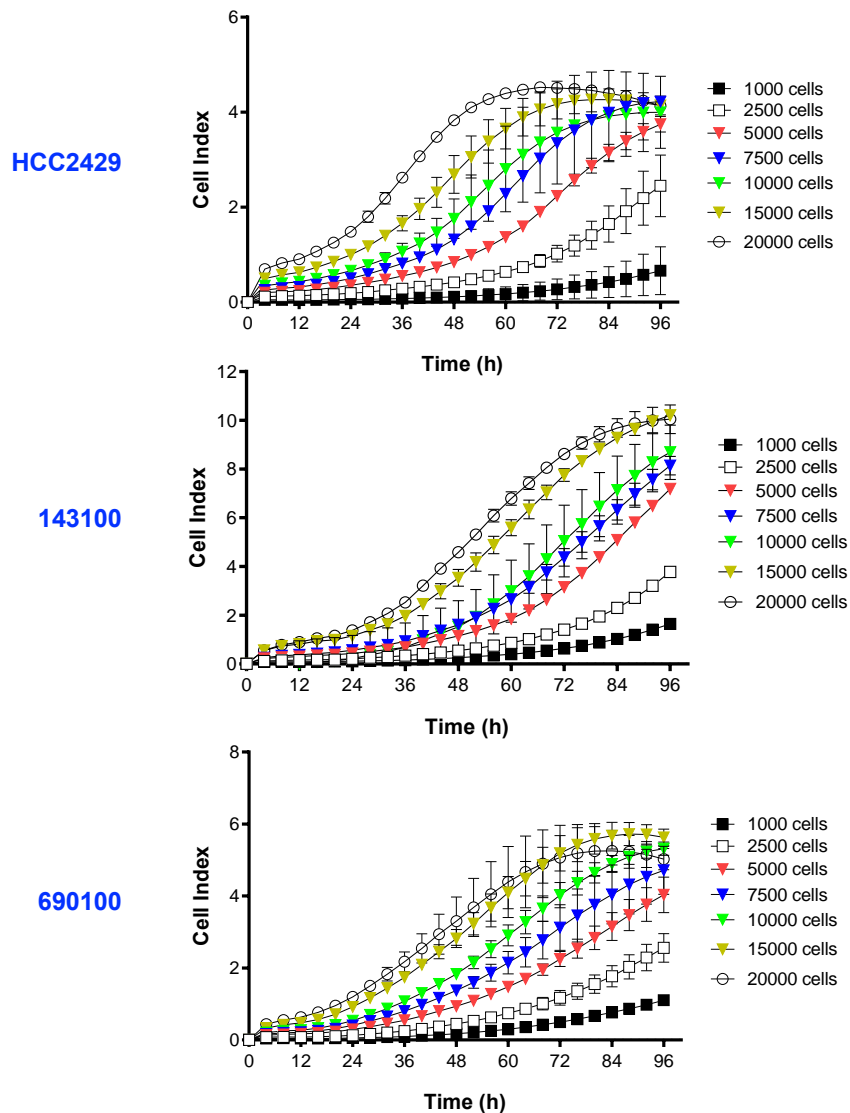


Figure 12: Cell proliferation of the NC cell lines HCC2429, 143100 and 690100.

Different cell numbers of the NUT carcinoma cell lines HCC2429, 143100 and 690100 were seeded in xCELLigence® E-96-well-plates. The impedance was measured for 96 h using the xCELLigence RTCA SP system. Displayed are mean values and SD of one experiment in which each number of cells was measured in quintuplicates.

As a result, 5,000 cells / well seemed to be the optimal number of cells for further experiments. At higher cell numbers the growth curve was no longer linear, while with a lower cell number, changes in the growth behavior would not have become as visible as with 5,000 cells (**Figure 12**).

### 3.2 Cytotoxic effect of oncolytic viruses on NC cell lines

To find out, whether immunovirotherapeutics can play a role in the therapy of NC, the cytotoxic potential of three different oncolytic viruses (MeV-GFP, GLV-0b347 and T-VEC) on three NC cell lines (HCC2429, 143100, 690100) containing the *BRD4-NUT* fusion protein was tested using the Sulforhodamine B (SRB) assay. For each virus five different multiplicities of infection (MOIs) were used, ranging from MOI 0.001 - MOI 10 for MeV-GFP and from MOI 0.0001 - MOI 1 for GLV-0b347 and T-VEC. The remnant cell mass was measured at 72 hpi and 96 hpi.

For the two non-adherent NC cell lines Ty-82 (*BRD4-NUT*) and 10326 (*BRD3-NUT*) the RealTime-Glo™ cell viability assay was performed as the SRB assay is only suitable for cell lines with adherent growth. The same MOIs were used as for the other cell lines, but the readout was only carried out at 96 hpi. These further experiments were performed to get a broader insight in the generality of the results obtained with the first three cell lines. Also, differences in the response of cell lines with *BRD3-NUT* compared to *BRD4-NUT* translocation were of interest.

**3.2.1 Cytotoxic effect of MeV-GFP, GLV-0b347 and T-VEC on NC cell line HCC2429**

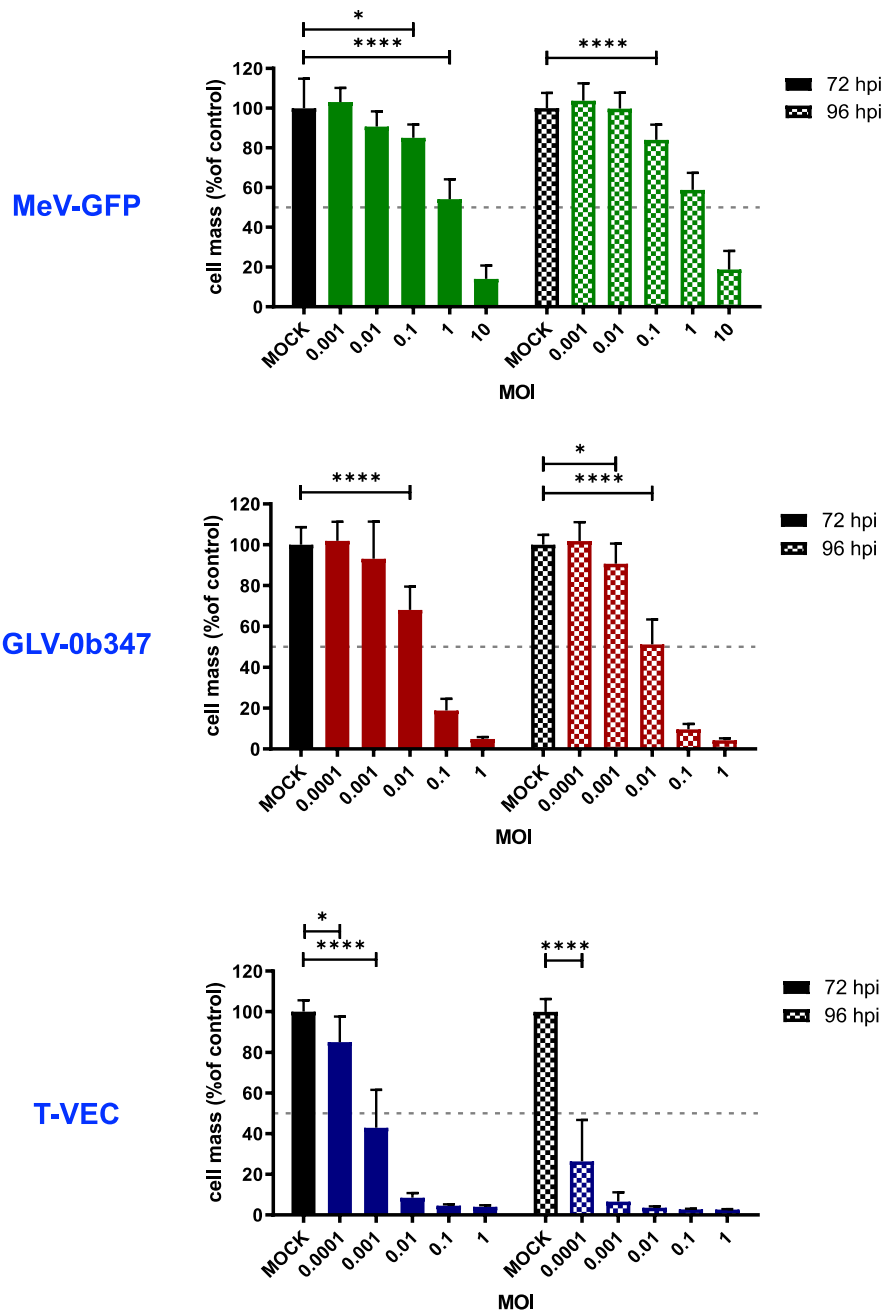


Figure 13: NC cell line HCC2429 infected with oncolytic viruses.

The NUT carcinoma cell line HCC2429 was infected with the oncolytic measles vaccine virus MeV-GFP (upper panel), the oncolytic vaccinia vaccine virus GLV-0b347 (middle panel) and the oncolytic herpes simplex virus T-VEC (lower panel) at indicated multiplicities of infection (MOI). Remaining cell masses were measured at 72 hpi and 96 hpi via Sulforhodamine B (SRB) assay. Displayed are mean values and SD of two (72 hpi) and three (96 hpi) independent experiments performed in quadruplicates. 50 % remaining cell mass is indicated by dotted lines. MOCK: uninfected control (black columns). Statistical significance: \*:  $p \leq 0.05$ ; \*\*:  $p \leq 0.01$ ; \*\*\*:  $p \leq 0.001$ ; \*\*\*\*:  $p \leq 0.0001$  - non-significant results are not indicated; significance is only displayed when a change to the next lower MOI occurred.

The NC cell line HCC2429 reacted to all tested oncolytic viruses in a MOI dependent manner, but the MOI values to achieve a remaining cell mass of < 50 % varied highly between the different oncolytic viruses: T-VEC proved to be the most effective therapeutic agent, followed by GLV-0b347, and the highest MOI for a significant reduction of cell mass was needed for MeV-GFP as displayed in **Figure 13**.

For MeV-GFP low MOIs of 0.001 and 0.01 did not lead to a significant reduction of cell mass. Starting at MOI 0.1, a MOI dependent decrease of cell mass could be observed at 72 hpi. Infection at MOI 0.1 reduced the cell mass to 85 %, at MOI 1 to 54 % and after infection at MOI 10 the remaining cell mass was only 14 % when compared to the mock infected control. Of note, in all concentrations the longer incubation time of 96 hpi could not lead to a further reduction of cell mass compared to the results after 72 hpi.

In contrast, GLV-0b347 already significantly reduced the cell mass at MOI of 0.01 (68 % at 72 hpi, 51 % at 96 hpi in comparison to MOCK). The lower tested MOIs 0.0001 and 0.001 did not lead to any noteworthy reduction of cell mass. When using higher MOIs of 0.1 and 1 nearly no cells were viable at 96 hpi (9 % and 4 %, respectively).

T-VEC showed even stronger oncolytic effects: Even a MOI of 0.001 already decreased the viable cell mass to 43 % at 72 hpi, MOI 0.01 led to a reduction of the remaining cell mass to 8 %. These effects were enhanced at 96 hpi: While MOI 0.0001 only reduced the cell mass to 85 % at 72 hpi, at 96 hpi a decrease to 26 % was observed. A high dropdown was also detected at MOI 0.001 (43 % at 72 hpi to 7 % at 96 hpi). When using higher MOIs of 0.01, 0.1 and 1 the remaining cell mass was already below 10 % at 72 hpi.

### 3.2.2 Cytotoxic effect of MeV-GFP, GLV-0b347 and T-VEC on NC cell line 143100

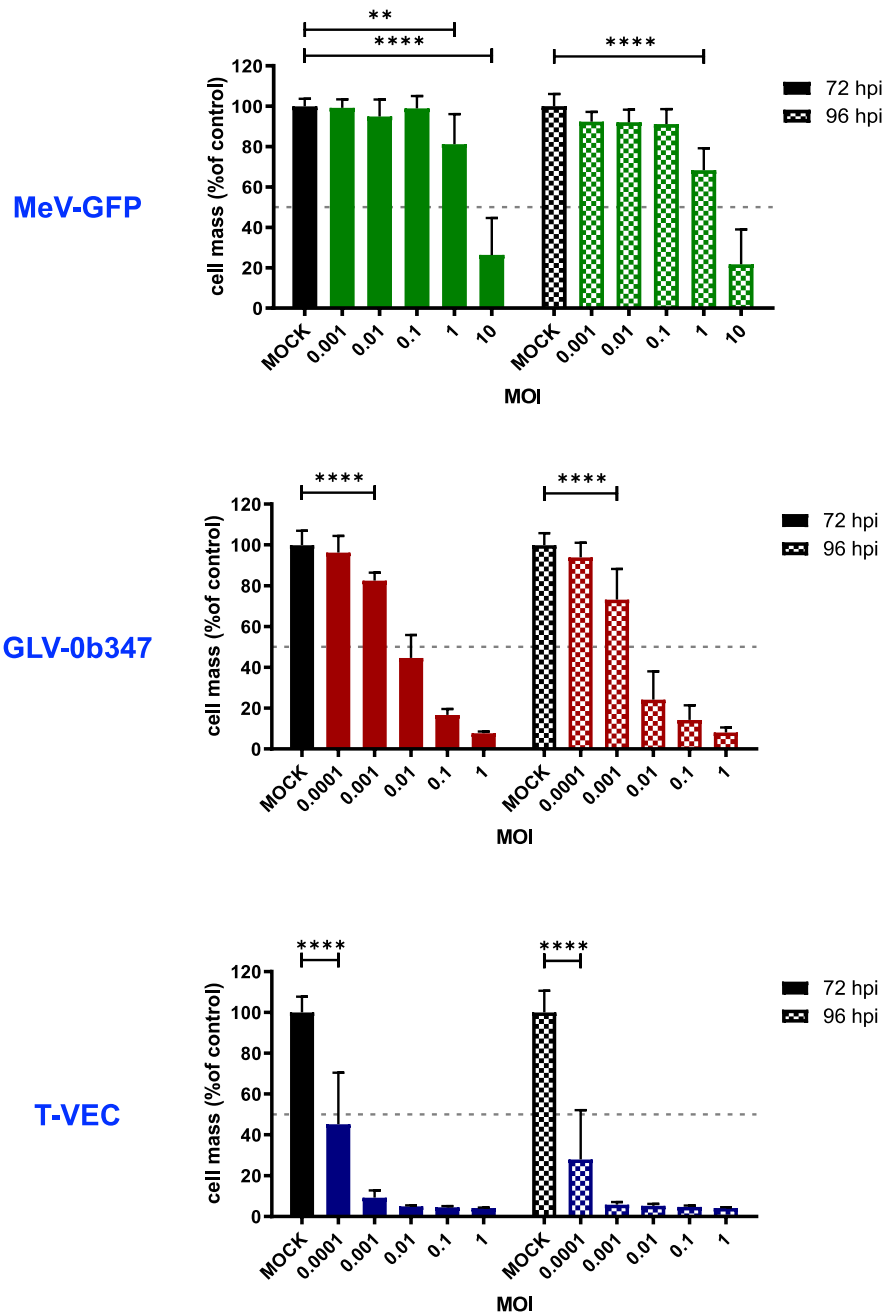


Figure 14: NC cell line 143100 infected with oncolytic viruses.

The NUT carcinoma cell line 143100 was infected with the oncolytic measles vaccine virus MeV-GFP (upper panel), the oncolytic vaccinia vaccine virus GLV-0b347 (middle panel) and the oncolytic herpes simplex virus T-VEC (lower panel) at indicated multiplicities of infection (MOI). Remaining cell masses were measured at 72 hpi and 96 hpi via Sulforhodamine B (SRB) assay. Displayed are mean values and SD of two (72 hpi) and three (96 hpi) independent experiments performed in quadruplicates. 50 % remaining cell mass is indicated by dotted lines. MOCK: uninfected control (black columns). Statistical significance: \*:  $p \leq 0.05$ ; \*\*:  $p \leq 0.01$ ; \*\*\*:  $p \leq 0.001$ ; \*\*\*\*:  $p \leq 0.0001$  - nonsignificant results are not indicated; significance is only displayed when a change to the next lower MOI occurred.

**Figure 14** indicates that all three tested immunovirotherapeutics lead to an induction of tumor cell death in the NC cell line 143100. Of note, T-VEC showed to be most powerful, followed by GLV-0b347 and MeV-GFP. Generally, the benefit of a longer incubation time of 96 hpi compared to 72 hpi was limited, with only selected MOIs showing a further reduction.

When infected with MeV-GFP, a shrinkage of remnant tumor cell mass to < 50 % in comparison to the mock infected control could only be observed with a MOI of 10 at 72 hpi, with no noteworthy further decrease at 96 hpi. While MOIs ranging from 0.001 to 0.1 did not show any effect at all, at MOI 1 MeV-GFP decreased the remaining cell mass to 81 % (72 hpi), respectively 68 % (96 hpi).

For GLV-0b347 the reduction of remnant cell mass to < 50 % could already be seen at a MOI of 0.01, where in addition the tumor cell mass dropped for further 21 % when comparing the results at 72 hpi and 96 hpi. The 10x lower MOI 0.001 also showed a small effect, leaving 73 % cell mass at 96 hpi viable, an effect that got also visible for MeV-GFP with MOI 10 and MOI 1. At the highest tested MOIs of 0.1 and 1 the viable cell mass decreased to 15 % respectively 8% for both incubation times.

For T-VEC, the effect of cell mass reduction to < 50 % at 72 hpi and further drop of ca. 20 % at 96 hpi became visible already at a MOI 0.0001. All higher tested MOIs (0.001 - 1) left no remarkable amount of viable tumor cells at both tested incubation times (4 - 9 %).

### 3.2.3 Cytotoxic effect of MeV-GFP, GLV-0b347 and T-VEC on NC cell line 690100

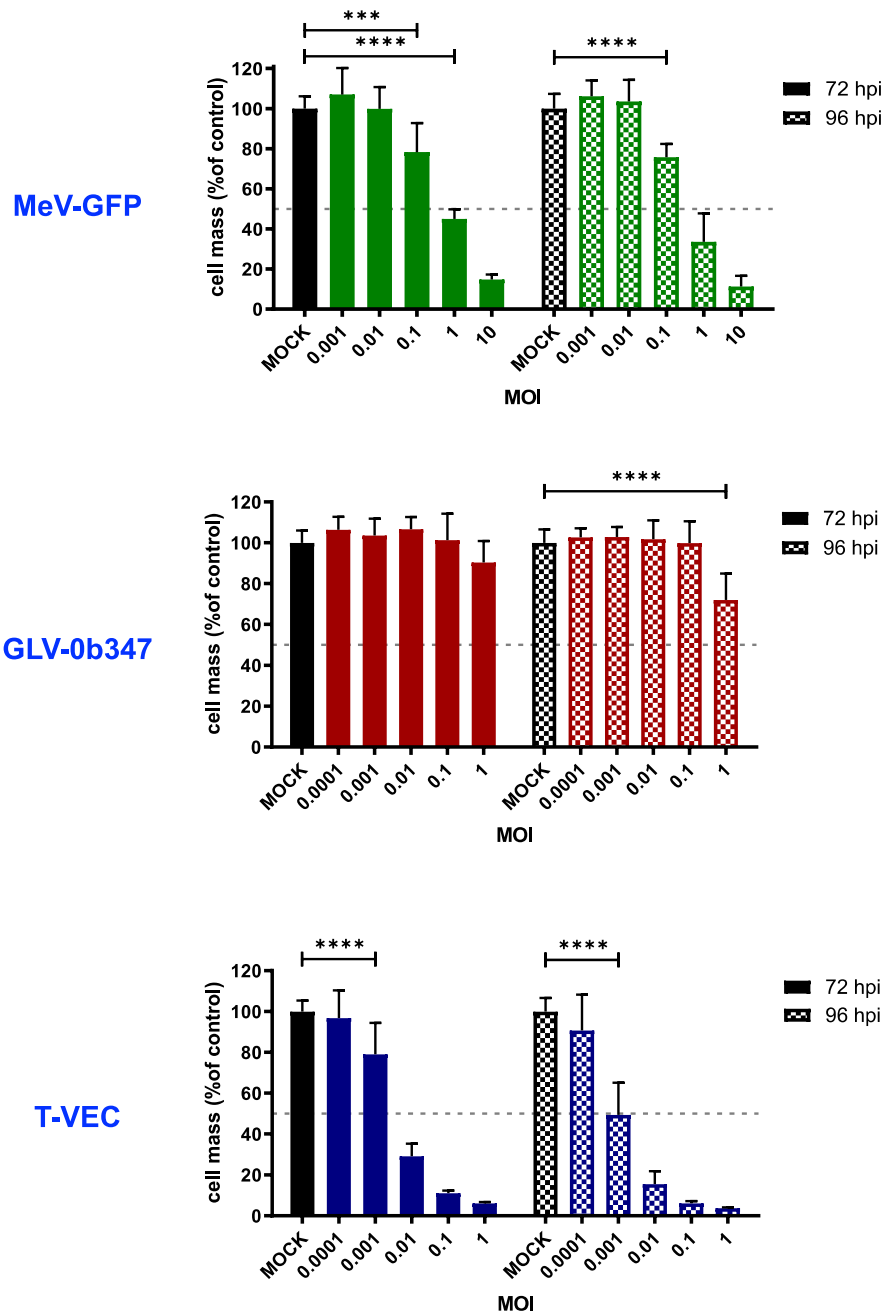


Figure 15: NC cell line 690100 infected with oncolytic viruses.

The NUT carcinoma cell line 690100 was infected with the oncolytic measles vaccine virus MeV-GFP (upper panel), the oncolytic vaccinia vaccine virus GLV-0b347 (middle panel) and the oncolytic herpes simplex virus T-VEC (lower panel) at indicated multiplicities of infection (MOI). Remaining cell masses were measured at 72 hpi and 96 hpi via Sulforhodamine B (SRB) assay. Displayed are mean values and SD of two (72 hpi) and three (96 hpi) independent experiments performed in quadruplicates. 50 % remaining cell mass is indicated by dotted lines. MOCK: uninfected control (black columns). Statistical significance: \*:  $p \leq 0.05$ ; \*\*:  $p \leq 0.01$ ; \*\*\*:  $p \leq 0.001$ ; \*\*\*\*:  $p \leq 0.0001$  - non-significant results are not indicated; significance is only displayed when a change to the next lower MOI occurred.



The cell masses of the third tested NC cell line, 690100, could only be reduced to < 50 % in comparison to MOCK with two of the three tested immunovirotherapeutics at the tested MOIs (**Figure 15**).

MeV-GFP did not reduce tumor cell masses at MOI 0.001 and MOI 0.01. At a MOI of 0.1, 78 % of the tumor cell mass was still viable, which got further reduced to 45 % at MOI 1 and 15 % at MOI 10 at 72 hpi, the results at 96 hpi only being slightly lower.

Completely different results could be seen after infection with GLV-0b347: At 72 hpi with none of the tested MOIs varying from 0.0001 to 1 a significant decrease of tumor cell mass got visible; at 96 hpi at least MOI 1 lead to a significant cell mass reduction to 72 % compared to the control.

While the MOI of 0.0001 did not show a significant effect at neither 72 hpi nor 96 hpi, at MOI 0.001 T-VEC lessened the tumor cell mass to 79 % at 72 hpi with an eminent further dropdown to 49 % at 96 hpi. With the MOIs 0.01 - 1 most cells were already killed at 72 hpi, but at 96 hpi an additional reduction of nearly 50 % (29 % to 15 % at MOI 0.01, 11 % to 6 % at MOI 0.1 and 6 % to 4 % at MOI 1) was viewable.

### 3.2.4 Comparison of the cytotoxic effect of different immunovirotherapeutics on adherent NC cell lines

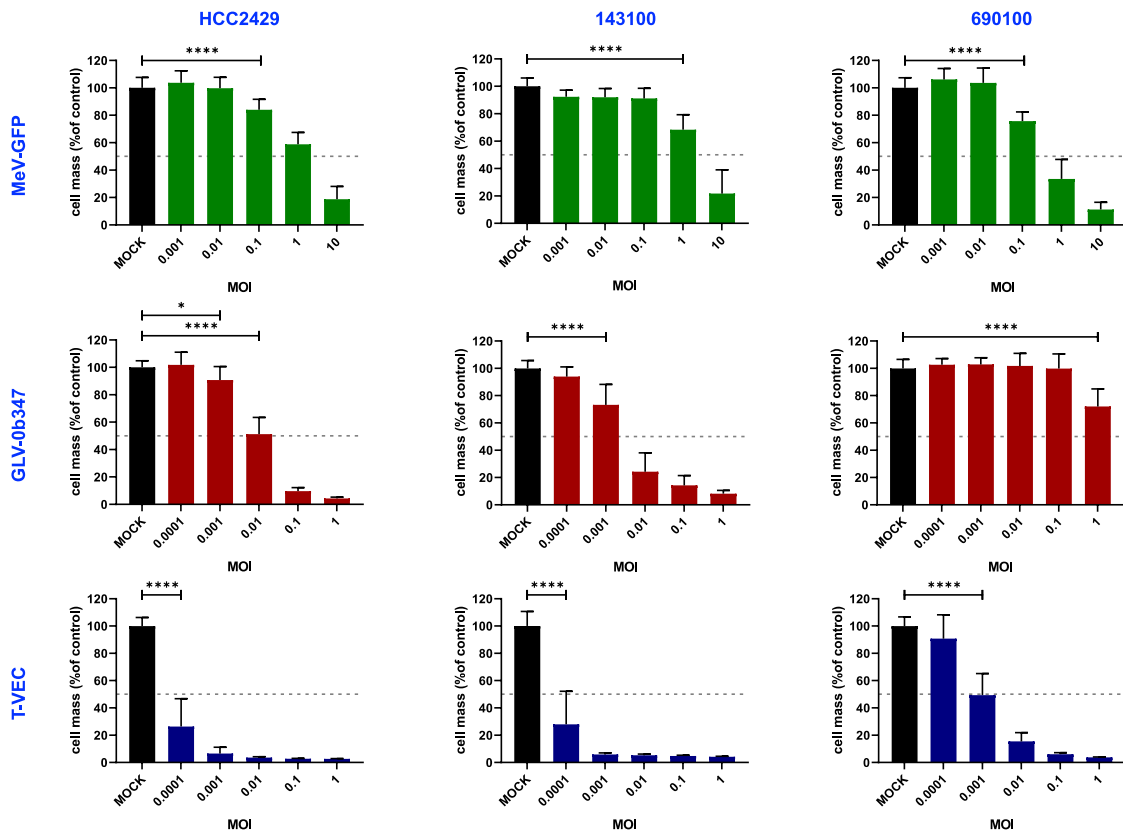


Figure 16: Comparison of the effect of oncolytic viruses on the NC cell lines HCC2429, 143100 and 690100. The NUT carcinoma cell lines HCC2429, 143100 and 690100 were infected with the oncolytic measles vaccine virus MeV-GFP (upper panel), the oncolytic vaccinia vaccine virus GLV-0b347 (middle panel) and the oncolytic herpes simplex virus T-VEC (lower panel) at indicated multiplicities of infection (MOI). The figure shows remaining cell masses measured via Sulforhodamine B (SRB) assay at 96 hpi. Displayed are mean values and SD of three independent experiments performed in quadruplicates. 50 % remaining cell mass is indicated by dotted lines. MOCK: uninfected control (black columns). Statistical significance: \*:  $p \leq 0.05$ ; \*\*:  $p \leq 0.01$ ; \*\*\*:  $p \leq 0.001$ ; \*\*\*\*:  $p \leq 0.0001$  - non-significant results are not indicated; significance is only displayed when a change to the next lower MOI occurred.

Generally, the obtained results lead to the conclusion that T-VEC is most efficient and led to highly reduced amounts of viable tumor cell masses in all of the cell lines even at very low MOIs (**Figure 16**). Hereby, the cell line 690100 proved to be least sensitive, as the MOI of 0.001 only led to a tumor cell mass reduction of 51 % at 96 hpi, whereas a reduction of ca. 75 % could be observed in the two other cell lines even at a 10 times lower MOI of 0.0001.

Also, when treated with GLV-0b347, the cell line 690100 reacted least sensitive. Here, the results obtained were even more diverging: The MOI of 0.01 reduced

the cell mass to 51 % in HCC2429 cells and even to 24 % in 143100 cells at 96 hpi compared to MOCK, whereas in 690100 cells no effect was visible at all. Here, 100x more virus particles (MOI 1) were needed to at least get a small decrease to 72 %.

Interestingly, the infection with MeV-GFP showed a reverse response intensity as 690100 reacted most sensitive in these experiments: While at MOI 1 the detectable remnant cell mass was 68 % for 143100, respectively 59 % for HCC2429, only 34 % of the 690100 cells were still viable.

## 3.2.5 First studies on semi-adherent BRD4-NUT cell line Ty-82

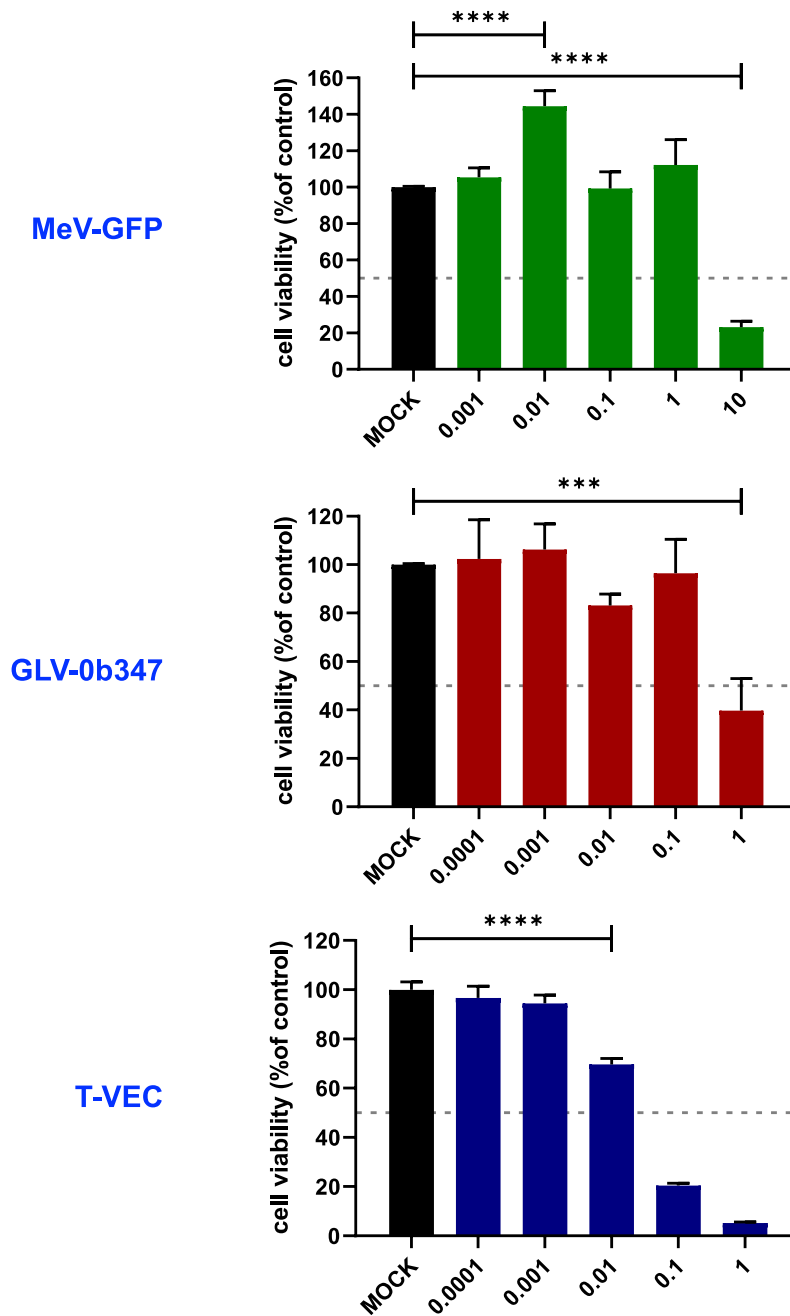


Figure 17: NC cell line Ty-82 infected with oncolytic viruses.

The NUT carcinoma cell line Ty-82 was infected with the oncolytic measles vaccine virus MeV-GFP (upper panel), the oncolytic vaccinia vaccine virus GLV-0b347 (middle panel) and the oncolytic herpes simplex virus T-VEC (lower panel) at indicated multiplicities of infection (MOI). The remaining cell masses were measured at 96 hpi via RealTime-Glo™ MT cell viability assay. Displayed are values and SD of one experiment performed in triplicates. 50 % remaining cell mass is indicated by dotted lines. MOCK: uninfected control (black columns). Statistical significance: \*:  $p \leq 0.05$ ; \*\*:  $p \leq 0.01$ ; \*\*\*:  $p \leq 0.001$ ; \*\*\*\*:  $p \leq 0.0001$  - nonsignificant results are not indicated; significance is only displayed when a change to the next lower MOI occurred.

**Figure 17** shows, that in NC cell line Ty-82 high MOIs of all three applied virotherapeutics led to a reduction of cell viability which was measured via the RealTime-Glo™ MT cell viability assay.

For MeV-GFP as well as for GLV-0b347 no effect got visible until the highest tested MOI of 10 or MOI of 1, respectively, where a significant decrease of viable cell masses to 23 %, respectively 40 % was measured. The lower tested MOIs did not show a MOI-dependent decrease of cell masses; MOI 0.01 of MeV-GFP even led to a significant increase of the cell mass compared to the MOCK treated control.

T-VEC treatment, on the contrary, led to a MOI-dependent decrease of cell mass being significant for MOI 0.01 and higher. While at MOI 0.01 70 % of the cell mass was still viable, this amount further decreased to 20 % (MOI 0.1), and at a MOI of 1 only 5 % of the cell mass was still viable.

## 3.2.6 First studies on floating BRD3-NUT cell line 10326

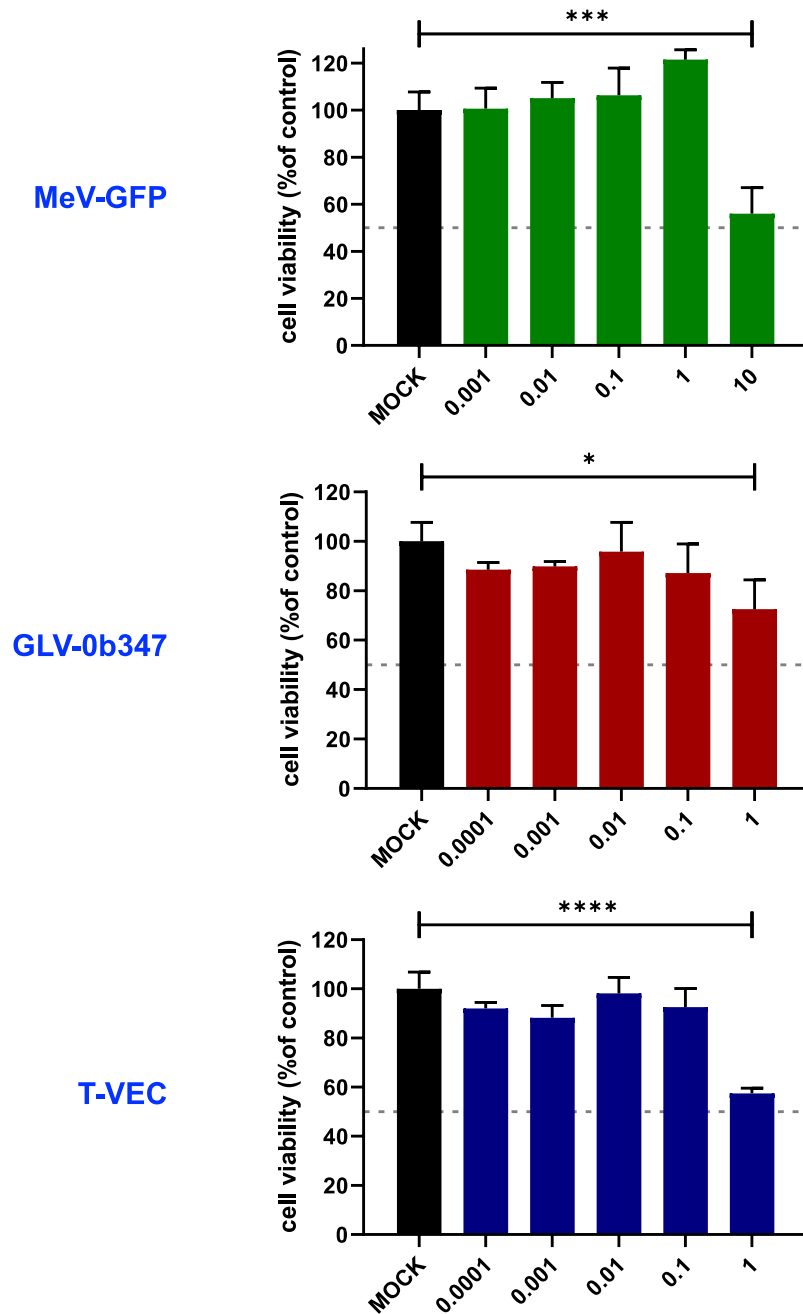


Figure 18: NC cell line 10326 infected with oncolytic viruses.

The NUT carcinoma cell line 10326 was infected with the oncolytic measles vaccine virus MeV-GFP (upper panel), the oncolytic vaccinia vaccine virus GLV-0b347 (middle panel) and the oncolytic herpes simplex virus T-VEC (lower panel) at indicated multiplicities of infection (MOI). The remaining cell masses were measured at 96 hpi via RealTime-Glo™ MT cell viability assay. Displayed are values and SD of one experiment performed in triplicates. 50 % remaining cell mass is indicated by dotted lines. MOCK: uninfected control (black columns). Statistical significance: \*:  $p \leq 0.05$ ; \*\*:  $p \leq 0.01$ ; \*\*\*:  $p \leq 0.001$ ; \*\*\*\*:  $p \leq 0.0001$  - nonsignificant results are not indicated; significance is only displayed when a change to the next lower MOI occurred.

The viability of the *BRD3-NUT* cell line 10326 after infection with the different OVs was measured via RealTime-Glo™ MT cell viability assay. Similar to Ty-82 cells, the non-adherent growth of the cell line 10326 did not allow the implementation of the SRB assay.

It is notable that none of the tested MOIs of all three oncolytic viruses, MeV-GFP, GLV-0b347 and T-VEC, decreased the cell viability to < 50 % in comparison to the MOCK treated control (**Figure 18**).

For all viruses it is also valid that only the highest tested MOI was able to achieve a significant reduction of the cell viability: MOI 10 of MeV-GFP led to a reduction to 56 % and MOI of 1 of T-VEC to 57 %. After GLV-0b347 infection with MOI 1 still 73 % of the cells were viable.

For all lower tested MOIs no MOI-dependent decrease of cell viability got visible; for MOI 1 of MeV-GFP even an increase in cell viability was measured, which was not significant though.

### 3.2.7 Comparison of SRB assay and RealTime-Glo™ assay

To see whether the results obtained via SRB assay are comparable to the results obtained via the RealTime-Glo™ assay, the RealTime-Glo™ assay was performed once with the adherent NC cell line 143100 (**Figure 19**).

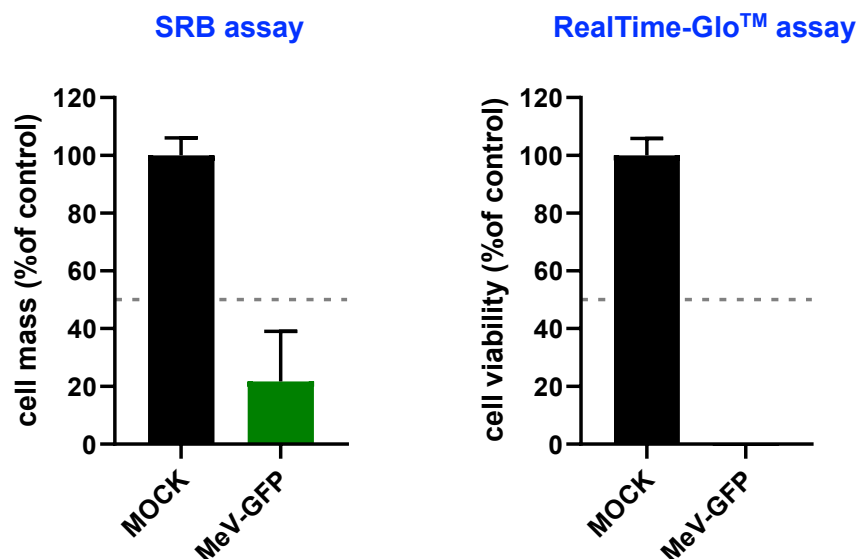


Figure 19: Comparison of the results measured via SRB assay and RealTime-Glo™ assay.

The NUT carcinoma cell line 143100 was treated with MeV-GFP (MOI 10). At 96 hpi the remnant cell mass was measured via SRB assay or the cell viability was measured via RealTime-Glo™ MT Cell Viability assay. SRB assay: Displayed are mean values and SD of three independent experiments performed in quadruplicates. RealTime-Glo™ assay: Displayed are mean values and SD of one experiment performed in triplicates. 50 % remaining cell mass is indicated by dotted lines. MOCK: uninfected control (black columns).

When the remnant cell mass was measured via SRB assay, 22 % of the cell mass in comparison to the MOCK treated control was still viable (see 3.3.2). The cell viability measured via the RealTime-Glo™ assay was found to be < 1 % of the MOCK treated control.



### 3.3 Effects of BET-inhibitors on proliferation and cell death of NC cell lines

Even though BET-Inhibitors were already tested in multiple *in vitro* studies on NUT carcinoma cell lines and even first clinical trials are currently running, the effect of these specific inhibitors had to be tested on each cell line, to find the suitable concentrations for combinatorial treatment of oncolytic viruses and iBET.

Two different iBET compounds, BI894999 (generated by Boehringer-Ingelheim, Vienna, Austria) and GSK525762 (generated by Glaxo-Smith-Kline, London-Brendford, Great Britain), were used in this thesis.

For both compounds the effect was tested via SRB assay at 24 h, 48 h, 72 h and 96 h post treatment (see 2.2.3.1). In contrast to infection with oncolytic viruses, first, the suitable range of iBET concentrations had to be identified, as there was little previous knowledge about its efficiency. Therefore, experiments with concentrations varying between 0.05 nM and 2.5  $\mu$ M (for BI894999) and 0.001  $\mu$ M and 10  $\mu$ M (for GSK525762) respectively were performed. First, a broad range of concentrations was used, which was narrowed down in the following experiments to get more precise results.

Additionally, an xCELLigence<sup>®</sup> assay was performed to monitor the real-time proliferation of the cell lines for 96 h post treatment with both iBET (see 2.2.5.4).

### 3.3.1 Reaction of NC cell line HCC2429 to iBET treatment

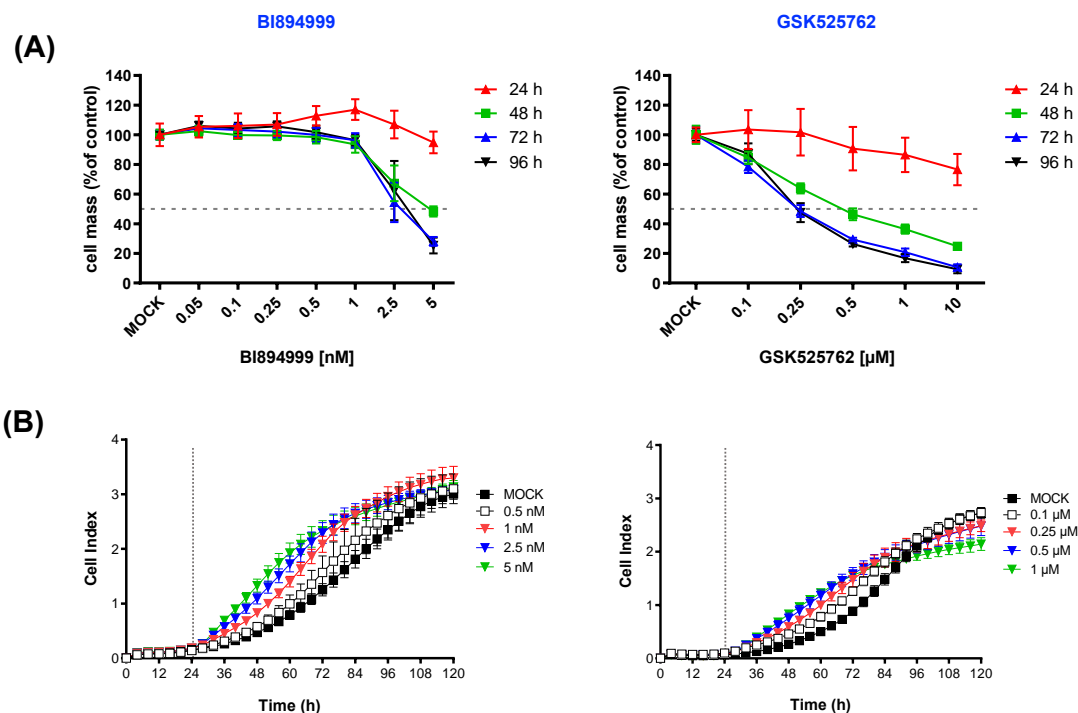


Figure 20: NC cell line HCC2429 after treatment with BET inhibitors (iBET).

NUT carcinoma cell line HCC2429 was treated with depicted concentrations of iBET BI894999 (left column) and iBET GSK525762 (“Molibresib”) (right column). **(A)** The remaining cell mass was measured via Sulforhodamine B assay at 24 h, 48 h, 72 h and 96 h after the treatment. Displayed are mean values and SD of at least three independent experiments performed in triplicates. 50 % remaining cell mass is indicated by dotted horizontal lines. MOCK: untreated control. **(B)** Real-time dynamic cell proliferation was monitored for 120 h using xCELLigence RTCA SP system. 24 h after seeding the iBET were added. For the iBET BI894999 one representative experiment out of two is shown. For GSK525762 only one proof-of-principle experiment was performed. Displayed are mean values and SD of one experiment performed in quadruplicates. Start of iBET treatment is indicated by dotted vertical lines. MOCK: untreated control.

When using sub-nanomolar concentrations of BI894999 (0.05 - 1 nM) no significant reduction of cell mass was achieved irrespectively of the incubation time (**Figure 20 A**). The first noteworthy reduction of cell mass was seen at a concentration of 2.5 nM, where cell mass decreased to 62 % after 96 h. The shortest incubation time of 24 h did not lead to any effect, while the maximal reduction was reached after 48 h, and a longer incubation of 72 h or 96 h did not result in any further reduction of cell mass. At the highest tested concentration of 5 nM the cell mass dropped to 48 % of control after 48 h. Only here, a further reduction to 28 % at 72 h of incubation could be noticed, which was similar to the result after 96 h (25 %).

---

The results for GSK525762 appeared similar regarding the different incubation times: While after 24 h only the highest tested concentration led to a minor cell mass reduction, after 48 h a dose dependent decrease of cell mass was observed starting at 0.1  $\mu\text{M}$ . This effect was enhanced after 72 h whereas after 96 h no further reduction of cell mass was observed.

Generally, higher concentrations of GSK5252762 than of BI894999 were needed to achieve cell mass reduction. Whereas the concentration of 0.1  $\mu\text{M}$  still left ca. 85 % of the cell viable at all timepoints  $\geq$  48 h, with the concentration of 0.25  $\mu\text{M}$  a decrease to less than 50 % could be reached after 72 h of incubation. For this concentration an additional effect of 15 - 20 % further cell mass reduction after 72 h of incubation compared to 48 h became visible. This enhancing effect could also be seen with all tested higher concentrations resulting in only 10 % viable cells with 10  $\mu\text{M}$  iBET after 72 h.

Interestingly, in the xCELLigence<sup>®</sup> assay no reduction of the impedance got visible (**Figure 20 B**). After iBET treatment at 24 h the treated cells show a concentration-dependent higher impedance signal compared to the control: The more inhibitor applied, the higher the signal. Interestingly, no increase of cell mass was observed at the 24 h post treatment measurement via SRB assay. After 120 h (96 h post iBET treatment) all groups ended with no significant difference between each other. These results were the same for both iBET tested, excluding the highest tested concentration of GSK525276 (1  $\mu\text{M}$ ) where a small decrease of the cell index after 120 h from 2.7 to 2.1 (78 % of MOCK value) got visible, which still showed no similarity to the SRB assay results in which after 96 h of incubation a decrease in cell mass to 10 % was noticed.

### 3 Results

---

#### 3.3.1.1 IC<sub>50</sub> values for the iBET in NC cell line HCC2429

The data of the SRB-assay results described in 3.3.1 were also used for the calculation of the half maximal inhibitory concentration (IC<sub>50</sub>). Hereby, only the values of 96 h incubation time were taken into account. The data were transformed and plotted using a non-linear regression (see 2.2.8).

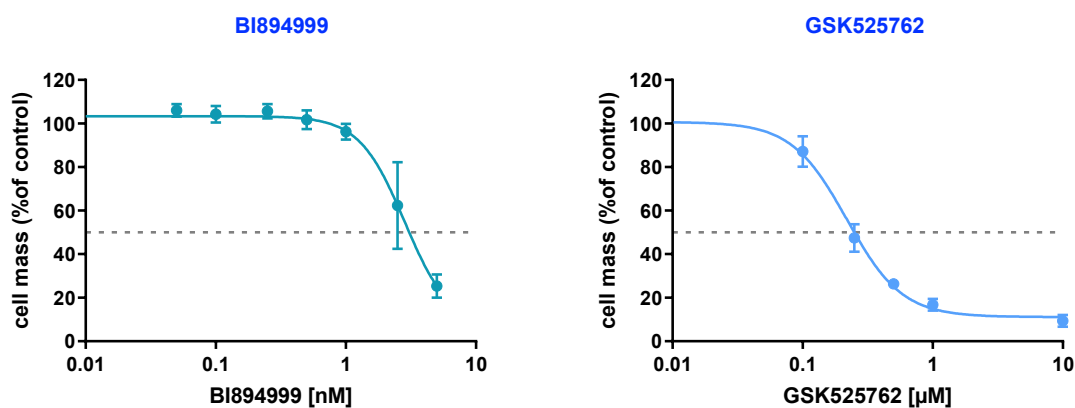


Figure 21: Graph used for calculation of the IC<sub>50</sub> values of iBET in NC cell line HCC2429.

The IC<sub>50</sub> values in the NC cell line HCC2429 were 2.835 nM for iBET BI894999 and 0.219 µM for GSK525762 (**Figure 21**).

### 3.3.2 Reaction of NC cell line 143100 to iBET treatment

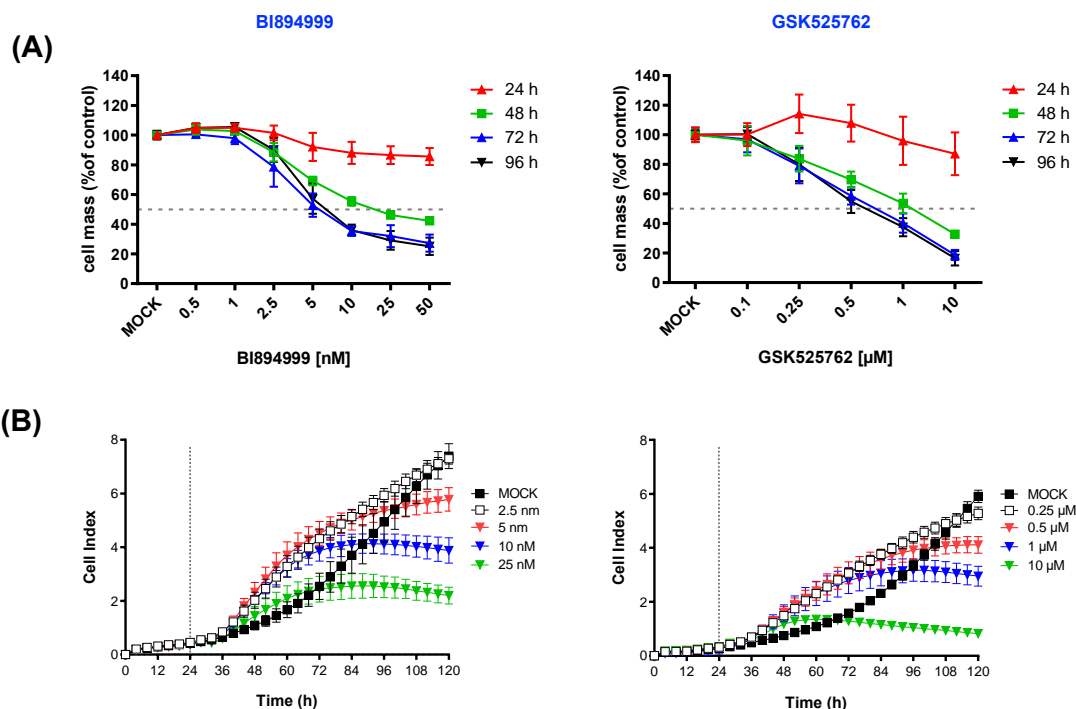


Figure 22: NC cell line 143100 after treatment with BET inhibitors (iBET).

NUT carcinoma cell line 143100 was treated with depicted concentrations of iBET BI894999 (left column) and iBET GSK525762 (“Molibresib”) (right column). **(A)** The remaining cell mass was measured via Sulforhodamine B assay at 24 h, 48 h, 72 h and 96 h after treatment. Displayed are mean values and SD of at least three independent experiments performed in triplicates. 50 % remaining cell mass is indicated by dotted horizontal lines. MOCK: untreated control. **(B)** Real-time dynamic cell proliferation was monitored for 120 h using xCELLigence RTCA SP system. 24 h after seeding iBET were added. For the iBET BI894999 one representative experiment out of two is shown. For GSK525762 only one proof-of-principle experiment was performed. Displayed are mean values and SD of one experiment performed in quadruplicates. Start of iBET treatment is indicated by dotted vertical lines. MOCK: untreated control.

For NC cell line 143100 the two tested iBET led to a decreasing cell mass when applied in higher concentrations for at least 48 h, which can be seen in the SRB assay results (**Figure 22 A**) as well as in the xCELLigence<sup>®</sup> assay results (**Figure 22 B**).

For the SRB assay the iBET BI894999 started to take effect at a concentration of 2.5 nM after 48 h (88 % remnant cell mass). The curve follows a for enzyme inhibition typical sigmoidal shape, leading to a decrease of cell mass to 42 % at the highest tested concentration of 50 nM after 48 h. The results for 72 h and 96 h of incubation time were almost identical and followed the course of the 48 h results just leaving approximately 15 - 20 % less viable cells at a concentration of 5 nM and higher.

### 3 Results

---

Essentially, these statements are also valid for iBET GSK525762. After 24 h no effect on the cell line was visible, independent of the applied concentration. While the lowest tested concentration of 0.1  $\mu\text{M}$  did also not lead to effects at any incubation time, first effects became visible with 0.25  $\mu\text{M}$  applied. While here still no differentiation between 48 h, 72 h and 96 h of incubation could be made (ca. 80 % remnant cell mass at all three timepoints), the curves for 48 h and the two longer incubation times started to separate at 0.5  $\mu\text{M}$  (remnant cell mass: 70 % after 48 h respectively ca. 55 % after 72 h / 96 h). This decrease continued for the higher concentrations of 1  $\mu\text{M}$  and 10  $\mu\text{M}$ , where after  $\geq 72$  h only 38 % and 17 % of the cells were still viable, respectively.

The findings of the SRB assay were confirmed by the xCELLigence<sup>®</sup> assay. For both iBET applies: The higher the inhibitor concentration applied the lower the cell index after 120 h was. But 12 h after the iBET were applied (36 h) first a faster increasing impedance signal could be detected. This higher signal lasted until 60 h after seeding, at a high concentration of 10  $\mu\text{M}$  GSK525762 it even lasted only until 48 h. Then, this increase for the treated cells slowed down. Interestingly, no increase of cell mass was observed at the 24 h post treatment measurement via SRB assay. In case of 10 nM and 25 nM BI894999 and 1  $\mu\text{M}$  GSK525762 respectively the cell mass even began to shrink again after 84 h. For 10  $\mu\text{M}$  GSK525762 this reduction of cell mass was noticed already after 60 h. The cell index at the endpoint of 120 h was 7.3 for MOCK as well as for 2.5 nM and dropped to 5.8 (79 % of MOCK) (5 nM), 3.9 (53 % of MOCK) (10 nM) respectively 2.4 (33 % of MOCK) (25 nM) for BI894999. So, the cell index in percentage of MOCK was slightly higher than the remnant cell mass measured at the same concentrations after 96 h.

For GSK762525 the MOCK value was 5.9 after 120 h dropping to 4.1 (69 % of MOCK) at 0.5  $\mu\text{M}$  and 2.9 (49 % of MOCK) at 1  $\mu\text{M}$ , respectively. A concentration of 10  $\mu\text{M}$  decreased the cell index to 0.8 (14 % of MOCK). Therefore, the decrease of the impedance signal correlates well with the decrease of viable cell mass at the same concentrations after 96 h.

### 3.3.2.1 IC<sub>50</sub> values for the iBET in NC cell line 143100

The data of the SRB-assay results described in 3.3.2 were also used for the calculation of the half maximal inhibitory concentration (IC<sub>50</sub>). Hereby only the values of 96 h incubation time were taken into account. The data were transformed and plotted using a non-linear regression (see 2.2.8).

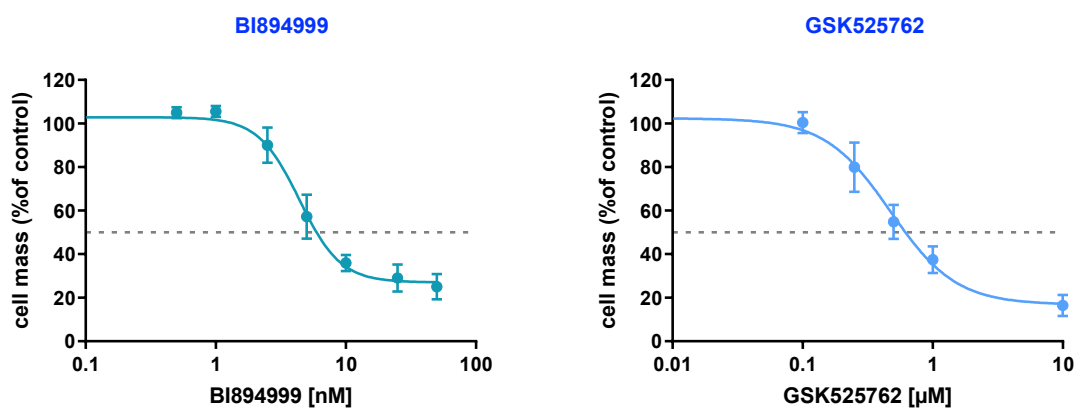


Figure 23: Graph used for calculation of the IC<sub>50</sub> values of iBET in NC cell line 143100.

The IC<sub>50</sub> values in the NC cell line HCC2429 were 4.397 nM for iBET BI894999 and 0.473 µM for GSK525762 (**Figure 23**).

### 3.3.3 Reaction of NC cell line 690100 to iBET treatment

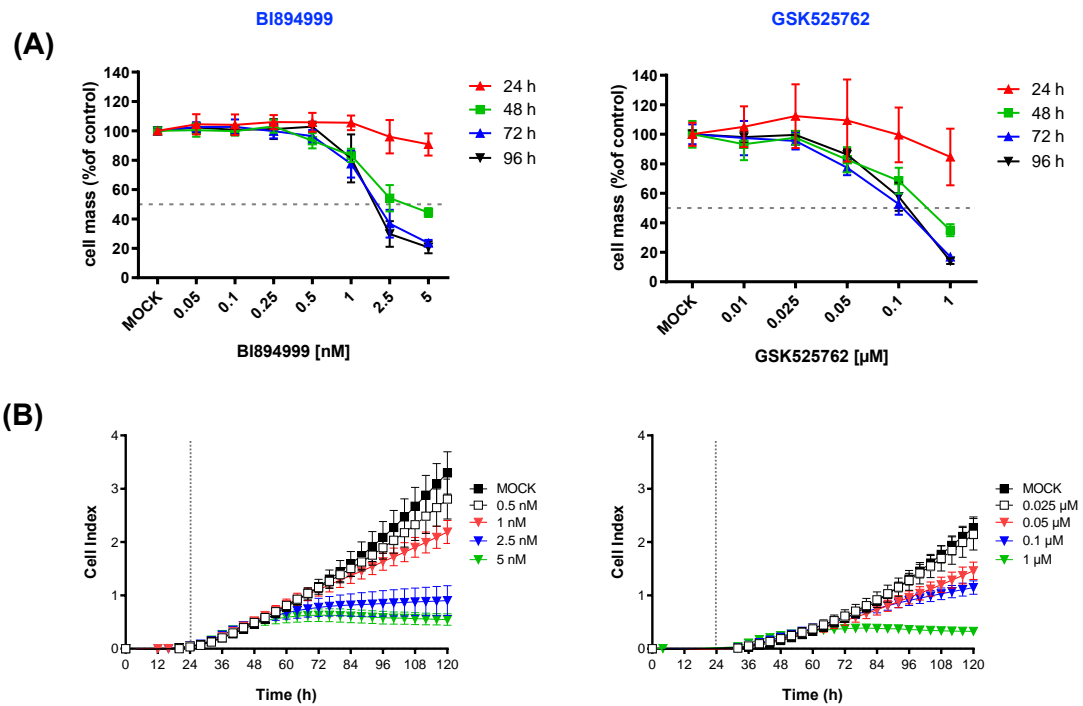


Figure 24: NC cell line 690100 after treatment with BET inhibitors (iBET).

NUT carcinoma cell line 690100 was treated with depicted concentrations of iBET BI894999 (left column) and iBET GSK525762 (“Molibresib”) (right column). **(A)** The remaining cell mass was measured via Sulforhodamine B assay at 24 h, 48 h, 72 h and 96 h after treatment. Displayed are mean values and SD of at least three independent experiments performed in triplicates. 50 % remaining cell mass is indicated by dotted horizontal lines. MOCK: untreated control. **(B)** Real-time dynamic cell proliferation was monitored for 120 h using xCELLigence RTCA SP system. 24 h after seeding the iBET were added. For the iBET BI894999 one representative experiment out of two is shown. For GSK525762 only one proof-of-principle experiment was performed. Displayed are mean values and SD of one experiment performed in quadruplicates. Start of iBET treatment is indicated by dotted vertical lines. MOCK: untreated control.

As displayed in **Figure 24 A**, treatment with both iBET tested led to a decreasing cell mass of 690100 cells in a concentration-dependent matter.

For both iBET the treatment was only effective if it was applied for at least 48 h; at no tested concentration a reduction of cell mass got visible after 24 h of incubation already.

The first concentration of BI894999 resulting in cell mass reduction was 1 nM (80 % in comparison to MOCK), the lower tested concentrations of 0.05 - 0.5 nM did not lead to a change at any tested incubation time. While for 1 nM no benefit of an incubation time longer than 48 h was visible, at the concentrations of 2.5 nM and 5 nM after 72 h a further cell mass reduction of ca. 20 % (54 %



---

compared to 36 % and 44 % compared to 24 %) occurred. The effect was not additionally intensified after 96 h.

A concentration of 0.05  $\mu\text{M}$  of GSK762525 was needed to achieve a reduction of cell mass to ca. 80 % at timepoints  $\geq 48$  h of incubation. A further reduction of cell mass at  $> 48$  h post infection was only noticed at the highest tested concentration of 1  $\mu\text{M}$  leading to an additive reduction of cell mass from 34 % (48 h) to 15 % ( $\geq 72$  h).

The xCELLigence<sup>®</sup> assay confirmed these results (**Figure 24 B**). A change in cell index was also found at a concentration of 1 nM for BI894999 and 0.05  $\mu\text{M}$  for GSK762525.

Corresponding to the SRB assay results, 2.5 nM of BI894999 led to an eminent further reduction of the cell index (30 % of MOCK value), whereas doubling the concentration to 5 nM brought only a small additional benefit (16 % of MOCK value). However, treatment with 5 nM resulted in a decrease of cell index after 72 h, whereas in contrast to the concentration of 2.5 nM a minimal increase of the cell index was noticed for the whole observation period of 120 h. The results are very similar between cell index in the xCELLigence<sup>®</sup> assay and remnant cell mass after 96 h in the SRB assay.

Also, the results of GSK762525 treatment showed the same tendency seen in the SRB assay. The drop in the cell index from MOCK value 2.3 to 1.1 at 0.1  $\mu\text{M}$ , equating 48 % of MOCK value, as well as the reduction to 0.3 for 1  $\mu\text{M}$ , equating 13 % of MOCK value, resemble the results of the SRB assay.

### 3 Results

---

#### 3.3.3.1 IC<sub>50</sub> values for the iBET in NC cell line 143100

The data of the SRB-assay results described in 3.3.3 were also used for the calculation of the half maximal inhibitory concentration (IC<sub>50</sub>). Hereby only the values of 96 h incubation time were taken into account. The data were transformed and plotted using a non-linear regression (see 2.2.8).

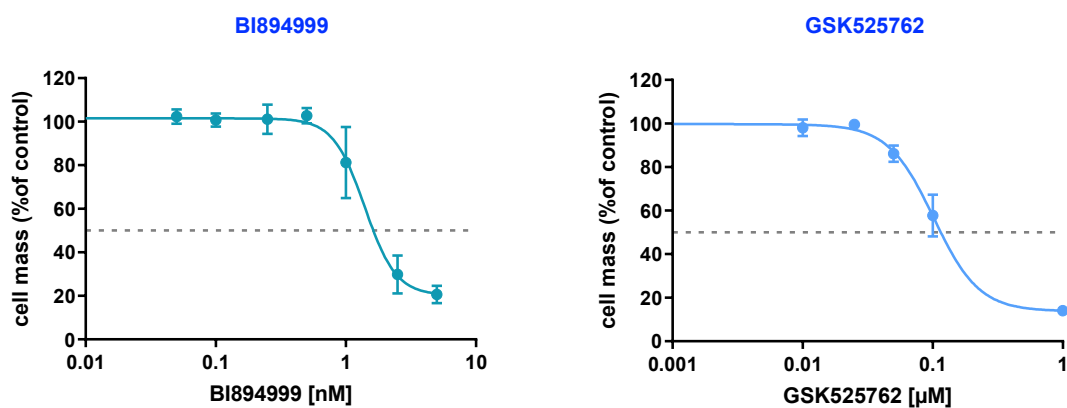


Figure 25: Graph used for calculation of the IC<sub>50</sub> values of iBET in NC cell line 690100.

The IC<sub>50</sub> values in the NC cell line HCC2429 were 1.396 nM for iBET BI894999 and 0.102 µM for GSK525762 (**Figure 25**).

### 3.3.4 Comparison of the effects of iBET on the different tested NC cell lines

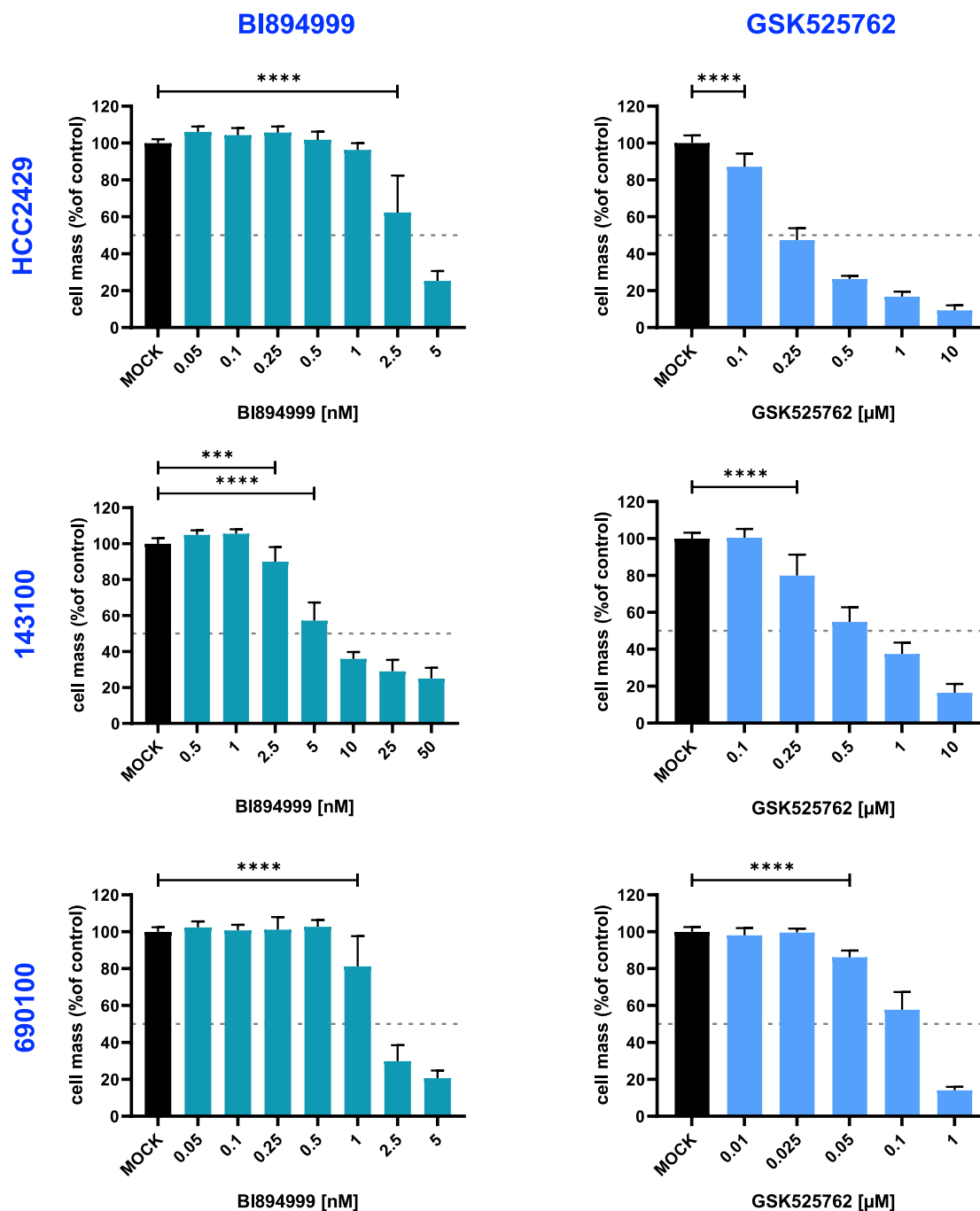


Figure 26: Comparison of SRB-assay results of NC cell lines HCC2429, 143100, 690100 after treatment with BET inhibitors (iBET).

The NUT carcinoma cell lines HCC2429, 143100 and 690100 were treated with depicted concentrations of iBET BI894999 (upper panel) and iBET GSK525762 ("Molibresib") (lower panel). The remaining cell mass was measured via Sulforhodamine B (SRB) assay at 96 h after iBET treatment. Displayed are mean values and SD of at least three independent experiments performed in triplicates. 50 % remaining cell mass is indicated by dotted lines. MOCK: uninfected control. Statistical significance: \*:  $p \leq 0.05$ ; \*\*:  $p \leq 0.01$ ; \*\*\*:  $p \leq 0.001$ ; \*\*\*\*:  $p \leq 0.0001$  - nonsignificant results are not indicated; significance is only displayed when a change to the next lower concentration occurred.

**Figure 26** compares the remaining cell masses measured via SRB assay of the three NC cell lines HCC2429, 143100 and 690100 96 h after iBET treatment.

When treated with BI894999 the cell lines HCC2429 and 690100 reacted similar: Nearly no effect of the iBET on the cell mass was seen for concentrations  $\leq 1$  nM. A concentration of 5 nM led to a highly reduced cell mass of about 25 % in comparison to MOCK. The only major difference was seen at 2.5 nM: While 62 % of HCC2429 cells were still viable, this was true for only 30 % of 690100 cells. The third cell line 143100 proved to be the most resistant cell line. Here a concentration of 5 nM only led to a reduction to 57 %; to achieve only 25 % remnant cell mass 50 nM of the iBET was needed.

Also, for the iBET GSK762525 it was observed that 143100 is the most resistant cell line and HCC2429 and 690100 cells reacted quite similar, the largest difference occurred in a concentration at which the first effects got visible (0.1  $\mu$ M). Once more, this change disappeared at a higher concentration of GSK762525 (1  $\mu$ M).

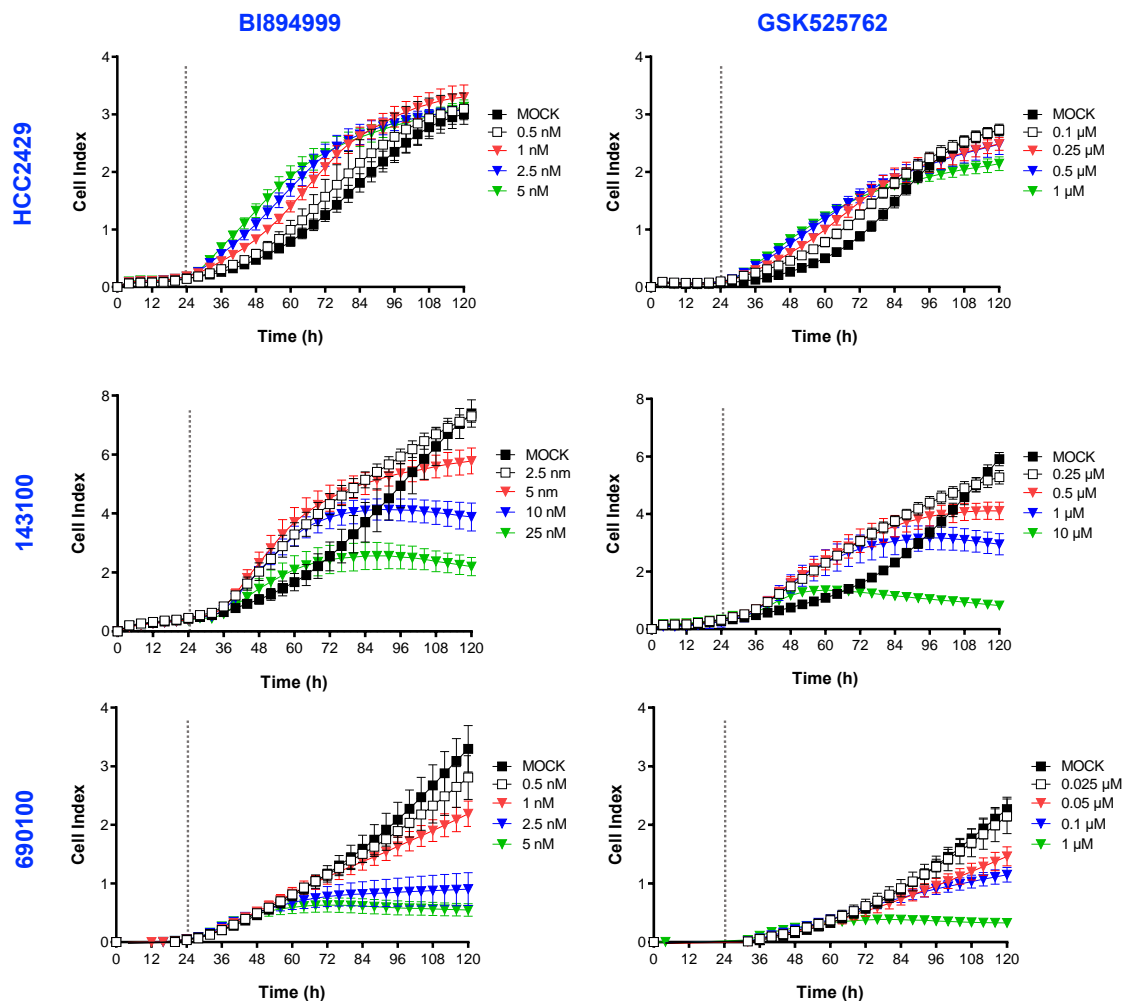


Figure 27: Comparison of xCELLigence®-assay results of NC cell lines HCC2429, 143100, 690100 after treatment with BET inhibitors (iBET).

NUT carcinoma cell lines HCC2429, 143100 and 690100 were treated with depicted concentrations of iBET BI894999 (upper panel) and iBET GSK525762 (“Molibresib”) (lower panel). Real-time dynamic cell proliferation was monitored for 120 h using the xCELLigence® RTCA SP system. 24 h after seeding the iBET was added. For the iBET BI894999 one representative experiment out of two is shown. For GSK525762 only one proof-of-principle experiment was performed. Displayed are mean values and SD of one experiment performed in quadruplicates. Start of iBET treatment is indicated by dotted lines. MOCK: untreated control.

Comparison of the proliferation curves observed via xCELLigence® assay shows different growth characteristics of the three NC cell lines HCC2429, 143100 and 690100 both without and after iBET treatment (**Figure 27**). While untreated HCC2429 and 690100 cells showed an increase of cell index to three, the value for 143100 cells increased to six, indicating a much faster cell growth. Interestingly, all three cell lines showed different growth characteristics, although they were fairly consistent in one cell line for both iBET.

In cell line HCC2429 a concentration-dependent increasing cell proliferation for approximately 24 h (compared to the MOCK treated cells) starting 12 h post treatment could be noticed. However, at the endpoint the cell index had not decreased in a concentration dependent matter.

Cell line 143100 also showed the concentration-dependent increasing cell proliferation. But in this cell line the proliferation started to decrease highly resulting in a concentration dependent lower cell index at the endpoint.

For the third cell line 690100 though, there was no concentration-dependent increase of cell proliferation in the first hours after treatment. But as in cell line 143100 the proliferation reduced concentration dependently after 60 h.

#### **3.4 Combinatorial therapy of NC cell lines with immunovirotherapeutics and BET-inhibitors**

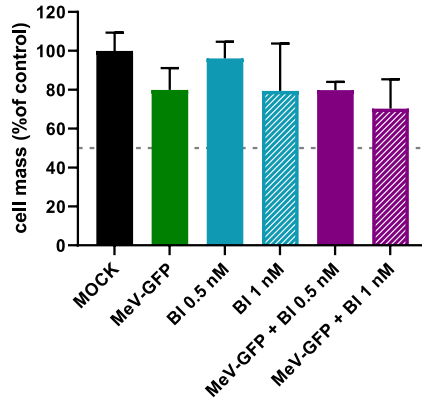
Since iBET therapy proved insufficient as a monotherapeutic to treat NC in most clinical trials, it was tested, if a combination of iBET and oncolytic virotherapy might be a powerful therapeutic option.

The concentrations of iBET and OV were chosen to leave 50 % to 75 % of remaining cell mass after respective monotherapy, thus additional effects as well as inhibitory effects of the combination of both agents were observable. All three oncolytic viruses were combined with both iBET, to see whether the effect of the combination differed between the selected OV or iBET.

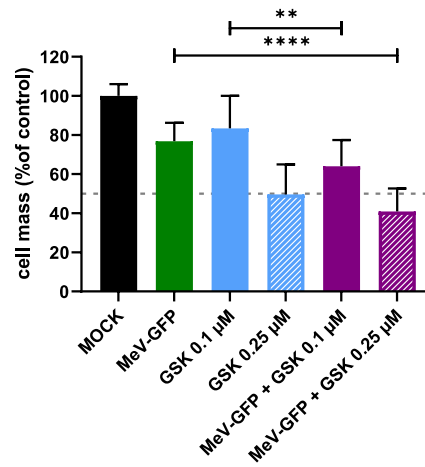
In order to determine whether a benefit occurred with the combinatorial treatment, this treatment always had to be compared with the most efficient monotherapeutic agent. Therefore, a significant benefit was only seen when OV and iBET monotherapy showed a significantly higher remaining cell mass than the corresponding combination.

### 3.4.1 Combinatorial iBET and OV treatment of the NC cell line HCC2429

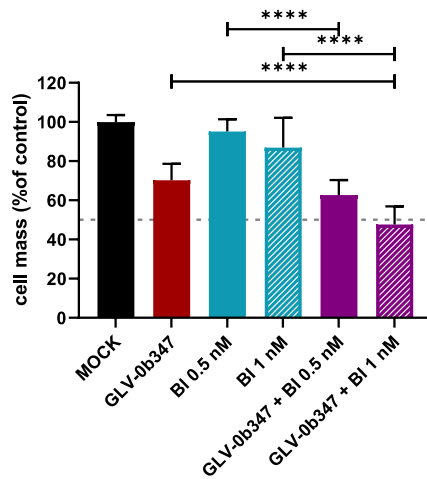
MeV-GFP + BI894999



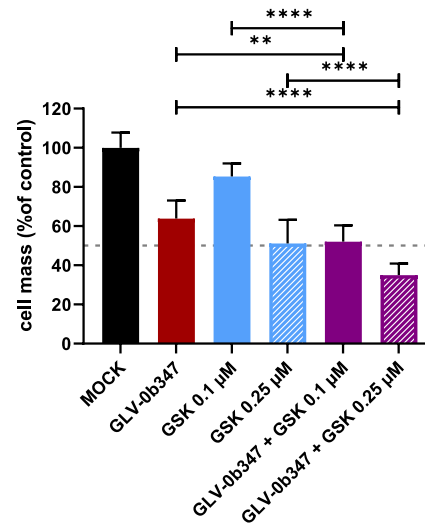
MeV-GFP + GSK525762



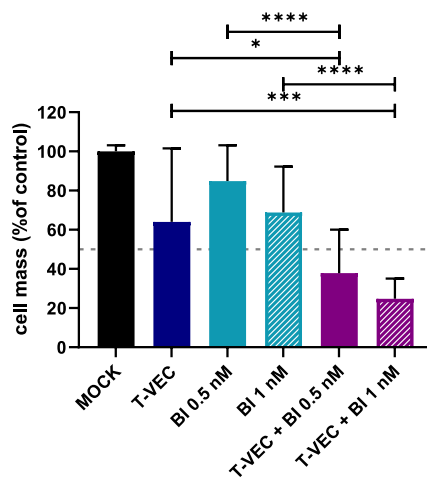
GLV-0b347 + BI894999



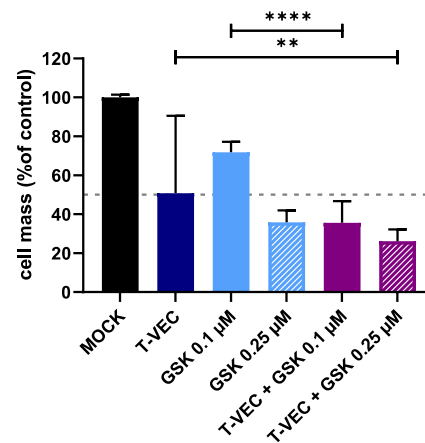
GLV-0b347 + GSK525762



T-VEC + BI894999



T-VEC + GSK525762



### 3 Results

---

*Figure 28: NC cell line HCC2429 treated with different oncolytic viruses in combination with two different iBET.*

The NUT carcinoma cell line HCC2429 was infected with MeV-GFP (MOI 0.1), GLV-0b347 (MOI 0.005) or T-VEC (MOI 0.0001). At 3 hpi (for MeV-GFP) and 1 hpi (for GLV-0b347 and T-VEC) the inoculum was removed and medium with or without iBET was added. The MOIs and iBET concentrations were chosen to leave between 50 % and 75 % of the cell mass in the respective monotherapy. The remaining cell mass was measured at 96 hpi via Sulforhodamine B (SRB) assay. Displayed are mean values of three independent experiments performed *in quadruplicates*. 50 % remaining cell mass is indicated by dotted lines. *MOCK: uninfected control (black columns)*. Statistical significance: \*:  $p \leq 0.05$ ; \*\*:  $p \leq 0.01$ ; \*\*\*:  $p \leq 0.001$ ; \*\*\*\*:  $p \leq 0.0001$  - nonsignificant results are not indicated; significance is only displayed between the monotherapeutic approaches and the corresponding combinatorial treatment.

For NC cell line HCC2429 only two of the six tested combinations (GLV-0b347 + GSK525762 and T-VEC + BI894999) showed a significant decrease of the remaining cell mass in the combinatorial therapy, regardless the iBET concentration (**Figure 28**).

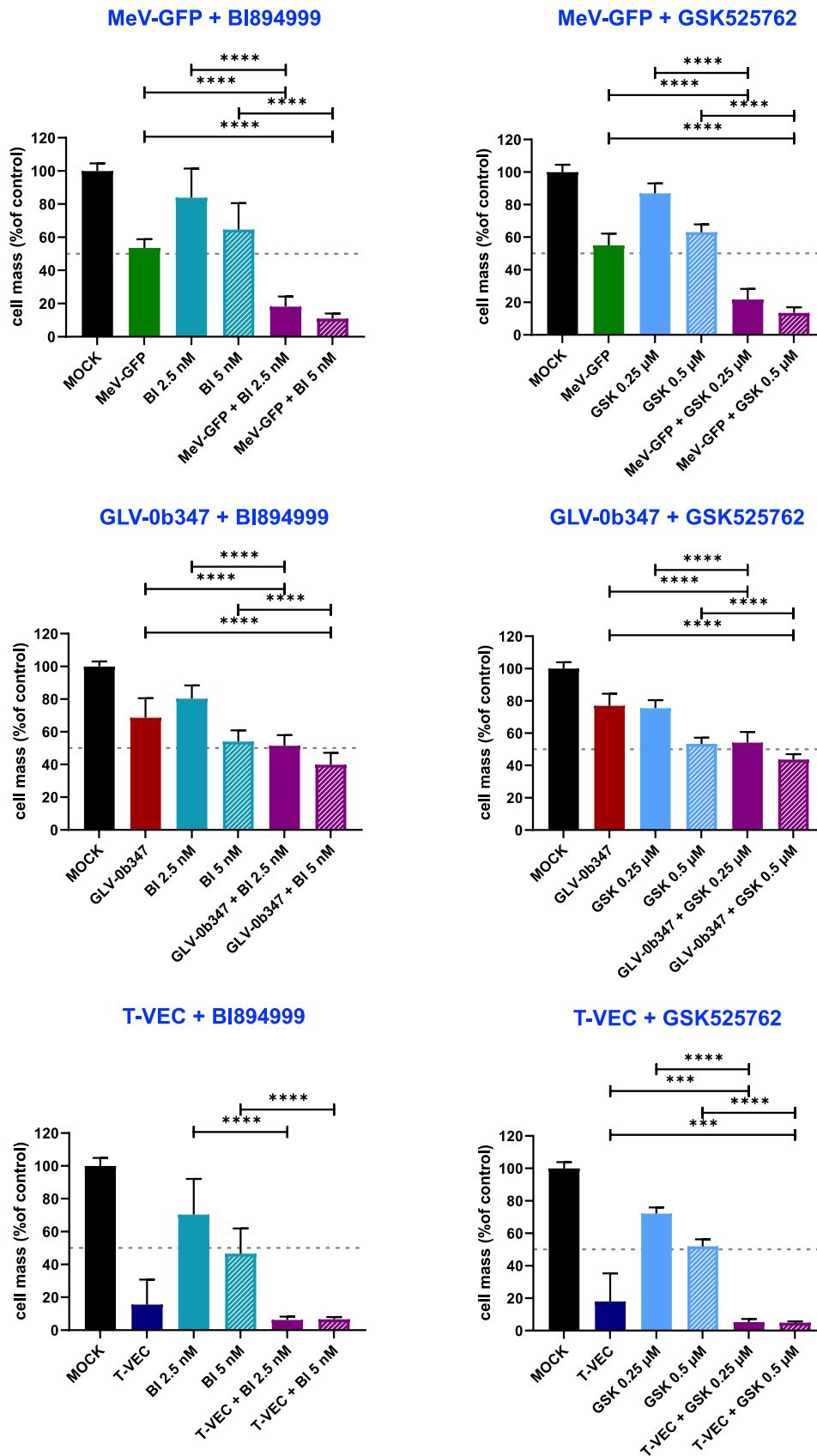
The combination of MeV-GFP with iBET did not lead to a significant decrease when compared to the monotherapeutic approaches.

However, this was different for the combination of GLV-0b347 with iBET. While for GLV-0b347 + BI894999 only a significant decrease got visible for the higher tested iBET concentration of 1 nM (70% remnant cell mass with GLV-0b347 respectively 48% with GLV-0b347 + 1 nM BI894999), GLV-0b347 in combination with GSK525762 proved to be more efficient with both concentrations of iBET tested.

Interestingly, for T-VEC the combinatorial treatment with BI894999 proved to be more effective with both tested concentrations of iBET (64 % remnant cell mass with T-VEC respectively 38 % with T-VEC + 0.5 nM iBET and 25 % with T-VEC + 1 nM iBET). However, when combined with GSK525762, no significant decrease was noticed. Of note, in both experiments the error bars for T-VEC monotherapy are very high.



### 3.4.2 Combinatorial iBET and OV treatment of the NC cell line 143100



### 3 Results

---

*Figure 29: NC cell line 143100 treated with different oncolytic viruses in combination with two different iBET.* The NUT carcinoma cell line 143100 was infected with MeV-GFP (MOI 1), GLV-0b347 (MOI 0.001) or T-VEC (MOI 0.0001). At 3 hpi (for MeV-GFP) and 1 hpi (for GLV-0b347 and T-VEC) the inoculum was removed and medium with or without iBET was added. The MOIs and iBET concentrations were chosen to leave between 50 % and 75 % of the cell mass in the respective monotherapy. The remaining cell mass was measured at 96 hpi via Sulforhodamine B (SRB) assay. Displayed are mean values of three independent experiments performed in quadruplicates. 50 % remaining cell mass is indicated by dotted lines. MOCK: uninfected control (black columns). Statistical significance: \*:  $p \leq 0.05$ ; \*\*:  $p \leq 0.01$ ; \*\*\*:  $p \leq 0.001$ ; \*\*\*\*:  $p \leq 0.0001$  - nonsignificant results are not indicated; significance is only displayed between the monotherapeutic approaches and the corresponding combinatorial treatment.

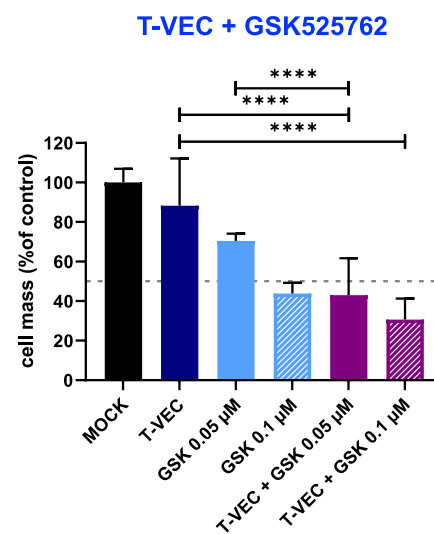
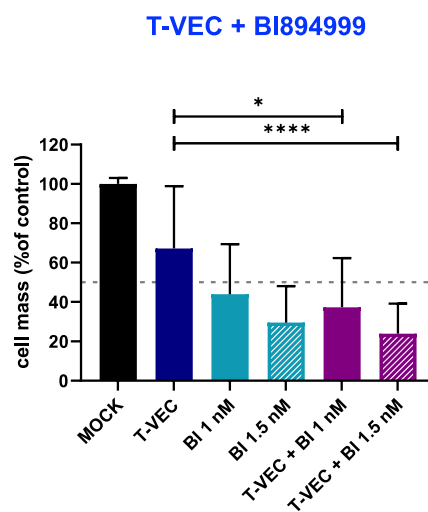
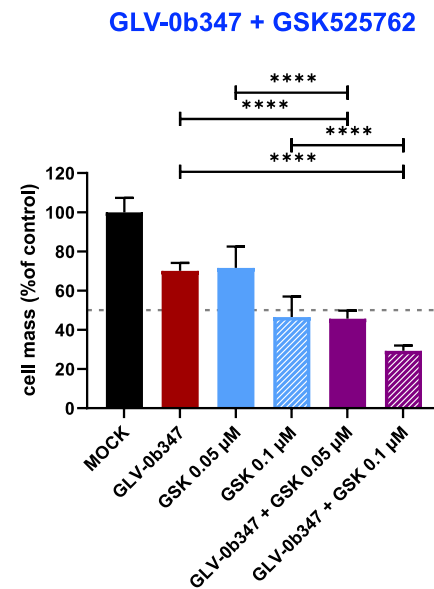
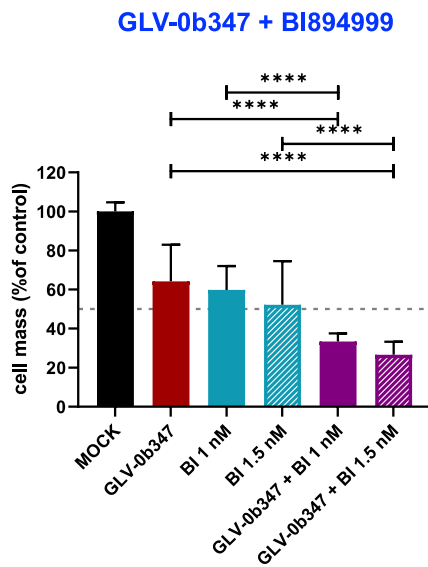
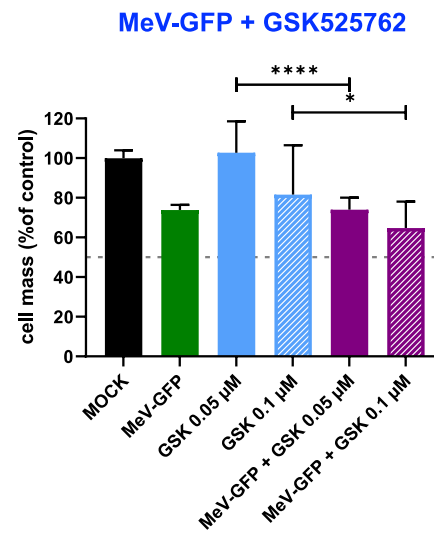
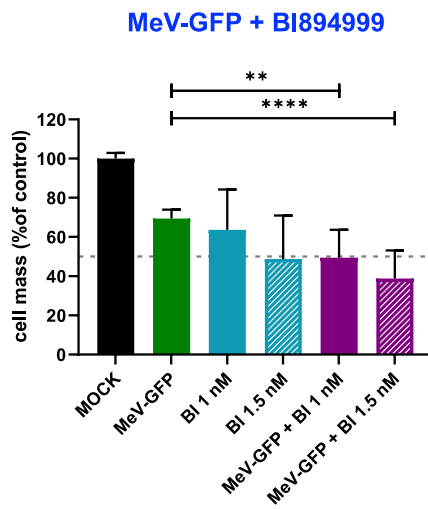
The combinatorial treatment with OV and iBET in the NC cell line 143100 showed a significant decrease of cell mass in five of six combinations, excluding only the combination of T-VEC + BI894999 (**Figure 29**).

Of note, combining MeV-GFP with either of the two iBET led to an eminent further decrease of the cell mass: The monotherapeutic approach with MeV-GFP at a MOI of 1 reduced the cell mass to 55 %, the combinatory treatment with the higher concentration of either iBET led to a further reduction of > 40 %, leaving only a viable cell mass of ca. 10 %.

The combinations of the other two OVs with the iBET were not able to achieve such a further reduction. For T-VEC only a further reduction of around 10 %, regardless the iBET used, got visible. For GLV-0b347 the further reduction was around 15 %, when comparing the monotherapy with the combinatorial approach with the lower tested iBET concentration. For the higher iBET concentration the benefit was even lower.

Since already a very low MOI of 0.0001 of T-VEC reduced the cell mass in the monotherapeutic approach to < 20 %, it was difficult to observe an additional decrease.

### 3.4.3 Combinatorial iBET and OV treatment of the NC cell line 690100



### 3 Results

---

*Figure 30: NC cell line 690100 treated with different oncolytic viruses in combination with two different iBET.* The NUT carcinoma cell line 690100 was infected with MeV-GFP (MOI 0.1), GLV-0b347 (MOI 1) or T-VEC (MOI 0.00025). At 3 hpi (for MeV-GFP) and 1 hpi (for GLV-0b347 and T-VEC) the inoculum was removed and medium with or without iBET was added. The MOIs and iBET concentrations were chosen to leave between 50 % and 75 % of the cell mass in the respective monotherapy. The remaining cell mass was measured at 96 hpi via Sulforhodamine B (SRB) assay. Displayed are mean values of three independent experiments performed in quadruplicates. 50 % remaining cell mass is indicated by dotted lines. MOCK: uninfected control (black columns). Statistical significance: \* :  $p \leq 0.05$ ; \*\* :  $p \leq 0.01$ ; \*\*\* :  $p \leq 0.001$ ; \*\*\*\* :  $p \leq 0.0001$  - nonsignificant results are not indicated; significance is only displayed between the monotherapeutic approaches and the corresponding combinatory treatment.

The combination of OV and iBET in the NC cell line 690100 generally only showed significant beneficial effects when OV GLV-0b347 was used (**Figure 30**). Here, the further reduction of cell mass under all tested approaches was around 15 %.

For MeV-GFP small further decreases of cell mass got visible with the combinatorial approaches as well, but none of the tested combinations showed a significant decrease.

When T-VEC was used as OV, significance could be observed for the combination of T-VEC + GSK525762 0.05  $\mu\text{M}$ , where the remnant cell mass was further reduced for 25 %. For all other approaches a decrease was also observed, however, it was not significant.

### 3.4.4 Fluorescence imaging of MeV-GFP and GLV-0b347 infection under *iBET* treatment

As the viruses MeV-GFP and GLV-0b347 are equipped with a fluorophore (MeV-GFP: GFP; GLV-0b347: turboFP635), their spreading in the cells could be monitored via fluorescence imaging. The more fluorescence signal got visible the more virus particles were present.

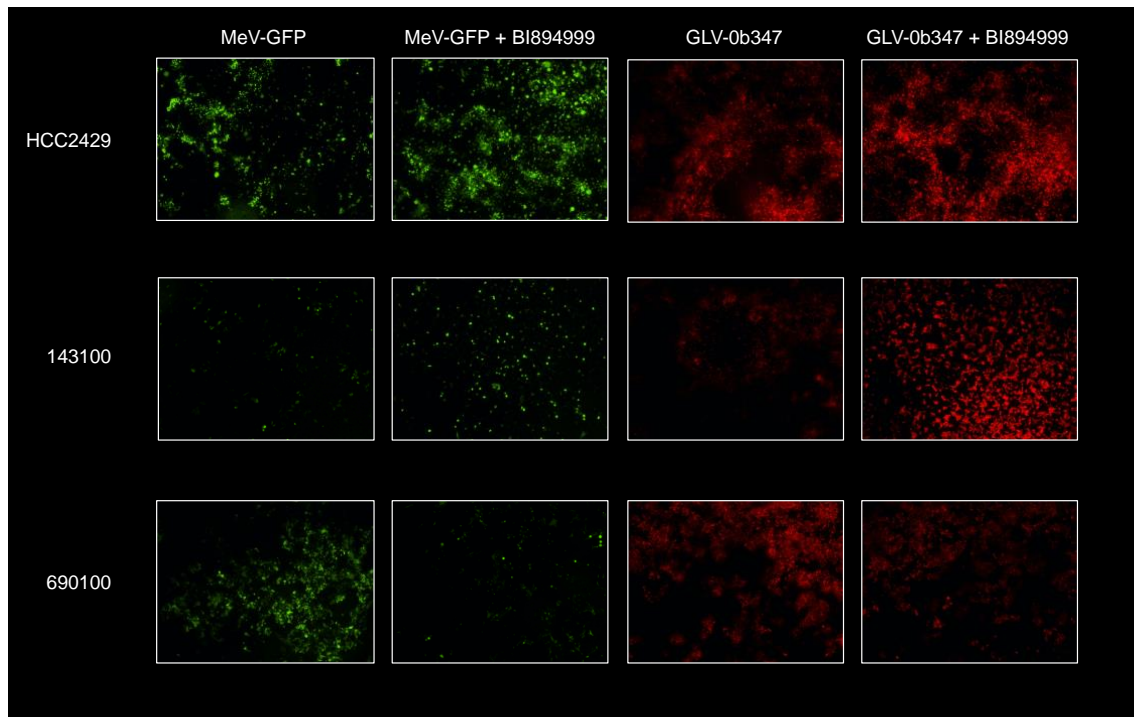
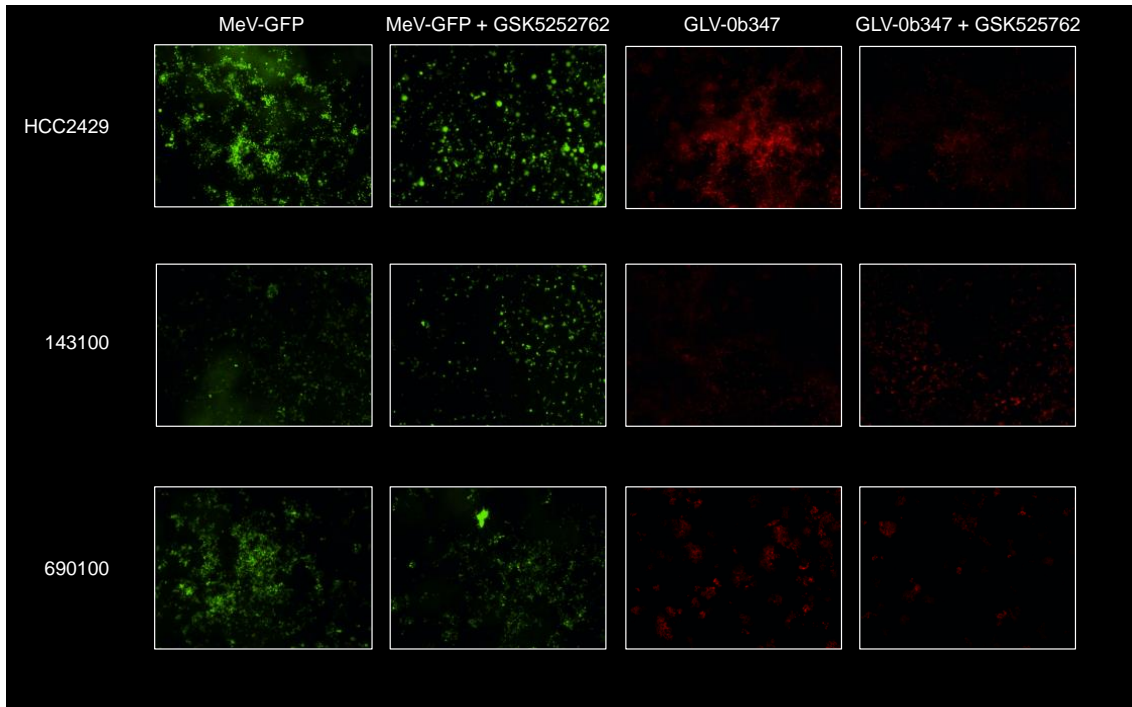


Figure 31: Fluorescence images of NC cells after treatment with MeV-GFP or GLV-0b347 with or without *iBET* BI894999.

Cells were treated with MeV-GFP (MOI 0.1 for HCC2429 and 690100; MOI 1 for 143100) or GLV-0b347 (MOI 0.005 for HCC2429; MOI 0.001 for 143100; MOI 1 for 690100). At 3 hpi (for MeV-GFP) and 1 hpi (for GLV-0b347) the inoculum was removed and medium with or without BI894999 (1 nM for HCC2429, 5 nM for 143100, 1.5 nM for 690100) was added. Images were taken at 96 hpi with a fluorescence microscope.

### 3 Results

---



*Figure 32: Fluorescence images of NC cells after treatment with MeV-GFP or GLV-0b347 with or without iBET GSK525762.*

Cells were treated with MeV-GFP (MOI 0.1 for HCC2429 and 690100; MOI 1 for 143100) or GLV-0b347 (MOI 0.005 for HCC2429; MOI 0.001 for 143100; MOI 1 for 690100). At 3 hpi (for MeV-GFP) and 1 hpi (for GLV-0b347) the inoculum was removed and medium with or without GSK525762 (0.25  $\mu$ M for HCC2429, 0.5  $\mu$ M for 143100, 0.05  $\mu$ M for 690100) was added. Images were taken at 96 hpi with a fluorescence microscope.

In general, it can be said that virus replication also took place in the presence of iBET. For iBET BI894999 the pictures indicate an enhanced virus replication in the cell lines HCC2429 and 143100, while the replication seemed to be lower under iBET treatment in cell line 690100 (**Figure 31**). For iBET GSK525762 an enhanced viral growth could only be seen for cell lines 143100, while for both other cell lines a slight reduction of fluorescence got visible (**Figure 32**).

### 3.5 Inhibition of T-VEC with Ganciclovir

T-VEC showed to be a very potent oncolytic virus to treat NUT carcinoma cell lines in monotherapy studies (see 3.2). Therefore, the risk of a tumor lysis syndrome has to be taken into account, when T-VEC is applied *in vivo*. As explained in chapter 1.2.5.1, the nucleoside analog Ganciclovir can slow down the synthesis of viral DNA. Since the drug already showed promising results in earlier experiments with neuroendocrine tumor (NET) cell lines (Kloker et al., 2019) regarding the inhibition of T-VEC replication, in this thesis only a proof-of-principle experiment was performed with the cell line 143100 (**Figure 33**).

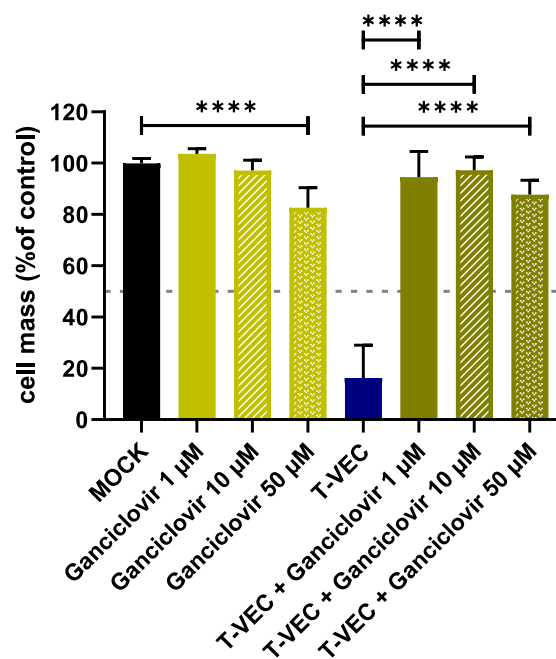


Figure 33: NC cell line 143100 treated with T-VEC in combination with Ganciclovir.

The NUT carcinoma cell line 143100 was infected with T-VEC at MOI 0.0001. At 1 hpi the Ganciclovir was added. The remaining cell mass was measured at 96 hpi via the Sulforhodamine B (SRB) assay. Displayed are mean values of three independent experiments performed in triplicates. 50 % remaining cell mass is indicated by dotted lines. MOCK: untreated control (black columns). Statistical significance: \*:  $p \leq 0.05$ ; \*\*:  $p \leq 0.01$ ; \*\*\*:  $p \leq 0.001$ ; \*\*\*\*:  $p \leq 0.0001$  - nonsignificant results are not indicated; significance is only displayed between MOCK and Ganciclovir treatment and between T-VEC and combinatorial treatment.

It could be shown that already the very low Ganciclovir concentration of 1 µM showed an intense effect: While T-VEC alone led to a reduction of viable cell mass at MOI 0.0001 to 16 %, the effect could completely be inhibited by 1 µM Ganciclovir (95 % viable cells). This concentration alone showed no cytotoxic effect on the cells when applied alone (104 % cell mass compared to MOCK), a

considerable cytotoxic effect could only be shown at Ganciclovir concentrations of 50  $\mu$ M, when the viable cell mass dropped to 83 %.

### 3.6 IFN- $\beta$ response of NC cell lines to OV treatment

Since one mechanism for fighting viral infection is the production of IFN- $\beta$ , it was tested whether the differences observed in the therapeutic approaches can be explained by a change in IFN- $\beta$  production. Therefore, the very effective combinatorial treatment of MeV-GFP + BI894999 (**Figure 34 A**) in the cell line 143100 was tested in comparison to the less efficient combination of GLV-0b347 + BI894999 (**Figure 34 B**) as well as all single treatment approaches of each therapeutic.

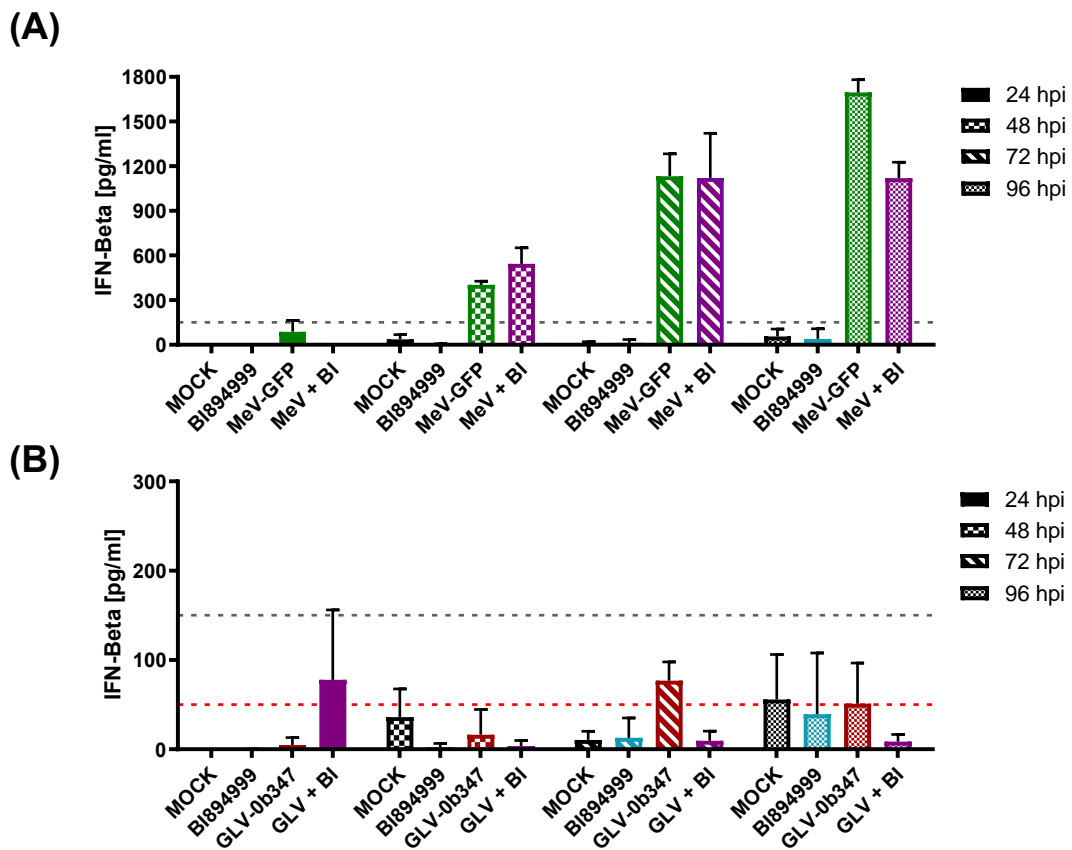


Figure 34: Concentration of IFN- $\beta$  after treatment with iBET and / or OV.

The NC cell line 143100 was treated in monotherapy with 5 nm iBET BI894999 and with OV MeV-GFP (MOI 1) (**A**) respectively GLV-0b347 (MOI 0.001) (**B**) and also in combinatorial treatment with both agents. The supernatants were harvested at the indicated timepoints and the concentration of IFN- $\beta$  was measured via ELISA. A concentration of 150 pg/ml is indicated by the black dotted lines, the red dotted line indicates the cut off value of the used assay (50 pg/ml). MOCK: untreated control



As expected, neither untreated cells nor cells receiving iBET monotherapy showed any significant IFN- $\beta$  production.

However, MeV-GFP treatment as monotherapy led to a strong increase of IFN- $\beta$  production. While the IFN- $\beta$  level was still low after 24 h (88 pg/ml), a first increase was visible after 48 h (403 pg/ml) which increased further after 72 h (1,133 pg/ml) and also after 96 h, where the maximal concentration of 1,695 pg/ml was reached (**Figure 34 A**).

Also, when treated with the combination of MeV-GFP and iBET a response of the IFN- $\beta$  production was visible: While after 48 h the IFN- $\beta$  level was slightly higher than in the single MeV-GFP treatment (503 pg/ml), it only heightened to 1,121 pg/ml after 72 h and therefore was on the same level as seen in the single treatment. This level did not further increase after 96 h and therefore was lower when compared to the single MeV-GFP treatment (**Figure 34 A**).

Interestingly, when 143100 cells were treated with GLV-0b347 as monotherapy, no IFN- $\beta$  production was detectable. Furthermore, also combinatorial treatment with BI894999 did not lead to any change (**Figure 34 B**).

As the NC cell line 690100 showed to be very resistant against GLV-0b347 infection, it was tested, whether this pronounced resistance can be explained due to an increased IFN- $\beta$  response in comparison to cell line 143100.

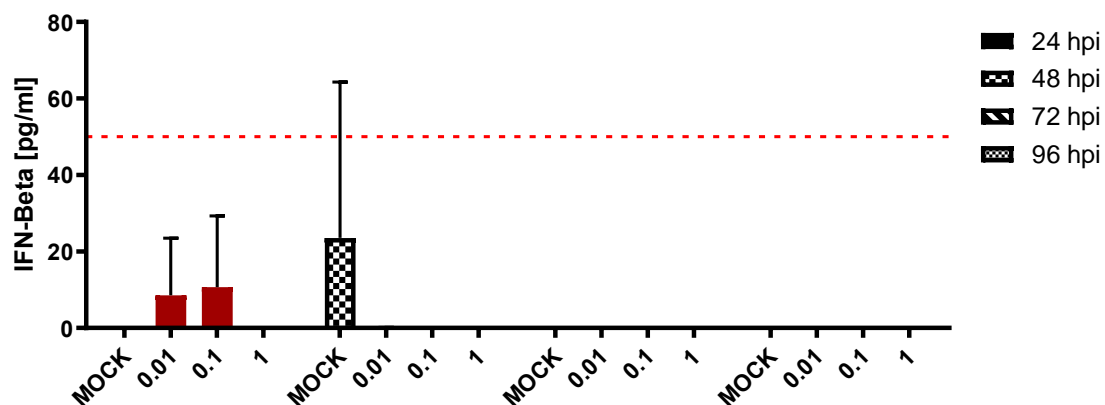


Figure 35: Concentration of IFN- $\beta$  after infection with GLV-0b347.

The NC cell line 690100 was treated in monotherapy with OV GLV-0b347 at the indicated MOIs. The supernatants were harvested at the indicated timepoints and the concentration of IFN- $\beta$  was measured. The red dotted line indicates the cut off value of the used assay (50 pg/ml). MOCK: untreated control.

### 3 Results

---

The results of the assay prove, that IFN- $\beta$  production is not the reason for decreased susceptibility, as all IFN- $\beta$  concentrations measured were below the cut off-value of the used assay (50 pg/ml) (**Figure 35**). A similar result was already attained for the NC cell line 143100 (**Figure 34 B**), in which GLV-0b347 showed strong oncolytic effects.

## 4 Discussion

The knowledge about NUT carcinoma has risen enormously in the past years and therefore also the therapeutic approaches to tackle this aggressive carcinoma have widened. But still none of the tested agents led to a breakthrough in the therapy, making more research in this field indispensable.

### 4.1 Oncolytic virotherapy - new hope for NC patients?

In this thesis the effect of the oncolytic viruses MeV-GFP, GLV-0b347 and T-VEC *in vitro* on a panel of five NUT carcinoma cell lines, four of which harboring a *BRD4-NUT* translocation and one with a *BRD3-NUT* translocation, was investigated.

#### 4.1.1 OV Treatment in *BRD4-NUT* cell lines leads to promising results

All three oncolytic viruses were found to lead to a significant reduction of cell mass or cell viability respectively when applied in sufficient high MOIs.

Noll et al. defined a cell line as susceptible for MeV-SCD treatment when a MOI of 1 led to a decrease to < 50 % of remnant cell mass in comparison to MOCK treatment (Noll et al., 2013). As the genomic structure of MeV-SCD is very similar to MeV-GFP, this concept is transferrable to the measles virus used in this thesis. On this basis, only the *BRD4-NUT* cell line 690100 can be marked as susceptible for MeV-GFP infection. The cell lines HCC2429 and 143100 showed a decrease to < 75 % and can therefore be marked as partially resistant. Taking into account that more than 50 % of the NCI-60 tumor panel cell lines were found to be susceptible for MeV-SCD infection, partial resistance might already be seen as a contraindication for MeV-GFP therapy. Both cell lines being analyzed with the RealTime-Glo™ assay showed a high resistance (> 75 % remnant cell mass), which was only found in six NCI-60 cell lines. However, since a different assay was used, these results have to be acknowledged with great care (see 4.1.2).

Berchtold et al. performed analogical experiments using the vaccinia virus GLV-1h68 (Berchtold et al., 2020). Even if this virus construct is derived from a different strain (“Lister”) and has more gene insertions ( $\beta$ -glucuronidase and  $\beta$ -galactosidase) compared to GLV-0b347, the otherwise high similarities should

still allow a comparison. They defined cell lines in which the remnant cell mass decreased > 50 % in comparison to MOCK at a MOI of 0.1 as susceptible. This is valid for two of the five tested NC cell lines: HCC2429 and 143100. On the other hand, cell line 690100 has to be marked partial resistant and the cell lines analyzed via RealTime-Glo™ assay were again found to be highly resistant.

For T-VEC no systematic study has been made yet, so a structured comparison to other cell lines is not possible. However, experiments with neuroendocrine tumor (NET) cell lines and SRB assay read-out were performed, resulting in a cell mass < 50 % in all three tested cell lines at a MOI of 0.0001 at 96 hpi (Kloker et al., 2019). Considering this, a MOI of 0.0001 to compare the susceptibility might be advisable. Following the studies of Noll et al. and Berchtold et al. taking 50 % (for susceptible) and 75 % (for partial resistant) remnant cell mass as cut-off values, in this case the NC cell lines HCC2429 and 143100 could be graded as susceptible, cell line 690100 as partially resistant, while Ty-82 and 10326 would need to be graded highly resistant. A higher MOI does not seem appropriate as the strong effect in some cell lines show the high potential of T-VEC and no differences between cell lines would be monitorable. As the application of higher doses always carries the risk of inducing stronger adverse effects it also makes sense to use the lowest possible MOI from a clinical point of view. T-VEC was the only tested OV in which the longer incubation time of 96 hpi compared to the effect at 72 hpi in some cases led to large additional effects. A reason for this might be an excessive replication and therefore extended spreading of the viral particles. This would also explain why the small initial number of viral particles is sufficient to achieve a strong oncolytic effect. Since this virus has no fluorophore integrated in its genome, it was unfortunately not possible to monitor viral spreading using fluorescence microscopy. For quantification of replication and spreading of T-VEC viral growth curves could provide more precise data.

Concluding these results, the response rates of the different tested NC cell lines tested with one and the same oncolytic virus vary greatly. This matches with the finding of Noll et al. who could also not find a pattern in the response rate (Noll et al., 2013). Therefore, a general statement to the effect of immunovirotherapeutics

for treatment of NC seems not possible. Thus, as with other cancer therapy modalities, immunovirotherapy in NC patients also will work mostly on a personalized approach.

Many different factors can lead to the different responses of different cell lines. Since the primary tumor site of the patients from whom the cell lines were derived is only known from HCC2429 (lung), different primary tumor sites cannot be excluded. Therefore, the cell lines might have different surface receptors (relevant for the cell entry of MeV-GFP and T-VEC) and surface molecules (relevant for the cell entry of GLV-0b347) and hence give the viruses different conditions for cell entry. Furthermore, the different morphology of the cell lines has to be taken into account. While the cell line 143100 distributes evenly over the whole area, HCC2429 and 690100 show a grouped growth (see 2.1.1). As for example the apoptotic effect of MeV-GFP is induced by syncytia formation with neighboring cells (Galanis, 2010), the influence of different growth behavior should not be underestimated. Of course, this effect can be influenced by the number of cells seeded: As soon as a confluent cell layer is reached the same effect as with grouped growth behavior will be noticed. This effect might also explain the slower response of cell line 143100 when treated with MeV-GFP: In the still thin cell layer at 72 hpi the reduction of cell mass was lower compared to both other cell lines. At 96 hpi though, a further decrease of 13 % got visible at a MOI of 1 in 143100 cells, an effect not noticed in the other cell lines. If the higher cell density really is the most relevant factor for this aspect could be found out in further experiments with different numbers of seeded cells. Additionally, the type of the viral genome can influence the cell response to viral infection, e.g. the pathways for induction of the IFN response differ (Matz et al., 2019). While T-VEC and GLV-0b347 have a ds[±] DNA genome, MeV-GFP has a ss[-] RNA genome. Since cell line 690100 proved to be less sensitive when treated with both DNA-viruses but showed good response when treated with the RNA-virus MeV-GFP, further research on the different viral response pathways might bring new insights.

This research about the reasons of different responses was started by comparing the IFN- $\beta$  responses after GLV-0b347 infection of the highly resistant cell line 690100 to the susceptible cell line 143100. However, no increased IFN- $\beta$  response in the resistant cell line was noticeable; the IFN- $\beta$  levels measured were all still lower than the cut-off value of the used assay. It is known that vaccinia viruses have developed powerful ways to block IFN synthesis (Hof and Schlüter, 2019, Smith et al., 2018). But also, other interferons, IFN- $\alpha$  as well as IFN- $\gamma$ , play a role in the immune response against viruses, as well as IFN independent pathways. One example for an IFN independent immune response is the transcription of telomere repeat-containing RNA (TERRA), especially after infection with DNA viruses (Wang et al., 2017). However, the testing of the IFN- $\beta$  response of cell line 143100 after treatment with MeV-GFP gave insights about the higher resistance noticed after treatment with this OV compared to GLV-0b347 or T-VEC. As early as at 24 hpi values above the cut-off value of 50 mg/ml got measurable. Even though a decrease of cell mass to 80 % (72 hpi), respectively 70 % (96 hpi) was noticed in the SRB assay, the IFN- $\beta$  values rose constantly over the time, indicating an ongoing excessive IFN production of the remaining cells still fighting successfully against the viral infection.

Still, immunovirotherapy is certainly a new option for NC treatment, as its approach can help to overcome deficiencies of other therapy approaches: Due to the location and early metastatic spread surgical R0 resection often is impossible. Even with (neo-)adjuvant chemoradiation a small number of tumor cells can often evade apoptosis. With the fast growth of NC these few surviving tumor cells often appear to be sufficient for tumor recurrence, as shown by the high progression rates after therapy and only few long-time survivors (Chau et al., 2020, Giridhar et al., 2018, Bauer et al., 2012). Oncolytic viruses are able to indirectly combat these small tumor centers because they can activate the body's own immune system and enable *in situ* vaccination (Toda et al., 1999).

### **4.1.2 Does the translocation type influence the resistance against OVs?**

The NC cell line 10326, harboring a *BRD3-NUT* translocation instead of *BRD4-NUT* as all other tested cell lines, proved to be highly resistant against all three

tested OV<sub>s</sub> in the RealTime-Glo™ assay. Hence, the question occurred if this high resistance can be explained by the different translocation of the cell line. This is especially interesting, as the *BRD4-NUT* fusion was recently found to lead to a lower overall survival rate (OS) than a *BRD3-NUT* fusion in non-thoracic NC<sub>s</sub> (Chau et al., 2020). However, this finding has to be noticed with care, as earlier analyses did not find a relation between OS and the translocation type (Giridhar et al., 2018, Bauer et al., 2012).

When comparing the results of this cell line to the others two important differences have to be taken into account: the different morphology of the cell line and the different assay type used.

Due to the different growth characteristics, it was not possible to use the same assay for cell viability analysis for all cell lines used. To analyze the differences of both assays, for cell line 143100 both assay types, RealTime-Glo™ assay and SRB assay, were performed. It could be shown that the RealTime-Glo™ assay does also show a signal reduction for cells treated with oncolytic viruses. However, when using the same MOI of MeV-GFP, the measured cell mass compared to the measured cell viability showed a huge difference (22 % respectively < 1 %). The much lower measured cell viability compared to the cell mass might be due to the longer incubation time of the virus: As in the SRB assay protocol MeV-GFP containing medium was taken off again at 3 hpi, the virus containing medium was left on the cell layer for the whole incubation time when the RealTime-Glo™ assay was performed. Furthermore, a possible inaccuracy of the SRB assay has to be included: Even though multiple times of washing should detach and wash out all dead cells, it cannot be excluded that a small number of dead cells stays in the well. This would falsify the measurement resulting in a higher cell mass. The RealTime-Glo™ assay, on the other hand, directly measures the living cells, so this problem does not occur.

Consequently, any comparison between cell viability measured via RealTime-Glo™ assay and cell mass measured via SRB assay must be considered with great care.

Interestingly, both cell lines analyzed via RealTime-Glo™ assay showed the highest resistances against the OV infection. Applying the noticed difference between SRB assay and RealTime-Glo™ assay in cell line 143100 an even higher resistance when measured via SRB assay can be expected. But another remarkable difference in the RealTime-Glo™ assay itself has to be taken into account: While for cell lines Ty-82 and 10326 absolute luminescence values < 6,000 RLU were measured, for cell line 143100 an absolute luminescence > 70,000 RLU was noticed. One possible explanation for this difference might be the smaller cell size of Ty-82 and 10326 in comparison to 143100. This difference was possibly partly equalized by a higher number of seeded cells though. Of note, only one experiment with biological triplicates with one OV at one MOI was performed.

Unfortunately, in the literature no direct comparison of the result obtained via the SRB assay and the RealTime-Glo™ assay can be found. Comparisons with the RealTime-Glo™ assay were only made with different cell viability assays (ATP assay, live cell protease (Duellman et al., 2015) and MTT assay (Orbach et al., 2018)) where a high similarity to the RealTime-Glo™ assay was found. A study comparing the MTT and the SRB assay also found a high correlation (Perez et al., 1993), leading to the suggestion that also SRB assay and RealTime-Glo™ assay should correlate.

Nevertheless, the findings of this thesis can only be considered preliminary and further experiments are needed to systematically test the differences between both assay types. Accordingly, at current stage it remains unclear whether the translocation type has any importance towards resistance phenomena against OVs.

### ***4.1.3 Ganciclovir can impede a possible tumor lysis syndrome***

The tumor lysis syndrome (TLS) must always be considered as a possible severe adverse effect of potent oncological treatment.

Even though solid tumors are most often classified as low risk tumors for TLS (Rahmani et al., 2019), for NC some risk factors accumulate: high rate of cell proliferation leading to a high tumor mass and the early formation of metastases;



---

in some cases also organ infiltration, especially of the kidneys (Howard et al., 2011).

Therefore, for example the very potent treatment with T-VEC has to be performed with great care in clinical studies, as it is difficult to estimate the right amount of T-VEC needed.

The virostatic Ganciclovir has already proven to powerfully inhibit T-VEC replication in neuroendocrine tumor (NET) cell lines (Kloker et al., 2019). The same strong impact got visible in the tested NC cell line. The needed low concentration of Ganciclovir itself (1  $\mu\text{M}$  to inhibit MOI 0.0001) did not show any cytotoxic effect *in vitro*. Also, clinical studies came to the result, that an average concentration of 5  $\mu\text{M}$  over 24 h is well tolerated (Lalezari et al., 2002). Consequently, Ganciclovir can assure a safe treatment of a T-VEC overdose, which otherwise could lead to the development of a TLS.

#### **4.2 iBET therapy in NC cell lines**

The experiments could show that the cell mass of NC can be reduced in a concentration-dependent manner *in vitro* by iBET monotherapy. Hereby, a reduction in cell mass to < 50 % with a concentration of 1  $\mu\text{M}$  of GSK525762 in all three cell lines could be seen. First clinical studies using GSK525762 for NC treatment found a dose of 80 mg/d well tolerable, leading to plasma concentrations of 2.5  $\mu\text{M}$  in the beginning of the therapy (Piha-Paul et al., 2020). Therefore, the results can be assumed to validate the already seen benefit of GSK525762 for NC treatment. The first clinical study using BI894999 is still recruiting participants (NCT02516553). Thus, still no data is available which plasma concentration can be administered safely. Certainty will be given by the currently running first in human dose finding study.

Several reasons might lead to the reduction of cell mass seen in the SRB assay, e.g. cell death, reduced proliferation or changes in morphology. To get better insight in the mechanism of cell mass reduction the xCELLigence RTCA SP assay was performed. In the case of cell death a rapid decrease of the cell index once the iBET takes effect would have been expected, which was shown in earlier studies after apoptotic OV treatment (Ma et al., 2020). This appears in outline in

cell line 143100 at the highest iBET concentrations. A logarithmic shape of the graph, which can be seen at all other iBET concentrations in cell line 143100 as well as in cell line 690100, can be seen as an index for stopping proliferation rather than cell death. But, of course, also a change in morphology could lead to smaller changes in the cell index. Why no change in the cell index of the iBET treated HCC2429 cells could be observed can unfortunately not be said with certainty. One possible explanation can again be a change in morphology leading to the same covered area by a smaller number of cells. To monitor these changes precisely a repetition of the experiment should be performed using the xCELLigence RTCA eSight™ system, which allows real time cell imaging. This system could also ensure the presumption of proliferation stoppage in the other two cell lines. Furthermore, determining the proliferation via the Ki-67 index, which was already found to be reduced in a NC cell line after treatment with iBET JQ1 (Filippakopoulos et al., 2010), might give more insights in the mechanism leading to the reduced cell mass. Also, assays analyzing cellular senescence, which was found to be induced in mucoepidermoid carcinoma (MEC) cell lines after treatment with the iBET GSK525762 (Markman et al., 2019), could contribute to this.

### **4.3 Oncolytic viruses and iBET - combined therapy as an answer?**

Since growth of NUT carcinoma progresses rapidly, no time should be wasted after diagnosis before starting the first therapy. In many clinical studies carried out with different iBET agents NC initially responded well, but progression often started again after weeks or month [Molibresib / GSK525762: (Piha-Paul et al., 2020); TEN-010: (Shapiro et al., 2015); Birabresib / OTX015: (Lewin et al., 2018)]. These first studies indicate that (neo-)adjuvant iBET treatment might be a suitable treatment option for patients before or after surgical resection but failed to offer a sufficient and long-lasting therapy option for NC patients as monotherapy. Therefore, combining iBET with other agents is in the focus of current research. Until now, mostly other small molecules were used as treatment partner. The combination with virotherapeutics is a new approach, especially since studies with other immunotherapeutic agents have rarely been performed (Doroshov et al., 2017).

With the performed experiments it could be shown that when combining iBET and oncolytic viruses for NC therapy no inhibitory effects can be expected: In none of the performed experiments a higher cell mass was measured after combinatory treatment compared to monotherapeutic treatment approaches. Most often a significant beneficial effect was noticed with the combinatory treatment, which, however, did not lead to a massive further cell mass reduction.

In 2006 it has been shown that BRD4 represses gene translation of the human papillomavirus (HPV) (Wu et al., 2006). Detecting a similar mechanism for the OVs and therefore see an induced viral replication after application of iBET and consequently a further reduced cell mass was hoped. Via fluorescence microscopy it could be shown that replication and spreading of used viral vectors is not impaired by iBET compounds; some of the pictures even indicate an enhanced replication and spreading of the viral vectors. As fluorescence microscopy does not allow a quantitative analysis, viral growth curves can help to reveal, if a change of the viral replication can be expected.

Interestingly, the beneficial effect of the combinatory therapy varied highly between the different cell lines as well as the different viruses used, while showing a similarity for both tested iBET. Especially one combination, MeV-GFP + iBET in the cell line 143100, proved to be powerful. In order to find an explanation for these differences in the combinatorial effects, it was tested whether a change in the IFN- $\beta$  response of the cells might be the cause, since reduced IFN- $\beta$  production of cells leads to higher susceptibility to viral infection if they have not lost their IFN responsiveness through mutations (Stojdl et al., 2000). But in the experiments no pronounced change of IFN- $\beta$  levels was measured comparing MeV-GFP monotherapy with MeV-GFP + iBET therapy. The differences in the IFN- $\beta$  levels especially after 96 h might be explainable with only a very small number of viable cells left in the combinatorial treatment (ca. 10 % viable cell mass). A changed IFN- $\beta$  response does not seem to be the reason for the more effective combinatorial therapy, which can only be confirmed by testing the IFN responsiveness of the cell lines. Therefore, further research exploiting this as well as other possible mechanisms is valuable on this field.

Nonetheless, these results indicate that simultaneous application of both substance classes can possibly lead to an improved therapy of NC.

### 4.4 Perspectives

This thesis aimed to establish a new therapy approach to treat the very aggressive NUT carcinoma in preclinical trials using iBET and oncolytic viruses as monotherapeutic approaches as well as in combination.

The effect of iBET on NC in these *in vitro* studies could be confirmed and it could be shown that the completely novel approach tackling NCs with oncolytic viruses has great potential. These findings alone show the need of further investigation of the effectiveness of the different OVs on NC *in vivo*, e.g. in immunocompetent murine models as well as in first clinical trials. First patient derived murine models with NC cell lines have already been successfully established (Morrison-Smith et al., 2020, Sun et al., 2017, Filippakopoulos et al., 2010). As the most potent OV T-VEC is already approved for other neoplasms by the FDA and EMA a fast implementation of the laboratory experiments to clinical studies is possible. Therefore, T-VEC in particular should be considered as an OV for further studies so that a new treatment option can be offered to NC patients as soon as possible. Another advantage of T-VEC is the possibility to start with individual healing approaches from which individual patients could benefit even earlier, as it has already been approved by governmental authorities. One possible problem could be the difficulty of an intratumoral injection, the only type of application of T-VEC approved to date, as the *primarius* of NC, unlike melanoma, is usually difficult to reach without surgery.

But not only the results of the monotherapeutic approach with OV offer new perspectives. Since the benefits of the simultaneous application of iBET and OVs varied highly, further *in vitro* studies aimed at finding a pattern or a marker suggesting an improved simultaneous therapy, could lead to an efficient therapy for certain NC patients.

Furthermore, since the results of the monotherapy studies did not lead to the conclusion that one specific virotherapeutic is the best to use for all kinds of NC, individual studies might have to be carried out before treatment. Hence, time,

which cannot be wasted when tackling NC, would be needed until the right virotherapeutic in the right concentration is found. Additionally, as a previous clinical trial with T-VEC showed, it can take multiple weeks after the beginning of an OV treatment until a measurable shrinkage of tumor mass can be observed (Andtbacka et al., 2016). During that time patients might suffer from progression lowering the probability to reach a stabilization of the disease or even a regression. With iBET therapy on the contrary the first patients show response after a few weeks (Piha-Paul et al., 2020). Therefore, a new treatment regimen imposes: iBET could be used to bridge over time, until OV is available and effective. The timespan while iBET still achieve a stable disease (SD) or even a partial response (PR) can be used for the development of the best virotherapeutic option and start of the OV treatment. In this way, an initial effect of the OV therapy can be achieved before the progression under iBET monotherapy begins. However, this treatment regimen has not been explored in this thesis and further *in vitro* studies testing the effect of a combinatorial treatment applying iBET before the oncolytic viruses are needed. With successfully conducted *in vitro* studies this treatment regimen offers the potential of rapid progression from “bench to bedside”, as both iBETs are already under clinical investigation.

### 5 Summary

NUT carcinoma (NC) is a rare but very aggressive tumor with more and more cases diagnosed as the awareness about this tumor rises. The prognosis of patients having NC is still very poor despite intensified research leading to new treatment approaches.

BET inhibitors (iBET) are one of the agents being tested already in clinical studies, where they could prove their efficacy against NC. Unfortunately, the tumor often recurs after a few months of iBET treatment. Therefore, the focus of further research lies on the combination of iBET with other substances.

The aim of this thesis was to find out if oncolytic viruses (OVs) could be a future option for NC treatment, either as single therapy or in combination with iBET. To test this, *in vitro* studies analyzing the oncolytic potential of different OVs and iBET, in monotherapeutic approaches as well as in combination, were performed.

It was found, that the different OVs could mostly lead to a significantly reduced cell mass in the tested NC cell lines when applied in sufficiently high concentrations. Thereby, the OV T-VEC, which is already approved for treatment of advanced melanoma, proved to be the most efficient OV. To forestall the possibility of a tumor lysis syndrome, the inhibitory effect of Ganciclovir on T-VEC replication and spreading was successfully tested.

In this thesis the potential of iBET treatment could also be verified. The studies showed that the efficacy is mostly explainable by reduced proliferation rates of the cells.

When combining both substances, no inhibitory interaction was monitored; on the contrary, mostly a further induced oncolysis got visible.

These promising results encourage further tests of OVs as a treatment option for NC in preclinical *in vivo* models as well as in first clinical trials. A further possible treatment approach is revealed by the additive effect of the combination of OV and iBET: Since a rapid response of NC to iBET therapy could be shown in clinical trials, iBET therapy could be used to bridge the time until the start of OV therapy,

during which it often takes longer for an initial response to become visible, as has been shown in clinical studies on other tumors. Therefore, this approach should also be evaluated further and tested in a clinical setting as it bears the opportunity of a fast and efficient treatment.

As the OV T-VEC is already licensed for clinical applications and the iBETs are also tested at present in phase-I/II trials, this therapeutic approach has the possibility of a fast transfer from the laboratory into clinical practice.

### 6 Zusammenfassung

Das NUT Karzinom (NC) ist eine seltene, aber sehr aggressiv wachsende Tumorentität, welche durch steigende Kenntnis und Aufmerksamkeit immer häufiger diagnostiziert wird. Auch wenn die Forschung nach therapeutischen Optionen in letzter Zeit intensiviert wurde, ist die Prognose des NC weiterhin sehr schlecht.

Als eine mögliche Behandlungsoption stellten sich BET-Inhibitoren (iBET) heraus, welche nun bereits in klinischen Studien zur NC Therapie eingesetzt werden. In diesen Studien konnte zwar ein gutes Ansprechen des Tumors zu Therapiebeginn festgestellt werden; allerdings kam es nach einigen Monaten der iBET Therapie sehr oft zu Rückfällen. Aus diesem Grund fokussiert sich die aktuelle Forschung auf die Kombination von iBET mit anderen Therapeutika.

Ziel dieser Arbeit war es herauszufinden, ob onkolytische Viren (OVs) entweder alleine oder als Kombinationspartner von iBET eine neuartige Behandlungsoption des NC darstellen können. Dafür wurden *in vitro* Versuche durchgeführt, die das onkolytische Potential von verschiedenen OVs und iBET Wirkstoffen, sowohl einzeln als auch in Kombination, testeten.

Es konnte gezeigt werden, dass bei den verschiedenen NC Zelllinien bei ausreichender Virusmenge fast immer eine deutliche Reduktion der Zellmasse zu verzeichnen war. Dabei stellte sich T-VEC, ein schon für die Melanom-Behandlung zugelassenes OV, als potentestes OV heraus. Um einem durch die Therapie induzierten möglichen Tumor-Lyse-Syndrom zuvorzukommen, wurde die inhibitorische Wirkung von Ganciclovir auf die Replikation und Ausbreitung von T-VEC in einer NC Zelllinie exemplarisch getestet und erfolgreich nachgewiesen.

Die Wirkung der iBET Therapie konnte in dieser Arbeit *in vitro* verifiziert werden. Dabei konnte gezeigt werden, dass die Wirkung vor allem durch verminderte Proliferation zustande kommt.



Bei der Untersuchung der Effekte der Kombination beider Wirkstoffe konnte gezeigt werden, dass keine inhibitorische Wechselwirkung zwischen beiden Therapeutika stattfindet. In fast allen Versuchen konnte zudem eine leicht verstärkte Onkolyse beobachtet werden.

Diese vielversprechenden Ergebnisse ermutigen zu der weiteren Testung von OV<sub>s</sub> in präklinischen *in vivo* Modellen oder ersten klinischen Studien. Eine potentielle Einsatzmöglichkeit ergibt sich auf Grund der leicht additiven (und sicher nicht inhibitorischen) Wechselwirkung zwischen OV<sub>s</sub> und iBET<sub>s</sub>: Das festgestellte schnelle Ansprechen des NC auf eine iBET Therapie könnte genutzt werden, um die Zeit bis zum Ansprechen des Karzinoms auf eine Virotherapie, welche in anderen Tumorentitäten bisher meist ein zeitverzögertes Ansprechen zeigte, zu überbücken. Auch diese Möglichkeit sollte in einer ersten klinischen Studie weiter evaluiert werden.

Durch die bereits erfolgte Zulassung des OV T-VEC und der laufenden iBET Studien hat diese Behandlung das Potential, zügig im klinischen Alltag zur Anwendung zu kommen.

---

## 7 Appendix

### 7.1 List of figures

Figure 1: Schematic display of the genomic structure of the most relevant NUT carcinoma fusion proteins. ....	3
Figure 2: Principle of oncolytic virotherapy.....	11
Figure 3: Structure of the measles virus and its genome.....	12
Figure 4: Replication cycle of Poxviridae.....	16
Figure 5: Genome of the GLV-0b347 virus.....	17
Figure 6: Genomic structure of Talimogene laherparepvec.....	21
Figure 7: Grid of the improved Neubauer hemocytometer.....	34
Figure 8: Setting of MeV-GFP single agent treatment for adherent cell lines. ...	36
Figure 9: Setting of GLV-0b347 and T-VEC single agent treatment for adherent cell lines. ....	36
Figure 10: Setting of MeV-GFP, GLV-0b347 and T-VEC single agent treatment for non-adherent cell lines.....	37
Figure 11: Setting of iBET single agent treatment for adherent cell lines. ....	37
Figure 12: Cell proliferation of the NC cell lines HCC2429, 143100 and 690100. ....	43
Figure 13: NC cell line HCC2429 infected with oncolytic viruses. ....	44
Figure 14: NC cell line 143100 infected with oncolytic viruses.....	46
Figure 15: NC cell line 690100 infected with oncolytic viruses.....	48
Figure 16: Comparison of the effect of oncolytic viruses on the NC cell lines HCC2429, 143100 and 690100.....	50
Figure 17: NC cell line Ty-82 infected with oncolytic viruses.....	52
Figure 18: NC cell line 10326 infected with oncolytic viruses.....	54
Figure 19: Comparison of the results measured via SRB assay and RealTime-Glo™ assay. ....	56
Figure 20: NC cell line HCC2420 after treatment with BET inhibitors (iBET)....	58
Figure 21: Graph used for calculation of the IC <sub>50</sub> values of iBET in NC cell line HCC2429.....	60
Figure 22: NC cell line 143100 after treatment with BET inhibitors (iBET).....	61

---

Figure 23: Graph used for calculation of the IC <sub>50</sub> values of iBET in NC cell line 143100.....	63
Figure 24: NC cell line 690100 after treatment with BET inhibitors (iBET).....	64
Figure 25: Graph used for calculation of the IC <sub>50</sub> values of iBET in NC cell line 690100.....	66
Figure 26: Comparison of SRB-assay results of NC cell lines HCC2429, 143100, 690100 after treatment with BET inhibitors (iBET).....	67
Figure 27: Comparison of xCELLigence®-assay results of NC cell lines HCC2429, 143100, 690100 after treatment with BET inhibitors (iBET). ....	69
Figure 28: NC cell line HCC2429 treated with different oncolytic viruses in combination with two different iBET.....	72
Figure 29: NC cell line 143100 treated with different oncolytic viruses in combination with two different iBET.....	74
Figure 30: NC cell line 690100 treated with different oncolytic viruses in combination with two different iBET.....	76
Figure 31: Fluorescence images of NC cells after treatment with MeV-GFP or GLV-0b347 with or without iBET BI894999.....	77
Figure 32: Fluorescence images of NC cells after treatment with MeV-GFP or GLV-0b347 with or without iBET GSK525762.....	78
Figure 33: NC cell line 143100 treated with T-VEC in combination with Ganciclovir. ....	79
Figure 34: Concentration of IFN-β after treatment with iBET and / or OV.....	80
Figure 35: Concentration of IFN-β after infection with GLV-0b347.....	81

**7.2 List of tables**

Table 1: Currently published NUT carcinoma cell lines ..... 4  
Table 2: NUT carcinoma cell lines used in this thesis ..... 27  
Table 3: Oncolytic viruses used in this thesis..... 28  
Table 4: Conditions used for the different assay types ..... 35

## 8 Citations

- ADEEGBE, D. O., LIU, S., HATTERSLEY, M. M., BOWDEN, M., ZHOU, C. W., LI, S., VLAHOS, R., GRONDINE, M., DOLGALEV, I., IVANOVA, E. V., QUINN, M. M., GAO, P., HAMMERMAN, P. S., BRADNER, J. E., DIEHL, J. A., RUSTGI, A. K., BASS, A. J., TSIRIGOS, A., FREEMAN, G. J., CHEN, H. & WONG, K.-K. 2018. BET Bromodomain Inhibition Cooperates with PD-1 Blockade to Facilitate Antitumor Response in Kras-Mutant Non-Small Cell Lung Cancer. *Cancer immunology research*, 6, 1234-1245.
- ADEYINKA, A. & BASHIR, K. 2020. Tumor Lysis Syndrome. *StatPearls*. Treasure Island (FL): StatPearls Publishing, Copyright © 2020, StatPearls Publishing LLC.
- AKHTAR, J. & SHUKLA, D. 2009. Viral entry mechanisms: cellular and viral mediators of herpes simplex virus entry. *Febs j*, 276, 7228-36.
- ALEKSEYENKO, A. A., WALSH, E. M., ZEE, B. M., PAKOZDI, T., HSI, P., LEMIEUX, M. E., DAL CIN, P., INCE, T. A., KHARCHENKO, P. V., KURODA, M. I. & FRENCH, C. A. 2017. Ectopic protein interactions within BRD4-chromatin complexes drive oncogenic megadomain formation in NUT midline carcinoma. *Proc Natl Acad Sci U S A*, 114, E4184-e4192.
- ANDERSSON, A. K., MA, J., WANG, J., CHEN, X., GEDMAN, A. L., DANG, J., NAKITANDWE, J., HOLMFELDT, L., PARKER, M., EASTON, J., HUETHER, R., KRIWACKI, R., RUSCH, M., WU, G., LI, Y., MULDER, H., RAIMONDI, S., POUNDS, S., KANG, G., SHI, L., BECKSFORT, J., GUPTA, P., PAYNE-TURNER, D., VADODARIA, B., BOGGS, K., YERGEAU, D., MANNE, J., SONG, G., EDMONSON, M., NAGAHAWATTE, P., WEI, L., CHENG, C., PEI, D., SUTTON, R., VENN, N. C., CHETCUTI, A., RUSH, A., CATCHPOOLE, D., HELDRUP, J., FIORETOS, T., LU, C., DING, L., PUI, C.-H., SHURTLEFF, S., MULLIGHAN, C. G., MARDIS, E. R., WILSON, R. K., GRUBER, T. A., ZHANG, J., DOWNING, J. R. & ST. JUDE CHILDREN'S RESEARCH HOSPITAL-WASHINGTON UNIVERSITY PEDIATRIC CANCER GENOME, P. 2015. The landscape of somatic mutations in infant MLL-rearranged acute lymphoblastic leukemias. *Nature genetics*, 47, 330-337.
- ANDTBACKA, R. H., ROSS, M., PUZANOV, I., MILHEM, M., COLLICHIO, F., DELMAN, K. A., AMATRUDA, T., ZAGER, J. S., CRANMER, L., HSUEH, E., CHEN, L., SHILKRUT, M. & KAUFMAN, H. L. 2016. Patterns of Clinical Response with Talimogene Laherparepvec (T-VEC) in Patients with Melanoma Treated in the OPTiM Phase III Clinical Trial. *Ann Surg Oncol*, 23, 4169-4177.
- ANDTBACKA, R. H. I., COLLICHIO, F. A., AMATRUDA, T., SENZER, N. N., CHESNEY, J., DELMAN, K. A., SPITLER, L. E., PUZANOV, I., DOLEMAN, S., YE, Y., VANDERWALDE, A. M., COFFIN, R. & KAUFMAN, H. 2013. OPTiM: A randomized phase III trial of talimogene laherparepvec (T-VEC) versus subcutaneous (SC) granulocyte-

- macrophage colony-stimulating factor (GM-CSF) for the treatment (tx) of unresected stage IIIB/C and IV melanoma. *Journal of Clinical Oncology*, 31, LBA9008-LBA9008.
- AREF, S., BAILEY, K. & FIELDING, A. 2016. Measles to the Rescue: A Review of Oncolytic Measles Virus. *Viruses*, 8, 294.
- BARQUET, N. & DOMINGO, P. 1997. Smallpox: The Triumph over the Most Terrible of the Ministers of Death. *Annals of Internal Medicine*, 127, 635-642.
- BAUER, D. E., MITCHELL, C. M., STRAIT, K. M., LATHAN, C. S., STELOW, E. B., LÜER, S. C., MUHAMMED, S., EVANS, A. G., SHOLL, L. M., ROSAI, J., GIRALDI, E., OAKLEY, R. P., RODRIGUEZ-GALINDO, C., LONDON, W. B., SALLAN, S. E., BRADNER, J. E. & FRENCH, C. A. 2012. Clinicopathologic features and long-term outcomes of NUT midline carcinoma. *Clin Cancer Res*, 18, 5773-9.
- BECHTER, O. & SCHÖFFSKI, P. 2020. Make your best BET the emerging role of BET inhibitor treatment in malignant tumors. *Pharmacology & therapeutics*, 107479-107479.
- BEESELEY, A. H., STIRNWEISS, A., FERRARI, E., ENDERSBY, R., HOWLETT, M., FAILES, T. W., ARNDT, G. M., CHARLES, A. K., COLE, C. H. & KEES, U. R. 2014. Comparative drug screening in NUT midline carcinoma. *British journal of cancer*, 110, 1189-1198.
- BERCHTOLD, S., BEIL, J., RAFF, C., SMIRNOW, I., SCHELL, M., D'ALVISE, J., GROSS, S. & LAUER, U. M. 2020. Assessing and Overcoming Resistance Phenomena against a Genetically Modified Vaccinia Virus in Selected Cancer Cell Lines. *Int J Mol Sci*, 21.
- BERCHTOLD, S., LAMPE, J., WEILAND, T., SMIRNOW, I., SCHLEICHER, S., HANDGRETINGER, R., KOPP, H. G., REISER, J., STUBENRAUCH, F., MAYER, N., MALEK, N. P., BITZER, M. & LAUER, U. M. 2013. Innate immune defense defines susceptibility of sarcoma cells to measles vaccine virus-based oncolysis. *J Virol*, 87, 3484-501.
- BHADURY, J., NILSSON, L. M., MURALIDHARAN, S. V., GREEN, L. C., LI, Z., GESNER, E. M., HANSEN, H. C., KELLER, U. B., MCLURE, K. G. & NILSSON, J. A. 2014. BET and HDAC inhibitors induce similar genes and biological effects and synergize to kill in Myc-induced murine lymphoma. *Proceedings of the National Academy of Sciences of the United States of America*, 111, E2721-E2730.
- BIDGOOD, S. R. & MERCER, J. 2015. Cloak and Dagger: Alternative Immune Evasion and Modulation Strategies of Poxviruses. *Viruses*, 7, 4800-4825.
- BRÄGELMANN, J., DAMMERT, M. A., DIETLEIN, F., HEUCKMANN, J. M., CHOIDAS, A., BÖHM, S., RICHTERS, A., BASU, D., TISCHLER, V., LORENZ, C., HABENBERGER, P., FANG, Z., ORTIZ-CUARAN, S., LEENDERS, F., EICKHOFF, J., KOCH, U., GETLIK, M., TERMATHE, M., SALLOUH, M., GREFF, Z., VARGA, Z., BALKE-WANT, H., FRENCH, C. A., PEIFER, M., REINHARDT, H. C., ÖRFI, L., KÉRI, G., ANSÉN, S., HEUKAMP, L. C., BÜTTNER, R., RAUH, D., KLEBL, B. M., THOMAS, R. K. & SOS, M. L. 2017. Systematic Kinase Inhibitor Profiling Identifies CDK9 as a Synthetic Lethal Target in NUT Midline Carcinoma. *Cell Reports*, 20, 2833-2845.

- BREITBACH, C. J., ARULANANDAM, R., DE SILVA, N., THORNE, S. H., PATT, R., DANESHMAND, M., MOON, A., ILKOW, C., BURKE, J., HWANG, T. H., HEO, J., CHO, M., CHEN, H., ANGARITA, F. A., ADDISON, C., MCCART, J. A., BELL, J. C. & KIRN, D. H. 2013. Oncolytic vaccinia virus disrupts tumor-associated vasculature in humans. *Cancer Res*, 73, 1265-75.
- BREITBACH, C. J., BELL, J. C., HWANG, T.-H., KIRN, D. H. & BURKE, J. 2015. The emerging therapeutic potential of the oncolytic immunotherapeutic Pexa-Vec (JX-594). *Oncolytic virotherapy*, 4, 25-31.
- BUCKLAND, R. & WILD, T. F. 1997. Is CD46 the cellular receptor for measles virus? *Virus research*, 48, 1-9.
- BULLER, R. M., SMITH, G. L., CREMER, K., NOTKINS, A. L. & MOSS, B. 1985. Decreased virulence of recombinant vaccinia virus expression vectors is associated with a thymidine kinase-negative phenotype. *Nature*, 317, 813-5.
- CHAIDOS, A., CAPUTO, V., GOUVEDENOU, K., LIU, B., MARIGO, I., CHAUDHRY, M. S., ROTOLO, A., TOUGH, D. F., SMITHERS, N. N., BASSIL, A. K., CHAPMAN, T. D., HARKER, N. R., BARBASH, O., TUMMINO, P., AL-MAHDI, N., HAYNES, A. C., CUTLER, L., LE, B., RAHEMTULLA, A., ROBERTS, I., KLEIJNEN, M., WITHERINGTON, J. J., PARR, N. J., PRINJHA, R. K. & KARADIMITRIS, A. 2014. Potent antimyeloma activity of the novel bromodomain inhibitors I-BET151 and I-BET762. *Blood*, 123, 697-705.
- CHAU, N. G., HURWITZ, S., MITCHELL, C. M., ASERLIND, A., GRUNFELD, N., KAPLAN, L., HSI, P., BAUER, D. E., LATHAN, C. S., RODRIGUEZ-GALINDO, C., TISHLER, R. B., HADDAD, R. I., SALLAN, S. E., BRADNER, J. E. & FRENCH, C. A. 2016. Intensive treatment and survival outcomes in NUT midline carcinoma of the head and neck. *Cancer*, 122, 3632-3640.
- CHAU, N. G., MA, C., DANGA, K., AL-SAYEGH, H., NARDI, V., BARRETTE, R., LATHAN, C. S., DUBOIS, S. G., HADDAD, R. I., SHAPIRO, G. I., SALLAN, S. E., DHAR, A., NELSON, J. J. & FRENCH, C. A. 2020. An Anatomical Site and Genetic-Based Prognostic Model for Patients With Nuclear Protein in Testis (NUT) Midline Carcinoma: Analysis of 124 Patients. *JNCI Cancer Spectr*, 4, pkz094.
- CHEN, N., ZHANG, Q., YU, Y. A., STRITZKER, J., BRADER, P., SCHIRBEL, A., SAMNICK, S., SERGANOVA, I., BLASBERG, R., FONG, Y. & SZALAY, A. A. 2009. A Novel Recombinant Vaccinia Virus Expressing the Human Norepinephrine Transporter Retains Oncolytic Potential and Facilitates Deep-Tissue Imaging. *Molecular Medicine*, 15, 144-151.
- CHESNEY, J., PUZANOV, I., COLLICHIO, F., SINGH, P., MILHEM, M. M., GLASPY, J., HAMID, O., ROSS, M., FRIEDLANDER, P., GARBE, C., LOGAN, T. F., HAUSCHILD, A., LEBBE, C., CHEN, L., KIM, J. J., GANSERT, J., ANDTBACKA, R. H. I. & KAUFMAN, H. L. 2018. Randomized, Open-Label Phase II Study Evaluating the Efficacy and Safety of Talimogene Laherparepvec in Combination With Ipilimumab Versus Ipilimumab Alone in Patients With Advanced, Unresectable Melanoma. *J Clin Oncol*, 36, 1658-1667.

- CONO, J., CASEY, C. G., BELL, D. M., CENTERS FOR DISEASE, C. & PREVENTION 2003. Smallpox vaccination and adverse reactions. Guidance for clinicians. *MMWR. Recommendations and reports : Morbidity and mortality weekly report. Recommendations and reports*, 52, 1-28.
- CONRY, R. M., WESTBROOK, B., MCKEE, S. & NORWOOD, T. G. 2018. Talimogene laherparepvec: First in class oncolytic virotherapy. *Hum Vaccin Immunother*, 14, 839-846.
- CRUMPACKER, C. S. 1996. Ganciclovir. *New England Journal of Medicine*, 335, 721-729.
- DANG, T. P., GAZDAR, A. F., VIRMANI, A. K., SEPETAVEC, T., HANDE, K. R., MINNA, J. D., ROBERTS, J. R. & CARBONE, D. P. 2000. Chromosome 19 Translocation, Overexpression of Notch3, and Human Lung Cancer. *JNCl: Journal of the National Cancer Institute*, 92, 1355-1357.
- DENIS, G. V. & GREEN, M. R. 1996. A novel, mitogen-activated nuclear kinase is related to a Drosophila developmental regulator. *Genes & development*, 10, 261-271.
- DEY, A., CHITSAZ, F., ABBASI, A., MISTELI, T. & OZATO, K. 2003. The double bromodomain protein Brd4 binds to acetylated chromatin during interphase and mitosis. *Proc Natl Acad Sci U S A*, 100, 8758-63.
- DICKSON, B. C., SUNG, Y. S., ROSENBLUM, M. K., REUTER, V. E., HARB, M., WUNDER, J. S., SWANSON, D. & ANTONESCU, C. R. 2018. NUTM1 Gene Fusions Characterize a Subset of Undifferentiated Soft Tissue and Visceral Tumors. *Am J Surg Pathol*, 42, 636-645.
- DIGAN, M. E., HAYNES, S. R., MOZER, B. A., DAWID, I. B., FORQUIGNON, F. & GANS, M. 1986. Genetic and molecular analysis of fs(1)h, a maternal effect homeotic gene in Drosophila. *Developmental biology*, 114, 161-169.
- DISPENZIERI, A., TONG, C., LAPLANT, B., LACY, M. Q., LAUMANN, K., DINGLI, D., ZHOU, Y., FEDERSPIEL, M. J., GERTZ, M. A., HAYMAN, S., BUADI, F., O'CONNOR, M., LOWE, V. J., PENG, K. W. & RUSSELL, S. J. 2017. Phase I trial of systemic administration of Edmonston strain of measles virus genetically engineered to express the sodium iodide symporter in patients with recurrent or refractory multiple myeloma. *Leukemia*, 31, 2791-2798.
- DOCK, G. 1904. The influence of complicating diseases upon leukemia. *The American Journal of the Medical Sciences*.
- DONG, X., HU, X., CHEN, J., HU, D. & CHEN, L. F. 2018. BRD4 regulates cellular senescence in gastric cancer cells via E2F/miR-106b/p21 axis. *Cell Death Dis*, 9, 203.
- DÖRIG, R. E., MARCIL, A., CHOPRA, A. & RICHARDSON, C. D. 1993. The human CD46 molecule is a receptor for measles virus (Edmonston strain). *Cell*, 75, 295-305.
- DOROSHOW, D. B., EDER, J. P. & LORUSSO, P. M. 2017. BET inhibitors: a novel epigenetic approach. *Annals of Oncology*, 28, 1776-1787.
- DUELLMAN, S. J., ZHOU, W., MEISENHEIMER, P., VIDUGIRIS, G., CALI, J. J., GAUTAM, P., WENNERBERG, K. & VIDUGIRIENE, J. 2015.



- Bioluminescent, Nonlytic, Real-Time Cell Viability Assay and Use in Inhibitor Screening. *ASSAY and Drug Development Technologies*, 13, 456-465.
- EISSA, I. R., NAOE, Y., BUSTOS-VILLALOBOS, I., ICHINOSE, T., TANAKA, M., ZHIWEN, W., MUKOYAMA, N., MORIMOTO, T., MIYAJIMA, N., HITOKI, H., SUMIGAMA, S., ALEKSIC, B., KODERA, Y. & KASUYA, H. 2017. Genomic Signature of the Natural Oncolytic Herpes Simplex Virus HF10 and Its Therapeutic Role in Preclinical and Clinical Trials. *Frontiers in oncology*, 7, 149-149.
- ESTEVE-ARENYS, A., VALERO, J. G., CHAMORRO-JORGANES, A., GONZALEZ, D., RODRIGUEZ, V., DLOUHY, I., SALAVERRIA, I., CAMPO, E., COLOMER, D., MARTINEZ, A., RYMKIEWICZ, G., PEREZ-GALAN, P., LOPEZ-GUILLERMO, A. & ROUE, G. 2018. The BET bromodomain inhibitor CPI203 overcomes resistance to ABT-199 (venetoclax) by downregulation of BFL-1/A1 in in vitro and in vivo models of MYC+/BCL2+ double hit lymphoma. *Oncogene*, 37, 1830-1844.
- FILIPPAKOPOULOS, P., QI, J., PICAUD, S., SHEN, Y., SMITH, W. B., FEDOROV, O., MORSE, E. M., KEATES, T., HICKMAN, T. T., FELLETTAR, I., PHILPOTT, M., MUNRO, S., MCKEOWN, M. R., WANG, Y., CHRISTIE, A. L., WEST, N., CAMERON, M. J., SCHWARTZ, B., HEIGHTMAN, T. D., LA THANGUE, N., FRENCH, C. A., WIEST, O., KUNG, A. L., KNAPP, S. & BRADNER, J. E. 2010. Selective inhibition of BET bromodomains. *Nature*, 468, 1067-73.
- FISHELSON, Z., DONIN, N., ZELL, S., SCHULTZ, S. & KIRSCHFINK, M. 2003. Obstacles to cancer immunotherapy: expression of membrane complement regulatory proteins (mCRPs) in tumors. *Molecular Immunology*, 40, 109-123.
- FONG, C. Y., GILAN, O., LAM, E. Y. N., RUBIN, A. F., FTOUNI, S., TYLER, D., STANLEY, K., SINHA, D., YEH, P., MORISON, J., GIOTOPOULOS, G., LUGO, D., JEFFREY, P., LEE, S. C.-W., CARPENTER, C., GREGORY, R., RAMSAY, R. G., LANE, S. W., ABDEL-WAHAB, O., KOUZARIDES, T., JOHNSTONE, R. W., DAWSON, S.-J., HUNTLY, B. J. P., PRINJHA, R. K., PAPENFUSS, A. T. & DAWSON, M. A. 2015. BET inhibitor resistance emerges from leukaemia stem cells. *Nature*, 525, 538-542.
- FOURNIER, N., CHALUS, L., DURAND, I., GARCIA, E., PIN, J. J., CHURAKOVA, T., PATEL, S., ZLOT, C., GORMAN, D., ZURAWSKI, S., ABRAMS, J., BATES, E. E. & GARRONE, P. 2000. FDF03, a novel inhibitory receptor of the immunoglobulin superfamily, is expressed by human dendritic and myeloid cells. *J Immunol*, 165, 1197-209.
- FRENCH, C. A. 2016. Chapter Two - Small-Molecule Targeting of BET Proteins in Cancer. In: TEW, K. D. & FISHER, P. B. (eds.) *Advances in Cancer Research*. Academic Press.
- FRENCH, C. A. 2018. NUT Carcinoma: Clinicopathologic features, pathogenesis, and treatment. *Pathol Int*, 68, 583-595.
- FRENCH, C. A., MIYOSHI, I., ASTER, J. C., KUBONISHI, I., KROLL, T. G., DAL CIN, P., VARGAS, S. O., PEREZ-ATAYDE, A. R. & FLETCHER, J. A. 2001. BRD4 bromodomain gene rearrangement in aggressive

- carcinoma with translocation t(15;19). *The American journal of pathology*, 159, 1987-1992.
- FRENCH, C. A., MIYOSHI, I., KUBONISHI, I., GRIER, H. E., PEREZ-ATAYDE, A. R. & FLETCHER, J. A. 2003. BRD4-NUT Fusion Oncogene: A Novel Mechanism in Aggressive Carcinoma. *A Novel Mechanism in Aggressive Carcinoma*, 63, 304-307.
- FRENCH, C. A., RAHMAN, S., WALSH, E. M., KÜHNLE, S., GRAYSON, A. R., LEMIEUX, M. E., GRUNFELD, N., RUBIN, B. P., ANTONESCU, C. R., ZHANG, S., VENKATRAMANI, R., DAL CIN, P. & HOWLEY, P. M. 2014. NSD3-NUT fusion oncoprotein in NUT midline carcinoma: implications for a novel oncogenic mechanism. *Cancer Discov*, 4, 928-41.
- FRENCH, C. A., RAMIREZ, C. L., KOLMAKOVA, J., HICKMAN, T. T., CAMERON, M. J., THYNE, M. E., KUTOK, J. L., TORETSKY, J. A., TADAVARTHY, A. K., KEES, U. R., FLETCHER, J. A. & ASTER, J. C. 2008. BRD-NUT oncoproteins: a family of closely related nuclear proteins that block epithelial differentiation and maintain the growth of carcinoma cells. *Oncogene*, 27, 2237-2242.
- GALANIS, E. 2010. Therapeutic Potential of Oncolytic Measles Virus: Promises and Challenges. *Clinical Pharmacology & Therapeutics*, 88, 620-625.
- GALANIS, E., ATHERTON, P. J., MAURER, M. J., KNUTSON, K. L., DOWDY, S. C., CLIBY, W. A., HALUSKA, P., JR., LONG, H. J., OBERG, A., ADERCA, I., BLOCK, M. S., BAKKUM-GAMEZ, J., FEDERSPIEL, M. J., RUSSELL, S. J., KALLI, K. R., KEENEY, G., PENG, K. W. & HARTMANN, L. C. 2015. Oncolytic measles virus expressing the sodium iodide symporter to treat drug-resistant ovarian cancer. *Cancer research*, 75, 22-30.
- GALANIS, E., HARTMANN, L. C., CLIBY, W. A., LONG, H. J., PEETHAMBARAM, P. P., BARRETTE, B. A., KAUR, J. S., HALUSKA, P. J., JR., ADERCA, I., ZOLLMAN, P. J., SLOAN, J. A., KEENEY, G., ATHERTON, P. J., PODRATZ, K. C., DOWDY, S. C., STANHOPE, C. R., WILSON, T. O., FEDERSPIEL, M. J., PENG, K.-W. & RUSSELL, S. J. 2010. Phase I trial of intraperitoneal administration of an oncolytic measles virus strain engineered to express carcinoembryonic antigen for recurrent ovarian cancer. *Cancer research*, 70, 875-882.
- GALEN, B., CHESHENKO, N., TUYAMA, A., RAMRATNAM, B. & HEROLD, B. C. 2006. Access to nectin favors herpes simplex virus infection at the apical surface of polarized human epithelial cells. *J Virol*, 80, 12209-18.
- GARBER, K. 2006. China Approves World's First Oncolytic Virus Therapy For Cancer Treatment. *JNCI: Journal of the National Cancer Institute*, 98, 298-300.
- GENENAMES.ORG. *Symbol Report for NUTM1* [Online]. HGNC - Human Gene Nomenclature Available: [https://www.genenames.org/data/gene-symbol-report/#!/hgnc\\_id/HGNC:29919](https://www.genenames.org/data/gene-symbol-report/#!/hgnc_id/HGNC:29919) [Accessed 07.02. 2020].
- GIRIDHAR, P., MALLICK, S., KASHYAP, L. & RATH, G. K. 2018. Patterns of care and impact of prognostic factors in the outcome of NUT midline carcinoma: a systematic review and individual patient data analysis of 119 cases. *Eur Arch Otorhinolaryngol*, 275, 815-821.

- GRAYSON, A. R., WALSH, E. M., CAMERON, M. J., GODEC, J., ASHWORTH, T., AMBROSE, J. M., ASERLIND, A. B., WANG, H., EVAN, G., KLUK, M. J., BRADNER, J. E., ASTER, J. C. & FRENCH, C. A. 2014. MYC, a downstream target of BRD-NUT, is necessary and sufficient for the blockade of differentiation in NUT midline carcinoma. *Oncogene*, 33, 1736-1742.
- GREIG, S. L. 2016. Talimogene Laherparepvec: First Global Approval. *Drugs*, 76, 147-54.
- GRIFFIN, D. E. 2018. Measles Vaccine. *Viral immunology*, 31, 86-95.
- HARUKI, N., KAWAGUCHI, K. S., EICHENBERGER, S., MASSION, P. P., GONZALEZ, A., GAZDAR, A. F., MINNA, J. D., CARBONE, D. P. & DANG, T. P. 2005. Cloned fusion product from a rare t(15;19)(q13.2;p13.1) inhibit S phase in vitro. *J Med Genet*, 42, 558-64.
- HEINZERLING, L., KÜNZI, V., OBERHOLZER, P. A., KÜNDIG, T., NAIM, H. & DUMMER, R. 2005. Oncolytic measles virus in cutaneous T-cell lymphomas mounts antitumor immune responses in vivo and targets interferon-resistant tumor cells. *Blood*, 106, 2287-2294.
- HEO, J., REID, T., RUO, L., BREITBACH, C. J., ROSE, S., BLOOMSTON, M., CHO, M., LIM, H. Y., CHUNG, H. C., KIM, C. W., BURKE, J., LENCIONI, R., HICKMAN, T., MOON, A., LEE, Y. S., KIM, M. K., DANESHMAND, M., DUBOIS, K., LONGPRE, L., NGO, M., ROONEY, C., BELL, J. C., RHEE, B.-G., PATT, R., HWANG, T.-H. & KIRN, D. H. 2013. Randomized dose-finding clinical trial of oncolytic immunotherapeutic vaccinia JX-594 in liver cancer. *Nature Medicine*, 19, 329-336.
- HOF, H. & SCHLÜTER, D. 2019. *Medizinische Mikrobiologie, 7th Edition*, Thieme.
- HOSER, H. A., ZANES, R. P. & VON HAAM, E. 1949. The Association of „viral“ Hepatitis and Hodgkin's Disease. *Cancer Research*, 9, 473.
- HOWARD, S. C., JONES, D. P. & PUI, C. H. 2011. The tumor lysis syndrome. *N Engl J Med*, 364, 1844-54.
- HU, J. C., COFFIN, R. S., DAVIS, C. J., GRAHAM, N. J., GROVES, N., GUEST, P. J., HARRINGTON, K. J., JAMES, N. D., LOVE, C. A., MCNEISH, I., MEDLEY, L. C., MICHAEL, A., NUTTING, C. M., PANDHA, H. S., SHORROCK, C. A., SIMPSON, J., STEINER, J., STEVEN, N. M., WRIGHT, D. & COOMBES, R. C. 2006. A phase I study of OncoVEXGM-CSF, a second-generation oncolytic herpes simplex virus expressing granulocyte macrophage colony-stimulating factor. *Clin Cancer Res*, 12, 6737-47.
- HUANG, B., YANG, X. D., ZHOU, M. M., OZATO, K. & CHEN, L. F. 2009. Brd4 coactivates transcriptional activation of NF-kappaB via specific binding to acetylated RelA. *Mol Cell Biol*, 29, 1375-87.
- HUANG, Q. W., HE, L. J., ZHENG, S., LIU, T. & PENG, B. N. 2019. An Overview of Molecular Mechanism, Clinicopathological Factors, and Treatment in NUT Carcinoma. *Biomed Res Int*, 2019, 1018439.
- JOHNSTONE, R. W., LOVELAND, B. E. & MCKENZIE, I. F. 1993. Identification and quantification of complement regulator CD46 on normal human tissues. *Immunology*, 79, 341-7.

- KAUSCHE, G. A., PFANKUCH, E. & RUSKA, H. 1939. Die Sichtbarmachung von pflanzlichem Virus im Übermikroskop. *Naturwissenschaften*, 27, 292-299.
- KEES, U. R., MULCAHY, M. T. & WILLOUGHBY, M. L. 1991. Intrathoracic carcinoma in an 11-year-old girl showing a translocation t(15;19). *The American journal of pediatric hematology/oncology*, 13, 459-464.
- KELLY, E. & RUSSELL, S. J. 2007. History of oncolytic viruses: genesis to genetic engineering. *Molecular therapy : the journal of the American Society of Gene Therapy*, 15, 651-659.
- KIRN, D. H. 1996. Monthly Update: Oncologic, Endocrine & Metabolic: Replicating oncolytic viruses: An overview. *Expert Opinion on Investigational Drugs*, 5, 753-762.
- KLIJN, C., DURINCK, S., STAWISKI, E. W., HAVERTY, P. M., JIANG, Z., LIU, H., DEGENHARDT, J., MAYBA, O., GNAD, F., LIU, J., PAU, G., REEDER, J., CAO, Y., MUKHYALA, K., SELVARAJ, S. K., YU, M., ZYNDA, G. J., BRAUER, M. J., WU, T. D., GENTLEMAN, R. C., MANNING, G., YAUCH, R. L., BOURGON, R., STOKOE, D., MODRUSAN, Z., NEVE, R. M., DE SAUVAGE, F. J., SETTLEMAN, J., SESHAGIRI, S. & ZHANG, Z. 2015. A comprehensive transcriptional portrait of human cancer cell lines. *Nature biotechnology*, 33, 306-312.
- KLOKER, L. D., BERCHTOLD, S., SMIRNOW, I., SCHALLER, M., FEHRENBACHER, B., KRIEG, A., SIPOS, B. & LAUER, U. M. 2019. The Oncolytic Herpes Simplex Virus Talimogene Laherparepvec Shows Promising Efficacy in Neuroendocrine Cancer Cell Lines. *Neuroendocrinology*, 109, 346-361.
- KOHLHAPP, F. J. & KAUFMAN, H. L. 2016. Molecular Pathways: Mechanism of Action for Talimogene Laherparepvec, a New Oncolytic Virus Immunotherapy. *Clin Cancer Res*, 22, 1048-54.
- KUBONISHI, I., TAKEHARA, N., IWATA, J., SONOBE, H., OHTSUKI, Y., ABE, T. & MIYOSHI, I. 1991. Novel t(15;19)(q15;p13) chromosome abnormality in a thymic carcinoma. *Cancer research*, 51, 3327-3328.
- KUKHANOVA, M. K., KOROVINA, A. N. & KOCHETKOV, S. N. 2014. Human herpes simplex virus: life cycle and development of inhibitors. *Biochemistry. Biokhimiia*, 79, 1635-1652.
- KUZUME, T., KUBONISHI, I., TAKEUCHI, S., TAKEUCHI, T., IWATA, J., SONOBE, H., OHTSUKI, Y. & MIYOSHI, I. 1992. Establishment and characterization of a thymic carcinoma cell line (Ty-82) carrying t(15;19)(q15;p13) chromosome abnormality. *Int J Cancer*, 50, 259-64.
- LAL, S., CARRERA, D., PHILLIPS, J. J., WEISS, W. A. & RAFFEL, C. 2018. An oncolytic measles virus-sensitive Group 3 medulloblastoma model in immune-competent mice. *Neuro Oncol*, 20, 1606-1615.
- LALEZARI, J. P., FRIEDBERG, D. N., BISSETT, J., GIORDANO, M. F., HARDY, W. D., DREW, W. L., HUBBARD, L. D., BUHLES, W. C., STEMPIEN, M. J., GEORGIU, P., JUNG, D. T. & ROBINSON, C. A. 2002. High dose oral ganciclovir treatment for cytomegalovirus retinitis. *J Clin Virol*, 24, 67-77.
- LAUER, U. M., SCHELL, M., BEIL, J., BERCHTOLD, S., KOPPENHÖFER, U., GLATZLE, J., KÖNIGSRÄINER, A., MÖHLE, R., NANN, D., FEND, F.,

- PFANNENBERG, C., BITZER, M. & MALEK, N. P. 2018. Phase I Study of Oncolytic Vaccinia Virus GL-ONC1 in Patients with Peritoneal Carcinomatosis. *Clinical cancer research : an official journal of the American Association for Cancer Research*, 24, 4388-4398.
- LAWLER, S. E., SPERANZA, M.-C., CHO, C.-F. & CHIOCCA, E. A. 2017. Oncolytic Viruses in Cancer Treatment: A Review. *JAMA Oncology*, 3, 841-849.
- LEE, A. C., KWONG, Y. I., FU, K. H., CHAN, G. C., MA, L. & LAU, Y. L. 1993. Disseminated mediastinal carcinoma with chromosomal translocation (15;19). A distinctive clinicopathologic syndrome. *Cancer*, 72, 2273-2276.
- LEVADITI, C. & NICOLAU, S. 1922. Sur le culture du virus vaccinal dans les neoplasmes epithelioux. *CR Soc Biol*, 86, 928.
- LEWIN, J., SORIA, J.-C., STATHIS, A., DELORD, J.-P., PETERS, S., AWADA, A., AFTIMOS, P. G., BEKRADDA, M., REZAI, K., ZENG, Z., HUSSAIN, A., PEREZ, S., SIU, L. L. & MASSARD, C. 2018. Phase Ib Trial With Birabresib, a Small-Molecule Inhibitor of Bromodomain and Extraterminal Proteins, in Patients With Selected Advanced Solid Tumors. *Journal of Clinical Oncology*, 36, 3007-3014.
- LIAO, S., MAERTENS, O., CICHOWSKI, K. & ELLEDGE, S. J. 2018. Genetic modifiers of the BRD4-NUT dependency of NUT midline carcinoma uncovers a synergism between BETis and CDK4/6is. *Genes Dev*, 32, 1188-1200.
- LISZEWSKI, M. K., POST, T. W. & ATKINSON, J. P. 1991. Membrane cofactor protein (MCP or CD46): newest member of the regulators of complement activation gene cluster. *Annual review of immunology*, 9, 431-455.
- LIU, A., FAN, D. & WANG, Y. 2018. The BET bromodomain inhibitor i-BET151 impairs ovarian cancer metastasis and improves antitumor immunity. *Cell Tissue Res*, 374, 577-585.
- LIU, B. L., ROBINSON, M., HAN, Z. Q., BRANSTON, R. H., ENGLISH, C., REAY, P., MCGRATH, Y., THOMAS, S. K., THORNTON, M., BULLOCK, P., LOVE, C. A. & COFFIN, R. S. 2003. ICP34.5 deleted herpes simplex virus with enhanced oncolytic, immune stimulating, and anti-tumour properties. *Gene Ther*, 10, 292-303.
- LOPEZ, M., COCCHI, F., MENOTTI, L., AVITABILE, E., DUBREUIL, P. & CAMPADELLI-FIUME, G. 2000. Nectin2alpha (PRR2alpha or HveB) and nectin2delta are low-efficiency mediators for entry of herpes simplex virus mutants carrying the Leu25Pro substitution in glycoprotein D. *J Virol*, 74, 1267-74.
- MA, J., RAMACHANDRAN, M., JIN, C., QUIJANO-RUBIO, C., MARTIKAINEN, M., YU, D. & ESSAND, M. 2020. Characterization of virus-mediated immunogenic cancer cell death and the consequences for oncolytic virus-based immunotherapy of cancer. *Cell Death Dis*, 11, 48.
- MAHER, O. M., CHRISTENSEN, A. M., YEDURURI, S., BELL, D. & TAREK, N. 2015. Histone deacetylase inhibitor for NUT midline carcinoma. *Pediatric Blood & Cancer*, 62, 715-717.
- MARKMAN, R. L., WEBBER, L. P., NASCIMENTO FILHO, C. H. V., REIS, L. A., VARGAS, P. A., LOPES, M. A., ZANELLA, V., MARTINS, M. D., SQUARIZE, C. H. & CASTILHO, R. M. 2019. Interfering with

- bromodomain epigenome readers as therapeutic option in mucoepidermoid carcinoma. *Cell Oncol (Dordr)*, 42, 143-155.
- MARTUZA, R., MALICK, A., MARKERT, J., RUFFNER, K. & COEN, D. 1991. Experimental therapy of human glioma by means of a genetically engineered virus mutant. *Science*, 252, 854-856.
- MATZ, K. M., GUZMAN, R. M. & GOODMAN, A. G. 2019. The Role of Nucleic Acid Sensing in Controlling Microbial and Autoimmune Disorders. *International review of cell and molecular biology*, 345, 35-136.
- MEJÍAS-PÉREZ, E., CARREÑO-FUENTES, L. & ESTEBAN, M. 2018. Development of a Safe and Effective Vaccinia Virus Oncolytic Vector WR-Δ4 with a Set of Gene Deletions on Several Viral Pathways. *Mol Ther Oncolytics*, 8, 27-40.
- MELL, L. K., BRUMUND, K. T., DANIELS, G. A., ADVANI, S. J., ZAKERI, K., WRIGHT, M. E., ONYEAMA, S.-J., WEISMAN, R. A., SANGHVI, P. R., MARTIN, P. J. & SZALAY, A. A. 2017. Phase I Trial of Intravenous Oncolytic Vaccinia Virus (GL-ONC1) with Cisplatin and Radiotherapy in Patients with Locoregionally Advanced Head and Neck Carcinoma. *Clinical cancer research : an official journal of the American Association for Cancer Research*, 23, 5696-5702.
- MITELMAN, F., JOHANSSON, B. & MERTENS, F. 2020. *Mitelman Database of Chromosome Aberrations and Gene Fusions in Cancer* [Online]. <https://mitelmandatabase.isb-cgc.org>. [Accessed 05.03. 2020].
- MOORHEAD, P. S. 1965. Human tumor cell line with a quasi-diploid karyotype (RPMI 2650). *Experimental cell research*, 39, 190-196.
- MORRISON-SMITH, C. D., KNOX, T. M., FILIC, I., SOROKO, K. M., ESCHLE, B. K., WILKENS, M. K., GOKHALE, P. C., GILES, F., GRIFFIN, A., BROWN, B., SHAPIRO, G. I., ZUCCONI, B. E., COLE, P. A., LEMIEUX, M. E. & FRENCH, C. A. 2020. Combined targeting of the BRD4-NUT-p300 axis in NUT midline carcinoma by dual selective bromodomain inhibitor, NEO2734. *Molecular Cancer Therapeutics*, molcanther.0087.2020.
- MÜHLEBACH, M. D., MATEO, M., SINN, P. L., PRÜFER, S., UHLIG, K. M., LEONARD, V. H. J., NAVARATNARAJAH, C. K., FRENZKE, M., WONG, X. X., SAWATSKY, B., RAMACHANDRAN, S., MCCRAY, P. B., JR., CICHUTEK, K., VON MESSLING, V., LOPEZ, M. & CATTANEO, R. 2011. Adherens junction protein nectin-4 is the epithelial receptor for measles virus. *Nature*, 480, 530-533.
- NANICHE, D., VARIOR-KRISHNAN, G., CERVONI, F., WILD, T. F., ROSSI, B., RABOURDIN-COMBE, C. & GERLIER, D. 1993. Human membrane cofactor protein (CD46) acts as a cellular receptor for measles virus. *J Virol*, 67, 6025-32.
- NAPOLITANO, M., VENTURELLI, M., MOLINARO, E. & TOSS, A. 2019. NUT midline carcinoma of the head and neck: current perspectives. *Onco Targets Ther*, 12, 3235-3244.
- NICODEME, E., JEFFREY, K. L., SCHAEFER, U., BEINKE, S., DEWELL, S., CHUNG, C. W., CHANDWANI, R., MARAZZI, I., WILSON, P., COSTE, H., WHITE, J., KIRILOVSKY, J., RICE, C. M., LORA, J. M., PRINJHA, R.

- K., LEE, K. & TARAKHOVSKY, A. 2010. Suppression of inflammation by a synthetic histone mimic. *Nature*, 468, 1119-23.
- NOLL, M., BERCHTOLD, S., LAMPE, J., MALEK, N. P., BITZER, M. & LAUER, U. M. 2013. Primary resistance phenomena to oncolytic measles vaccine viruses. *International journal of oncology*, 43, 103-112.
- NOYCE, R. S., BONDRE, D. G., HA, M. N., LIN, L.-T., SISSON, G., TSAO, M.-S. & RICHARDSON, C. D. 2011. Tumor cell marker PVRL4 (nectin 4) is an epithelial cell receptor for measles virus. *PLoS pathogens*, 7, e1002240-e1002240.
- OHNESORGE, P. V., BERCHTOLD, S., BEIL, J., HAAS, S. A., SMIRNOW, I., SCHENK, A., FRENCH, C. A., LUONG, N. M., HUANG, Y., FEHRENBACHER, B., SCHALLER, M. & LAUER, U. M. 2022. Efficacy of Oncolytic Herpes Simplex Virus T-VEC Combined with BET Inhibitors as an Innovative Therapy Approach for NUT Carcinoma. *Cancers*, 14, 2761.
- ORBACH, S. M., EHRICH, M. F. & RAJAGOPALAN, P. 2018. High-throughput toxicity testing of chemicals and mixtures in organotypic multi-cellular cultures of primary human hepatic cells. *Toxicology in Vitro*, 51, 83-94.
- PASQUINUCCI, G. 1971. Possible effect of measles on leukaemia. *Lancet (London, England)*, 1, 136-136.
- PENG, Z. 2005. Current Status of Gendicine in China: Recombinant Human Ad-p53 Agent for Treatment of Cancers. *Human Gene Therapy*, 16, 1016-1027.
- PEREZ, R. P., GODWIN, A. K., HANDEL, L. M. & HAMILTON, T. C. 1993. A comparison of clonogenic, microtetrazolium and sulforhodamine B assays for determination of cisplatin cytotoxicity in human ovarian carcinoma cell lines. *European Journal of Cancer*, 29, 395-399.
- PIHA-PAUL, S. A., HANN, C. L., FRENCH, C. A., COUSIN, S., BRAÑA, I., CASSIER, P. A., MORENO, V., DE BONO, J. S., HARWARD, S. D., FERRON-BRADY, G., BARBASH, O., WYCE, A., WU, Y., HORNER, T., ANNAN, M., PARR, N. J., PRINJHA, R. K., CARPENTER, C. L., HILTON, J., HONG, D. S., HAAS, N. B., MARKOWSKI, M. C., DHAR, A., O'DWYER, P. J. & SHAPIRO, G. I. 2020. Phase 1 Study of Molibresib (GSK525762), a Bromodomain and Extra-Terminal Domain Protein Inhibitor, in NUT Carcinoma and Other Solid Tumors. *JNCI Cancer Spectr*, 4, pkz093.
- PUHLMANN, M., BROWN, C. K., GNANT, M., HUANG, J., LIBUTTI, S. K., ALEXANDER, H. R. & BARTLETT, D. L. 2000. Vaccinia as a vector for tumor-directed gene therapy: Biodistribution of a thymidine kinase-deleted mutant. *Cancer Gene Therapy*, 7, 66-73.
- RAHMANI, B., PATEL, S., SEYAM, O., GANDHI, J., REID, I., SMITH, N. & KHAN, S. A. 2019. Current understanding of tumor lysis syndrome. *Hematological Oncology*, 37, 537-547.
- REYNOIRD, N., SCHWARTZ, B. E., DELVECCHIO, M., SADOUL, K., MEYERS, D., MUKHERJEE, C., CARON, C., KIMURA, H., ROUSSEAU, S., COLE, P. A., PANNE, D., FRENCH, C. A. & KHOCHBIN, S. 2010. Oncogenesis by sequestration of CBP/p300 in

- transcriptionally inactive hyperacetylated chromatin domains. *Embo j*, 29, 2943-52.
- RIBAS, A., DUMMER, R., PUZANOV, I., VANDERWALDE, A., ANDTBACKA, R. H. I., MICHIELIN, O., OLSZANSKI, A. J., MALVEHY, J., CEBON, J., FERNANDEZ, E., KIRKWOOD, J. M., GAJEWSKI, T. F., CHEN, L., GORSKI, K. S., ANDERSON, A. A., DIEDE, S. J., LASSMAN, M. E., GANSERT, J., HODI, F. S. & LONG, G. V. 2017. Oncolytic Virotherapy Promotes Intratumoral T Cell Infiltration and Improves Anti-PD-1 Immunotherapy. *Cell*, 170, 1109-1119.e10.
- RIEDEL, S. 2005. Edward Jenner and the history of smallpox and vaccination. *Proc (Bayl Univ Med Cent)*, 18, 21-5.
- RKI.DE. 2014. *RKI-Ratgeber Masern* [Online]. Robert Koch Institut (RKI). Available: [https://www.rki.de/DE/Content/Infekt/EpidBull/Merkblaetter/Ratgeber\\_Masern.html#doc2374536bodyText2](https://www.rki.de/DE/Content/Infekt/EpidBull/Merkblaetter/Ratgeber_Masern.html#doc2374536bodyText2) [Accessed 07.02 2020].
- ROTA, J. S., WANG, Z. D., ROTA, P. A. & BELLINI, W. J. 1994. Comparison of sequences of the H, F, and N coding genes of measles virus vaccine strains. *Virus research*, 31, 317-330.
- RUSSELL, S. J. & PENG, K. W. 2007. Viruses as anticancer drugs. *Trends Pharmacol Sci*, 28, 326-33.
- SAKAMAKI, J.-I., WILKINSON, S., HAHN, M., TASDEMIR, N., O'PREY, J., CLARK, W., HEDLEY, A., NIXON, C., LONG, J. S., NEW, M., VAN ACKER, T., TOOZE, S. A., LOWE, S. W., DIKIC, I. & RYAN, K. M. 2017. Bromodomain Protein BRD4 Is a Transcriptional Repressor of Autophagy and Lysosomal Function. *Molecular cell*, 66, 517-532.e9.
- SAMUEL, C. E. 2001. Antiviral Actions of Interferons. *Clinical Microbiology Reviews*, 14, 778.
- SÁNCHEZ-SAMPEDRO, L., PERDIGUERO, B., MEJÍAS-PÉREZ, E., GARCÍA-ARRIAZA, J., DI PILATO, M. & ESTEBAN, M. 2015. The evolution of poxvirus vaccines. *Viruses*, 7, 1726-803.
- SANFORD, K. K., EARLE, W. R. & LIKELY, G. D. 1948. The Growth in Vitro of Single Isolated Tissue Cells. *JNCI: Journal of the National Cancer Institute*, 9, 229-246.
- SAVAGE, H. E., ROSSEN, R. D., HERSH, E. M., FREEDMAN, R. S., BOWEN, J. M. & PLAGER, C. 1986. Antibody development to viral and allogeneic tumor cell-associated antigens in patients with malignant melanoma and ovarian carcinoma treated with lysates of virus-infected tumor cells. *Cancer Res*, 46, 2127-33.
- SCHAEFER, I.-M., DAL CIN, P., LANDRY, L. M., FLETCHER, C. D. M., HANNA, G. J. & FRENCH, C. A. 2018. CIC-NUTM1 fusion: A case which expands the spectrum of NUT-rearranged epithelioid malignancies. *Genes, chromosomes & cancer*, 57, 446-451.
- SCHEUBECK, G., BERCHTOLD, S., SMIRNOW, I., SCHENK, A., BEIL, J. & LAUER, U. M. 2019. Starvation-Induced Differential Virotherapy Using an Oncolytic Measles Vaccine Virus. *Viruses*, 11.
- SCHMIDT, F. I., BLECK, C. K. E. & MERCER, J. 2012. Poxvirus host cell entry. *Current Opinion in Virology*, 2, 20-27.



- SCHNEIDER, U., VON MESSLING, V., DEVAUX, P. & CATTANEO, R. 2002. Efficiency of measles virus entry and dissemination through different receptors. *Journal of virology*, 76, 7460-7467.
- SCHWARTZ, B. E., HOFER, M. D., LEMIEUX, M. E., BAUER, D. E., CAMERON, M. J., WEST, N. H., AGOSTON, E. S., REYNOIRD, N., KHOCHBIN, S., INCE, T. A., CHRISTIE, A., JANEWAY, K. A., VARGAS, S. O., PEREZ-ATAYDE, A. R., ASTER, J. C., SALLAN, S. E., KUNG, A. L., BRADNER, J. E. & FRENCH, C. A. 2011. Differentiation of NUT midline carcinoma by epigenomic reprogramming. *Cancer Res*, 71, 2686-96.
- SENZER, N. N., KAUFMAN, H. L., AMATRUDA, T., NEMUNAITIS, M., REID, T., DANIELS, G., GONZALEZ, R., GLASPY, J., WHITMAN, E., HARRINGTON, K., GOLDSWEIG, H., MARSHALL, T., LOVE, C., COFFIN, R. & NEMUNAITIS, J. J. 2009. Phase II clinical trial of a granulocyte-macrophage colony-stimulating factor-encoding, second-generation oncolytic herpesvirus in patients with unresectable metastatic melanoma. *J Clin Oncol*, 27, 5763-71.
- SHAPIRO, G. I., DOWLATI, A., LORUSSO, P. M., EDER, J. P., ANDERSON, A., DO, K. T., KAGEY, M. H., SIRARD, C., BRADNER, J. E. & LANDAU, S. B. 2015. Abstract A49: Clinically efficacy of the BET bromodomain inhibitor TEN-010 in an open-label substudy with patients with documented NUT-midline carcinoma (NMC). *Molecular Cancer Therapeutics*, 14, A49.
- SHEN, Y. & NEMUNAITIS, J. 2006. Herpes simplex virus 1 (HSV-1) for cancer treatment. *Cancer Gene Therapy*, 13, 975-992.
- SHUKLA, D., LIU, J., BLAIKLOCK, P., SHWORAK, N. W., BAI, X., ESKO, J. D., COHEN, G. H., EISENBERG, R. J., ROSENBERG, R. D. & SPEAR, P. G. 1999. A Novel Role for 3-O-Sulfated Heparan Sulfate in Herpes Simplex Virus 1 Entry. *Cell*, 99, 13-22.
- SKEHAN, P., STORENG, R., SCUDIERO, D., MONKS, A., MCMAHON, J., VISTICA, D., WARREN, J. T., BOKESCH, H., KENNEY, S. & BOYD, M. R. 1990. New Colorimetric Cytotoxicity Assay for Anticancer-Drug Screening. *JNCI: Journal of the National Cancer Institute*, 82, 1107-1112.
- SMITH, G. L., TALBOT-COOPER, C. & LU, Y. 2018. How Does Vaccinia Virus Interfere With Interferon? *Adv Virus Res*, 100, 355-378.
- SMITH, R. R., HUEBNER, R. J., ROWE, W. P., SCHATTEEN, W. E. & THOMAS, L. B. 1956. Studies on the use of viruses in the treatment of carcinoma of the cervix. *Cancer*, 9, 1211-1218.
- SPEAR, P. G. 2004. Herpes simplex virus: receptors and ligands for cell entry. *Cellular Microbiology*, 6, 401-410.
- STATHIS, A. & BERTONI, F. 2018. BET Proteins as Targets for Anticancer Treatment. *Cancer Discovery*, 8, 24-36.
- STEVENS, T. M., MORLOTE, D., XIU, J., SWENSEN, J., BRANDWEIN-WEBER, M., MIETTINEN, M. M., GATALICA, Z. & BRIDGE, J. A. 2019. NUTM1-rearranged neoplasia: a multi-institution experience yields novel fusion partners and expands the histologic spectrum. *Modern Pathology*, 32, 764-773.

- STIRNWEISS, A., MCCARTHY, K., OOMMEN, J., CROOK, M. L., HARDY, K., KEES, U. R., WILTON, S. D., ANAZODO, A. & BEESLEY, A. H. 2015. A novel BRD4-NUT fusion in an undifferentiated sinonasal tumor highlights alternative splicing as a contributing oncogenic factor in NUT midline carcinoma. *Oncogenesis*, 4, e174-e174.
- STIRNWEISS, A., OOMMEN, J., KOTTECHA, R. S., KEES, U. R. & BEESLEY, A. H. 2017. Molecular-genetic profiling and high-throughput in vitro drug screening in NUT midline carcinoma-an aggressive and fatal disease. *Oncotarget*, 8, 112313-112329.
- STOJDL, D. F., LICHTY, B., KNOWLES, S., MARIUS, R., ATKINS, H., SONENBERG, N. & BELL, J. C. 2000. Exploiting tumor-specific defects in the interferon pathway with a previously unknown oncolytic virus. *Nature Medicine*, 6, 821-825.
- STONESTROM, A. J., HSU, S. C., WERNER, M. T. & BLOBEL, G. A. 2016. Erythropoiesis provides a BRD's eye view of BET protein function. *Drug discovery today. Technologies*, 19, 23-28.
- SUN, K., ATOYAN, R., BOREK, M. A., DELLAROCCHA, S., SAMSON, M. E. S., MA, A. W., XU, G.-X., PATTERSON, T., TUCK, D. P., VINER, J. L., FATTAEY, A. & WANG, J. 2017. Dual HDAC and PI3K Inhibitor CUDC-907 Downregulates MYC and Suppresses Growth of MYC-dependent Cancers. *Molecular Cancer Therapeutics*, 16, 285-299.
- TAQI, A. M., ABDURRAHMAN, M. B., YAKUBU, A. M. & FLEMING, A. F. 1981. Regression of Hodgkin's disease after measles. *Lancet (London, England)*, 1, 1112-1112.
- TATSUO, H., ONO, N., TANAKA, K. & YANAGI, Y. 2000. SLAM (CDw150) is a cellular receptor for measles virus. *Nature*, 406, 893-897.
- THOMPSON-WICKING, K., FRANCIS, R. W., STIRNWEISS, A., FERRARI, E., WELCH, M. D., BAKER, E., MURCH, A. R., GOUT, A. M., CARTER, K. W., CHARLES, A. K., PHILLIPS, M. B., KEES, U. R. & BEESLEY, A. H. 2013. Novel BRD4-NUT fusion isoforms increase the pathogenic complexity in NUT midline carcinoma. *Oncogene*, 32, 4664-74.
- TODA, M., RABKIN, S. D., KOJIMA, H. & MARTUZA, R. L. 1999. Herpes Simplex Virus as an in Situ Cancer Vaccine for the Induction of Specific Anti-Tumor Immunity. *Human Gene Therapy*, 10, 385-393.
- TORETSKY, J. A., JENSON, J., SUN, C.-C., ESKENAZI, A. E., CAMPBELL, A., HUNGER, S. P., CAIRES, A., FRANTZ, C., HILL, J. L. & STAMBERG, J. 2003. Translocation (11;15;19): a highly specific chromosome rearrangement associated with poorly differentiated thymic carcinoma in young patients. *American journal of clinical oncology*, 26, 300-306.
- VARGAS, S. O., FRENCH, C. A., FAUL, P. N., FLETCHER, J. A., DAVIS, I. J., DAL CIN, P. & PEREZ-ATAYDE, A. R. 2001. Upper respiratory tract carcinoma with chromosomal translocation 15;19: evidence for a distinct disease entity of young patients with a rapidly fatal course. *Cancer*, 92, 1195-203.
- WANG, R., LIU, W., HELFER, C. M., BRADNER, J. E., HORNICK, J. L., JANICKI, S. M., FRENCH, C. A. & YOU, J. 2014. Activation of SOX2 expression by BRD4-NUT oncogenic fusion drives neoplastic

- transformation in NUT midline carcinoma. *Cancer research*, 74, 3332-3343.
- WANG, Z., DENG, Z., TUTTON, S. & LIEBERMAN, P. M. 2017. The Telomeric Response to Viral Infection. *Viruses*, 9.
- WHO 1980. The global eradication of smallpox. Final Report of the Global Commission for the Certification of Smallpox Eradication. *History of International Public Health.*, 4, 122 pp.
- WHO.INT. 2017. *Fact Sheet Herpes Simplex Virus* [Online]. <https://www.who.int/news-room/fact-sheets/detail/herpes-simplex-virus#hsv1>. [Accessed 18.02 2020].
- WU, S. Y., LEE, A. Y., HOU, S. Y., KEMPER, J. K., ERDJUMENT-BROMAGE, H., TEMPST, P. & CHIANG, C. M. 2006. Brd4 links chromatin targeting to HPV transcriptional silencing. *Genes Dev*, 20, 2383-96.
- WU, T., WANG, G., CHEN, W., ZHU, Z., LIU, Y., HUANG, Z., HUANG, Y., DU, P., YANG, Y., LIU, C. Y. & CUI, L. 2018. Co-inhibition of BET proteins and NF-kappaB as a potential therapy for colorectal cancer through synergistic inhibiting MYC and FOXM1 expressions. *Cell Death Dis*, 9, 315.
- XIA, Z. J., CHANG, J. H., ZHANG, L., JIANG, W. Q., GUAN, Z. Z., LIU, J. W., ZHANG, Y., HU, X. H., WU, G. H., WANG, H. Q., CHEN, Z. C., CHEN, J. C., ZHOU, Q. H., LU, J. W., FAN, Q. X., HUANG, J. J. & ZHENG, X. 2004. [Phase III randomized clinical trial of intratumoral injection of E1B gene-deleted adenovirus (H101) combined with cisplatin-based chemotherapy in treating squamous cell cancer of head and neck or esophagus]. *Ai Zheng*, 23, 1666-70.
- YANG, Z., HE, N. & ZHOU, Q. 2008. Brd4 recruits P-TEFb to chromosomes at late mitosis to promote G1 gene expression and cell cycle progression. *Molecular and cellular biology*, 28, 967-976.
- ZEH, H. J., DOWNS-CANNER, S., MCCART, J. A., GUO, Z. S., RAO, U. N., RAMALINGAM, L., THORNE, S. H., JONES, H. L., KALINSKI, P., WIECKOWSKI, E., O'MALLEY, M. E., DANESHMAND, M., HU, K., BELL, J. C., HWANG, T. H., MOON, A., BREITBACH, C. J., KIRN, D. H. & BARTLETT, D. L. 2015. First-in-man study of western reserve strain oncolytic vaccinia virus: safety, systemic spread, and antitumor activity. *Mol Ther*, 23, 202-14.
- ZUBER, J., SHI, J., WANG, E., RAPPAPORT, A. R., HERRMANN, H., SISON, E. A., MAGOON, D., QI, J., BLATT, K., WUNDERLICH, M., TAYLOR, M. J., JOHNS, C., CHICAS, A., MULLOY, J. C., KOGAN, S. C., BROWN, P., VALENT, P., BRADNER, J. E., LOWE, S. W. & VAKOC, C. R. 2011. RNAi screen identifies Brd4 as a therapeutic target in acute myeloid leukaemia. *Nature*, 478, 524-528.
- ZYGIERT, Z. 1971. Hodgkin's disease: remissions after measles. *Lancet (London, England)*, 1, 593-593.

## **9 Erklärung zum Eigenanteil**

Die Arbeit wurde in der Inneren Medizin VIII des Universitätsklinikums Tübingen unter Betreuung von Herrn Prof. Dr. med. Ulrich M. Lauer durchgeführt.

Die Konzeption der Studie erfolgte in Zusammenarbeit mit Herrn Prof. Dr. med. Ulrich M. Lauer, Frau Dr. med. Susanne Berchtold [Laborleitung] und Frau Dr. rer. nat. Julia Beil [wiss. Mitarbeiterin].

Sämtliche Versuche - mit unten stehenden Ausnahmen - wurden nach Einarbeitung durch Frau Irina Smirnow [MTA] von mir eigenständig durchgeführt.

Frau Andrea Schenk [MTA] führte je eines der drei unabhängigen Experimente mit Auswertung nach 96 h der unter 3.2.1, 3.2.2 und 3.2.3 genannten Versuche zur Bestimmung der Resistenzen von NC Zelllinien durch.

Die statistische Auswertung erfolgte nach Beratung durch das Institut für Biometrie durch mich.

Ich versichere, das Manuskript selbständig (nach Anleitung durch Frau Dr. med. Susanne Berchtold, Frau Dr. rer. nat. Julia Beil [wiss. Mitarbeiterin] und Prof. Dr. med. Ulrich M. Lauer) verfasst zu haben und keine weiteren als die von mir angegebenen Quellen verwendet zu haben.

Tübingen, den 10.02.2021

Paul Vincent Ohnesorge

## **10 Veröffentlichungen**

Teile der Ergebnisse dieser Dissertation wurden am 02.06.2022 unter dem Titel „Efficacy of Oncolytic Herpes Simplex Virus T-VEC Combined with BET Inhibitors as an Innovative Therapy Approach for NUT Carcinoma“ in *Cancers* (Basel, Schweiz) bereits veröffentlicht (Ohnesorge et al., 2022).

### **11 Danksagung**

An dieser Stelle möchte ich mich ganz herzlich bei allen bedanken, die mich bei der Erstellung meiner Dissertation unterstützt haben.

Dabei gilt mein besonderer Dank natürlich meinem Doktorvater Prof. Dr. Ulrich M. Lauer für die Hilfe bei der Entwicklung meines Promotionsthemas, der Unterstützung für die Bewerbung bei dem IZKF Promotionskolleg und die vielen Ideen für weitere Experimente während meiner Forschungstätigkeit. Genauso dankbar bin ich über die überaus kompetente Betreuung durch die AG Lauer, namentlich Dr. Susanne Berchtold, Dr. Julia Beil, Irina Smirnow sowie Andrea Schenk. Während meiner Zeit im Labor konnte ich bei jeder Frage immer auf eure schnelle und fachkundige Unterstützung zählen, ohne welche die Anfertigung dieser Dissertation nicht möglich gewesen wäre. Frau Dr. Julia Beil und Frau Dr. Susanne Berchtold danke ich zusätzlich für die Beantwortung der zahlreichen Fragen, welche sich mir bei dem Verfassen dieser Arbeit stellten, als auch für das Korrekturlesen.

Des Weiteren möchte ich mich bei dem IZKF Promotionskolleg für die Förderung meiner Dissertation, die zahlreichen weiteren Einblicke in andere medizinische Forschungsbereiche und die Unterstützung bei allen formalen Fragen zu meiner Dissertation bedanken.

Bei dieser Arbeit wurde die methodische Beratung des Instituts für Klinische Epidemiologie und angewandte Biometrie der Universität Tübingen in Anspruch genommen. Für die Unterstützung möchte ich mich bei Frau You-Shan Feng herzlich bedanken.

Nicht zuletzt gilt großer Dank auch meiner Familie, welche mich immer unterstützt hat.